ISSN 1016-3115

wgn

21 - 4
august 1993

bimonthly journal of the international meteor organization

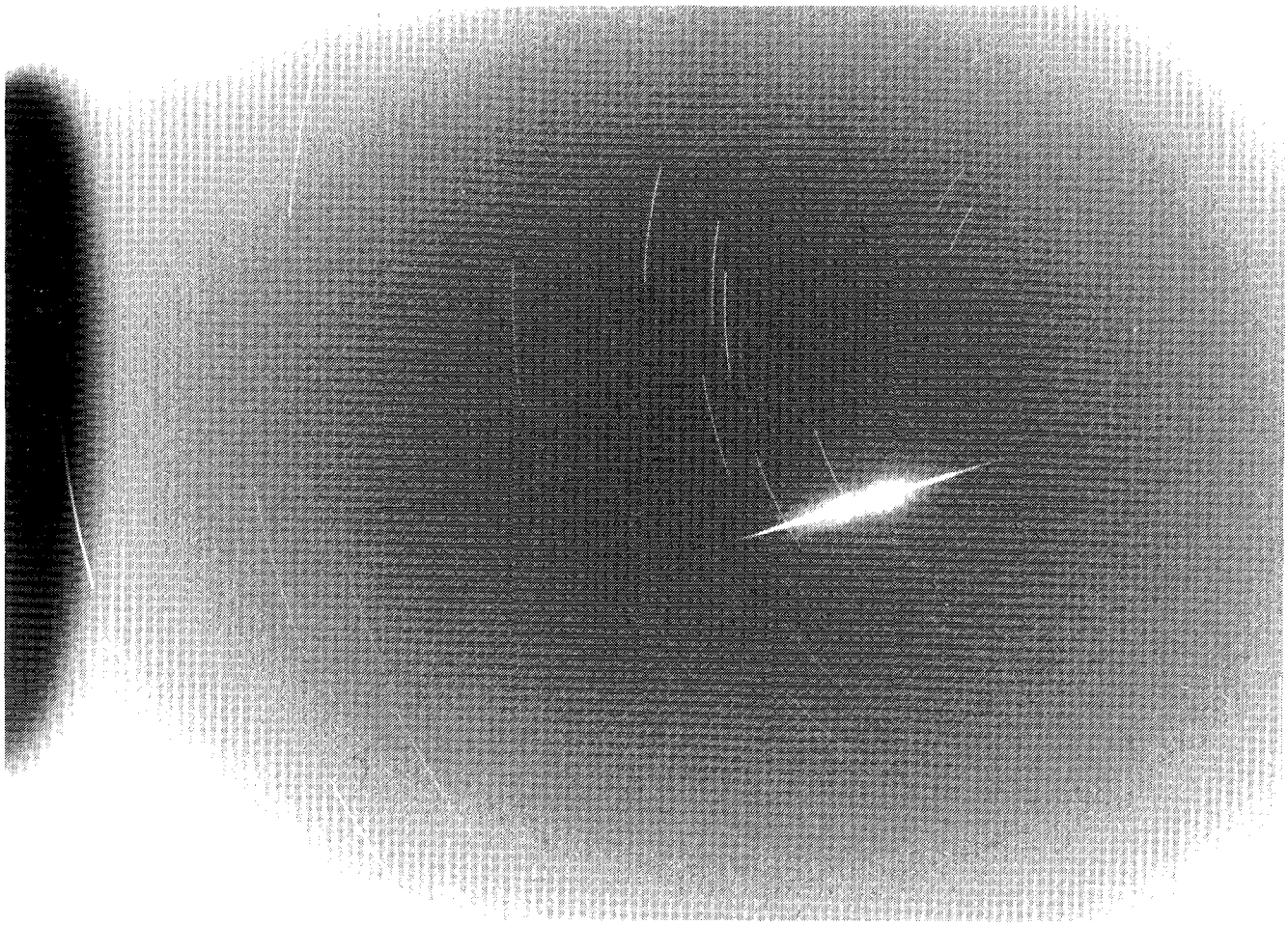

This bright −9.5 fireball was photographed by Ben Apeldoorn from Hoogmade, the Netherlands, on April 15, 1993, at $21^h14^m30^s \pm 5^s$ UT. A Nikkor fish-eye 16 mm $f/4$ was used with a Tmax-400 film and a shutter yielding 25 breaks per second. The fireball moved in the direction of the Polar Star. More information on this bright fireball can be found in this issue.

In this issue:

- Practical information for observers
- Global analysis of the 1991 and 1992 Perseids
- Observations of the 1863 Perseids
- Sporadic-E, Noctilucent clouds, aurorae, and meteors
- Fireballs and meteorites
- Video observational results

In case of non-delivery, return postage guaranteed. Please return to:
v.u.: Marc Gyssens, Heerbaan 74, B-2530 Boechout, Belgium

WGN, Vol. 21, No. 4, August 1993, pp. 143–218

Contents

Useful Information

The October Issue *(WGN 21:5)*

The *October issue* is expected to be a normal issue and will be mailed during the first or second week of October. Since the *IMC* partially interferes with the preparation of this issue, contributions are due early. The issue will primarily be devoted to the 1993 Perseids. Please prepare your reports on this shower immediately and send them still during August to *Marc Gyssens* (address on inside back cover). Authors of contributions not pertaining to the Perseids are advised that their contributions might be postponed to the December issue due to space considerations, for which we apologize.

WGN Subscription/IMO Membership 1993

The subscription rate for volume 21 (1993) is 25 DEM for six issues. Additional gifts are of course welcome. It is anticipated that volume 21 will contain over 260 pages.

From the Editor-in-Chief

Marc Gyssens

Most of you will receive this very thick issue of WGN *after the Perseid maximum is over. We hope you already supplied us with a summary of your findings as instructed in the previous issue, but please do also send us a more detailed report as soon as possible to help us provide everyone with an accurate account of what happened in the October issue.*

The next thing to look forward to now is the IMC *in Puimichel. As with previous* IMC*s it will provide an opportunity to meet your fellow meteor observers as well as provide a forum to make important decisions for meteor work during the upcoming years.*

Meanwhile, enjoy this issue!

Letters to WGN

compiled by Marc Gyssens

Changes in ionospherical radio emission caused by meteors

We received one more reaction on the article in the February issue (WGN 21:2, pp. 69-71) *by Andreić, Beg, and Korlević, reporting on a negative attempt to determine changes in ionospheric radio emission caused by meteors. The letter below is from Graham Wolf.*

It appears to me that what the authors were actually attempting, was a recording of electrophonic fireballs. As this is my specialist interest in meteoritics, and I have had some experience in this field, I hope the following comments and information may be of help to others who may be also considering making similar efforts.

The earliest known accounts of electrophonic sounds from fireballs, date back to Chinese observations of 817 AD [1,2], so the phenomena has been with us for a long time! V.A. Bronshten's catalogue of electrophonic sounds dates back to the mid 1500s [3]. Texas Engineering Professor J.A. Udden suggested as far back as 1917, that electrophonic sounds (where sounds appear to travel at the speed of light, under rather unusual physical circumstances) might just be electrical in origin [1,4].

Perhaps the ultimate electrophonic fireball is the United States' Space Shuttle! It has been observed by Americans to give off electrophonic sounds as it passes through the atmosphere at re-entry, below an altitude of some 40 km, above which any sounds are reflected off the ionosphere and back into space [5]. N. Kinzett [6] has remarked that the Space Shuttle re-enters the atmosphere at a velocity of some Mach 25 (nearly 8 km/s) and 122 km altitude, slowing to Mach 3.5 at 14 km altitude. The zenith angle of re-entry is rather mild: about 30° to the horizon, another requirement for the production of electrophonics [2]. G.S. Hawkins [7] suggested that it requires an object with a mass of at least 90 kg (sic) at meteor velocity, to produce a magnitude −12 glow, that is, a glow equal in brilliance to the Full Moon, and which would cast an appreciable shadow on the ground. McCrosky commented that most fireballs travel at velocities less than 25 km/s through the Earth's atmosphere [8]. Giving an extreme example, he pointed out that the famous Lost City fireball of 1970 in Oklahoma, had an end point velocity of 3.5 km/s at an altitude of 19.5 km, and dropped a meteorite weighing several kilograms [8].

Peter Lancaster Brown of the *BAA* reported in "Sky and Telescope" of the December 1965 fall over Barwell in England [9]. Brown remarked on several reports of electrophonic sounds, and in one case, horses in a nearby field bolted in panic, just a few seconds before the meteorite passed over [10] ... perhaps ultrasonic electrophonics were produced initially before the emission frequency dropped sufficiently for the human ear to detect. It appears that some animals such as cats, dogs, and horses, with much more accurate hearing, can perhaps detect electrophonic sounds better than humans.

R.W. Evans (Director of the *RASNZ* Aurora Section) has recently reported a case in New Zealand, where an observer's cat repeatedly became distressed and looked to the South whenever auroral activity was present [11]. Some people have reported hearing auroral "swishing" sounds, as I too have, on two separate occasions during an all-sky auroral "storm," which left strong shadows on the ground. These sounds took place, in my own instance, in 5 to 10 second "bursts" over a two hour period in the 1970s, when one of the strongest displays on record took place. However, in spite of all these observations, many professionals have long been skeptical of electrophonic sounds. In particular, W.F. Denning in 1915 [12] and C.C. Wylie [13] were rather strong in their condemnation of these sounds, applying the psychological illusion theory [1]. These criticisms flew in the face of rather veracious reports by numerous individuals who claimed that they first heard the electrophonic sound, then looked up and saw the fireball. I too, have recorded similar observations [2,14,15].

Many researchers have attempted to record electrophonic sounds, but until just a few years ago, all were unsuccessful. In particular, G.S. Hawkins spent several years in the 1950s trying to establish where in the electromagnetic spectrum these enigmatic sounds might reside [16,17,18]. Alas, the fireballs he studied, were well below the electrophonic threshold first postulated by Russian researcher I.S. Astopovich [19,20]. Historically, the first recording of electrophonic sounds were made by Japanese researchers Watanabe, Okada, and Suzuki from a −7 Perseid in August 1988 [21].

In the mid 1980s, in response to a "Sky and Telescope" request by Professor Colin S.L. Keay [5], I attempted to first record these sounds, using VLF and MF equipment set up at the R.F. Joyce Observatory at West Melton, near Christchurch, New Zealand [22].

To this end, 2000 turns of insulated copper wire helically wound around a 2 m long plastic drainpipe made the antenna, which was vertically oriented in free space with string, attached to four wooden poles. A simple 46 dB gain bipolar low noise transistor preamplifier (using a BC 548C device) running on 18 V DC, and having a frequency response of 30-30 kHz ±3 dB, was connected between the antenna and the penchart recorder, with a run of 50 m coaxial cabling to eliminate loudspeaker and antenna feedback from running into the system. The penchart recorder was preceded by a 50 W RMS stereo amplifier in cascade mode, that is, its left channel fed straight into its right channel for extra combined gain. The total gain was probably in excess of 120 dB. The AUX input of the stereo amplifier was used, as this matched the 10 000 Ω input and output impedances of the 46 dB preamp, that preceded it. Headphones provided aural monitoring of the detected signals.

Plenty of VLF whistlers were easily heard, and it was also possible to detect the impulse wave from a 105 mm caliber Howitzer being used by the Army at the local firing range just 2 km down the road from the Observatory [22].

No electrophonics were detected by this equipment during the period September 1985 to February 1986, as the device was not frequently switched on, and incidentally, no electrophonic fireballs appeared at all, during this time. In late 1986, at the same observatory, attempts were made with an HF radio telescope using a 1 km baseline that was half oriented North-South, and the other leg East-West in an "L" formation. A modified 0.1 μV sensitivity Communications Receiver was used as the "front end," and again the signals fed into the cascaded stereophonic amplifier, then the penchart recorder, which to save expensive recorder paper, was used only occasionally.

The main frequencies listened to were 1000 and 1044 kHz, the latter from a distant radio station in the AM broadcast band. The next step was to see if there could be any MF "enhancements" from electrophonic fireballs [23]. At $1^h22^m22^s$ UT on December 9, 1986, a magnitude −4 electrophonic fireball made a faint sound at the instant it passed over the Observatory, and was recorded on penchart paper. The fireball made a trail of 45° and lasted for 2 seconds. The voltage enhancement at 1044 kHz rose from an ambient level of 5 mV on the penchart paper to a high of about 75mV, and stayed there for about 5 seconds before decaying slowly over about 10 seconds back to ambient level.

The previous evening, a magnitude −7 fireball passed over the Observatory in a 150° track lasting nearly 10 seconds. The 50 W stereo amplifier was playing the 1044 kHz signal at a level of about 40 dBA with the volume wound full on. As the fireball passed overhead, an electrophonic sound was aurally heard outside, then about three seconds later, as it passed over Orion, an increasingly loud feedback shriek was heard, as the front end of the communications receiver went into saturation. The shriek rose to a crescendo of about 110 dBA and nearly blew out the high-powered loudspeakers. The shriek was also strongly doppler-shifted in pitch [23].

There appear to be several requirements for the production of electrophonic sounds from fireballs. Firstly, the fireball has to be of sufficient brightness... brighter than Full Moon will do nicely [2]. The entry has to be at a rather shallow angle, and the velocity relatively modest, usually below 20 km/s. Professor Keay has extensively reported on a New South Wales version that fell near Newcastle, Australia, in 1978 [18,19,20,24,25]. In other studies, Keay noted a strong correlation with cold dry months in North America [24], as I have also noted here in New Zealand [2,26].

There appear to have been several shortcomings in the efforts of Andreić and his Croatian team to record VLF emissions from bright meteors:

1. As Peter Brown of Canada has rightly pointed out, the maximum gain of a loop antenna is in the plane of the loop, so only horizontal meteors would have been detected at Croatia, if at all.
2. The overall gain of the detection system seems to be very low. Indeed, the diagram on page 70 of *WGN* 21:2 suggests that the gain of the system is only about 20 times the input voltage, when the detection signal itself is more likely to be in the vicinity of one microvolt, perhaps much less. A voltage gain of some 100 dB is really needed here for effective results. Peter Brown suggests that the Croatian device might detect whistlers, but I frankly have my doubts, as the preamplifier is just not sensitive enough. A cheap whistler detector, using a cascaded stereo amplifier and the antenna connected to the AUX socket can be made rather cheaply, as I have already described.

3. There were no electrophonic fireballs externally heard by the Croatian team. For VLF emissions to be produced into a VLF detector device, firstly an electrophonic sound has to be produced. This requires much brighter fireballs and more favorable physical conditions (still air, low humidity, low temperature, low velocity, deep penetration into the atmosphere, and low angle to the horizon) before this can happen. The meteors observed by Andreić and his team, were clearly too faint for this. Such events that produce electrophonic meteor sounds, are very rare, as Peter has stated at the end of the article, and I agree with him that many hours, perhaps in the thousands of hours, of observing would be required to successfully hear an electrophonic fireball.
4. Antenna and other circuit impedances (the electrical resistance that a circuit sees to a sinusoidal waveform) are not mentioned in the Croatian report. I suspect that the loop antenna used, has a very low RF impedance of only a few ohm and that input impedance of the preamplifier is of the order of 10 000 to 50 000 Ω at RF. Also, pencharts can have notoriously high impedances, depending on the design, of up to several million ohm, especially if a FET (Field Effect Transistor) "front end" is used. Mismatch of impedances means that much of the signal is absorbed by the system and not passed through to the next circuit stage. A mismatch of just 6:1, as can happen with a poorly installed TV antenna (300 Ω impedance into a 50 Ω coaxial cable) can result in as much as a 3/4 loss of signal, and in radio work, you need all the signal you can possibly extract! I have not heard an electrophonic fireball since December 1986 in over 1000 hours of observing meteors, and another 60 or so observed fireballs since. It may be cheaper and more appropriate to feed the detected signal into a tape recorder (in order to save on expensive penchart paper) and then when an electrophonic sound is successfully detected, it can be fed into the penchart recorder at varying speeds so that its waveform can be analyzed. This way, you also have a permanent record of the signal, which can be played over and over again at leisure.
5. A higher detection frequency might be more productive. Whistlers are more prevalent in the 5 kHz to 15 kHz range. Watanabe et al. got their successful electrophonics signal at a frequency of 27 kHz, so a detection frequency of 30 kHz to 50 kHz might be more appropriate here, certainly no more, and would mean that any whistlers about, were not accidentally detected.

I wish the Croatian team well in their efforts, and hope that my comments have been of constructive assistance to them, and to anyone else thinking of such a project. Certainly in electronics, a thousand dollar problem can be sometimes cured with a ten dollar solution, so goes the old proverb. There is no need to repeat other people's mistakes, when better methods have been attempted by some others. I am willing to write in answer to any interested persons with appropriate technical details to assist them, if they so wish.

[1] G.W. Wolf, in *Proceedings of the 1992 IMC*, Smolenice, pp. 86–91.
[2] G.W. Wolf, "New Zealand Observed Electrophonic Fireballs", unpublished paper, May 1992.
[3] J. Rendtel, *personal communications.*
[4] J.A. Udden, *Science* 46, 1917, pp. 616–617.
[5] C.S.L. Keay, *Sky and Telescope* 70, 1985, pp. 623–625.
[6] N. Kinzett, *Casmag*, August 1985, pp. 4–5.
[7] G.S. Hawkins, in *Meteors, Comets, and Meteorites*, McGraw-Hill Publishers, 1964.
[8] R.E. McCrosky, *Sky and Telescope*, March 1970, pp. 154-158.
[9] P.L. Brown, *Sky and Telescope*, November 1966, pp. 7–10.
[10] P.L. Brown, in *Comets, Meteorites, and Men*, Robert Hale and Company Publishers, 1973.
[11] R.W. Evans, *RASNZ Aurora Section Newsletter* 31, April 1993, p. 2.
[12] W.F. Denning, *J. Roy. Ast. Soc. Canada* 9, 1915, pp. 199–200.
[13] C.C. Wylie, *Popular Astronomy* 40, 1932, pp. 289–294.
[14] G.W. Wolf, in *Proceedings of the 1991 IMC*, Potsdam, pp. 67–71.
[15] G.W. Wolf, "Eyewitness Reports of Electrophonic Sounds from the 1985 Taieri Plains Fireball in New Zealand", *WGN* 20:6, December 1992, pp. 223–225.
[16] G.S. Hawkins, *Nature* 181, 1958, p. 1610.
[17] G.S. Hawkins, *Astroph. J.* 128, 1958, pp. 724–726.
[18] C.S.L. Keay, *Southern Stars* 31, 1984, pp. 11–16.
[19] C.S.L. Keay, *Science* 210, 1980, pp. 11–15.
[20] C.S.L. Keay, in *Proc. Asteroids, Comets, Meteors*, Flagstaff, Arizona, June 26, 1991.
[21] E. Budding, *personal communications*, 1991.
[22] G.W. Wolf, *Casmag*, December 1985, pp. 8–9.
[23] G.W. Wolf, *Casmag*, February 1987, pp. 10–11.
[24] C.S.L. Keay, *J. Roy. Ast. Soc. Canada* 74, 1980, pp. 253–260.
[25] C.S.L. Keay, *J. Roy. Ast. Soc. Canada* 84, 1990, pp. 373–382.
[26] G.W. Wolf, "Physical and Climatic Data for New Zealand Observed Electrophonic Fireballs", *WGN* 21:1, February 1993, pp. 44-46.

Graham Wolf, May 15, 1993

Fragmenting dusty meteoroids

In the previous issue (WGN 21:3, p. 81), *Dr. Duncan Steel asked for possible observations of fragmenting dusty meteoroids. The following reaction is from Malcolm Currie.*

In the last *WGN*, Duncan Steel asked whether or not clouds of meteoroids have been observed. During the 1970s, Sandy Allan of the *British Meteor Society* collated observations of *nebulous meteors*, commonly known as "shooting nebulae." There is a brief summary of his findings in [1]. There is even a photograph of an alleged nebulous meteor. I do not know if the full analysis ever appeared. The planned monograph *Peculiar Meteors* was shelved due to a lack of orders.

I myself saw several during well over 1000 hours of viewing as a visual observer at that time. So I should reckon my frequency was about one every 150–200 hours, though with more research examining the 20-odd thousand observations I could be more precise. Nebulous meteors tended to be faint, and although my limiting magnitude was faint, 6.7–6.8 being typical, such objects were only seen near the center of perception. Therefore I suspect that the true frequency is much higher. They might even be dismissed by some observers and not recorded. For me they looked like moving parts of the Milky Way, though some did have a nucleus, and one expanded as it traversed.

Given the number of visual observers in the *IMO* we could accumulate a large collection of such sightings so that we can derive meaningful statistics, and learn more about these peculiar meteors. However, to answer Duncan's question I think that we need optical aid to resolve the cloud, as a telescope resolves the Milky Way into stars. Therefore more telescopic and video observations are called for. (I have to admit that I have yet to recognize such a meteor during a telescopic watch.) If Duncan is correct, we shall need several telescopic sightings or one good video recording to convince the skeptics.

[1] R.A. Mackenzie, "Solar System Debris", British Meteor Society, Dover, 1980, pp. 60–61.

Malcolm Currie, July 28, 1993

The 1993 International Meteor Conference

Puimichel, France, September 23–26

Paul Roggemans

1. Update

As of the end of July, 1993 a total of 56 persons are expected to participate in the 1993 *IMC*. Each participant should have received the long *IMC* information letter (6 pages) by now. Please read the following lines which are relevant to the *IMC*:

- Presently, we are able to accommodate 4 to 6 additional people, but since we have to rent extra rooms to do this these people will have to pay an additional 200 FRF for the overnight accommodation during the *IMC*.
- In an effort to make your stay more comfortable and reduce the stress associated with travel to reach a deadline (September 23, the start of the *IMC*), it is possible to arrive any day before the start of the *IMC*. You may stay for 150 FRF per day full board in Puimichel before as well as after the *IMC*.
- The *IMC* will end with lunch on Sunday at Noon, September 26; this time may be too late for people who have to drive considerable distances by car. People traveling by train should be aware that special reduced fares generally do not allow travel on Sundays by train. For all of these people there is the possibility of staying until September 27 or longer at Puimichel.
- As was asked in the last information circular we now must have the more exact time of your arrival and departure for planning purposes.
- Be sure to bring money already converted to French Francs with you. Credit cards are not admissible in Puimichel and Eurocheques are too costly to cash in France.
- Lecturers should remember that the text of their oral or poster contribution should be brought with them for the Proceedings as at the last *IMC*.
- Finally, you are asked to bring a sleeping bag with you or at the very least some sheets as the stocks of these items are very limited at Puimichel.

Visual Observers' Notes: September–October 1993

Jeff Wood

1. Introduction

Following the excellent activity of the previous two months, observers tend to feel let down when rates return to normal during September and October. Because of this, nowhere near as much observational work has been carried out during this time even though there is much to see.

Table 1 gives a list of the active showers that occur in these months and Table 2 shows the observing conditions moon-wise. The illuminated part of the Moon is always given for 0^h UT on the date indicated. The dates of the phases of the Moon are also given in UT.

Table 1 – A list of meteor showers to be seen during September and October 1993.

Shower	Activity	Maximum		Radiant			Drift		V_∞	r	ZHR
		Date	$\lambda_\odot$	α	δ	Diam.	$\Delta\alpha$	$\Delta\delta$			
π-Eridanids	Aug 20–Sep 05	Aug 29	155°.7	52°	−15°	6°	+0°.8	+0°.2	59	2.8	
α-Aurigids	Aug 24–Sep 05	Sep 01	158°.6	84°	+42°	5°	+1°.1	0°.0	66	2.5	15
δ-Aurigids	Sep 05–Oct 09	Sep 10	166°.7	60°	+47°	5°	+1°.0	+0°.1	64	3.0	7
Piscids S	Aug 15–Oct 14	Sep 20	177°.7	8°	00°	8°	+0°.9	+0°.2	26	3.0	3
κ-Aquarids	Sep 08–Sep 30	Sep 21	178°.7	339°	−02°	5°	+1°.0	+0°.2	16	3.0	3
Capricornids (Oct)	Sep 20–Oct 14	Oct 02	189°.7	303°	−10°	5°	+0°.8	+0°.2	15	2.8	3
σ-Orionids	Sep 10–Oct 26	Oct 04	191°.7	86°	−03°	5°	+1°.2	0°.0	65	3.0	3
Draconids	Oct 06–Oct 10	Oct 10	197°.0	262°	+54°	5°			20	2.6	storm
ε-Geminids	Oct 14–Oct 27	Oct 20	206°.7	104°	+27°	5°	+1°.0	0°.0	71	3.0	5
Orionids	Oct 02–Nov 07	Oct 21	208°.4	95°	+16°	10°	+1°.2	+0°.1	66	2.9	25
Taurids S	Sep 15–Nov 25	Nov 03	220°.7	50°	+14°	10°/5°	Table 8		27	2.3	10
Taurids N	Sep 13–Nov 25	Nov 13	230°.7	60°	+23°	10°/5°	Table 8		29	2.3	8
Puppid/Velids	Sep 28–Jan 26	several		120°	−45°	10°			41	2.9	

Table 2 – Moonlight and observing conditions in September–October 1993.

Date	k	Date	k
Friday August 27	0.76+	Friday October 1	1.00−
Friday September 3	0.97−	Friday October 8	0.59−
Friday September 10	0.43−	Friday October 15	0.00−
Friday September 17	0.01+	Friday October 22	0.46+
Friday September 24	0.62+	Friday October 29	0.98+

New Moon:	September 16, October 15, November 13
First Quarter:	August 24, September 22, October 22
Full Moon:	September 1, September 30, October 30
Last Quarter:	September 9, October 8, November 7

For more details, we refer to the *IMO 1993 Meteor Shower Calendar*. Here we highlight some of the showers visible during September and October.

2. Southern Piscids

This weak ecliptic stream is active from August 15 through to October 14. Rates are generally one or two meteors per hour, but on occasions have passed 5 per hour around the maximum which occurs on September 20. With a Full Moon occurring on September 30, the Piscids can best be observed under dark sky conditions from the southern hemisphere during the periods September 8–26 and October 8–14. Observers should face the radiant area and plot all Southern Piscids seen taking care to distinguish them from the sporadic background. In particular, the angular velocity must be taken into account.

Table 3 – Radiant positions of the Southern Piscids.

Date	α	δ	Date	α	δ
Sep 15	0°	−02°	Sep 30	13°	+01°
Sep 20	4°	−01°	Oct 05	17°	+02°
Sep 25	9°	00°	Oct 15	26°	+04°

3. κ-Aquarids

This minor ecliptical stream has an activity period from September 8 to 30. It reaches a maximum ZHR of 3 on September 21. Since its period of activity and its radiant position is similar to that of the Southern Piscids, both showers can be observed simultaneously. In 1993, the Full Moon on September 30 means that the κ-Aquarids can be observed under dark sky conditions from September 8 to 26. Southern hemisphere observers should make their center of field of view somewhere around $\alpha = 345°$ to 0° and $\delta = -20°$ to $+20°$. All possible shower meteors should be plotted. Shower association should be carried out very carefully taking note of direction of travel, path length and appropriate angular velocity.

Table 4 – Radiant positions of the κ-Aquarids.

Date	α	δ	Date	α	δ
Sep 15	334°	−03°	Sep 25	344°	−01°
Sep 20	339°	−02°	Sep 30	349°	00°

4. δ-Aurigids

The radiant of this minor shower is well situated for observers in the northern hemisphere. The fast ($V_\infty = 64$ km/s) Perseid-like meteors are very striking and the ZHR reaches values of about 7 around September 10. But after more or less successful Perseid campaigns, most observers rest on their laurels at that time. That is why our knowledge of this shower is rather poor. With New Moon on September 16, the conditions to monitor its activity are very favorable in 1993. Observers in the northern hemisphere are called upon to pay special attention to this shower in their September observations. Except for the first two hours after dusk, the radiant is sufficiently high in the sky for useful observations with the best conditions in the morning when the radiant approaches the zenith of mid-northern latitudes. Therefore, the morning hours should be preferred for observations. Choose the center of your field of view at about 20° to 30° from the radiant.

Table 5 – Radiant positions of the δ-Aurigids.

Date	α	δ	Date	α	δ
Sep 01	51°	+46°	Sep 20	70°	+48°
Sep 10	60°	+47°			

5. October Capricornids

The October Capricornids were discovered in 1972 and provide variable activity from year to year. They are active from September 20 through to October 14 with an overall maximum on October 2, close to Full Moon.

Intending observers should ensure that they face the radiant position and plot all possible shower meteors. Care should be taken in identifying these meteors. At maximum the October Capricornid radiant is situated at $\alpha = 303°$ and $\delta = -10°$. Angular velocities are comparable to these of the κ-Aquarids.

6. Comet Findlay radiant

Observations during September and October have indicated that there is some evidence of meteor activity from the area of the predicted Comet Findlay radiant. Although there will be some interference from the Moon during mid October, southern hemisphere observers are requested to make observations of the Comet Findlay radiant a priority in 1993. Since they can be observed simultaneously with the October Capricornids, southern observers should endeavor to monitor both. To do this they should have a center of field of view situated around $\alpha = 285°$ and $\delta = -20°$, which is midway between both shower radiants. The Comet Findlay radiant should be monitored from September 20 through to October 20. The radiant area is from $\alpha = 260°$ to 280° and $\delta = -30°$ to $-42°$. All possible shower members should be plotted and great care should be taken in identifying any meteors coming from the radiant area as such. The angular velocity of meteors originating from the Comet Findlay radiant is comparable to these of the κ-Aquarids ($V_\infty \approx 15$ km/s).

7. σ-Orionids

This shower is active from September 10 through to October 26. Its maximum ZHR of 3 meteors per hour occurs on October 4 which means that the Moon interferes greatly with the strongest period of activity in 1993. The σ-Orionids have their radiant in the Belt of Orion and so after maximum great care needs to be taken to distinguish them from the October Orionids. This year, the *IMO* is particularly interested in the σ-Orionid activity profile for the periods September 10–27 and October 7–26 when the skies should be moon-free. Observers in both hemispheres should watch during the last few hours before sunrise and have a center of field situated no more than 30° west or northwest of the radiant. All possible shower members should be plotted.

Table 6 – Radiant positions of the σ-Orionids.

Date	α	δ	Date	α	δ
Sep 15	71°	−03°	Oct 15	93°	−03°
Sep 25	79°	−03°	Oct 25	101°	−03°
Oct 05	86°	−03°			

8. Orionids

This major shower has favorable Moon conditions in 1993 and is a must on the meteor observer's calendar. The Orionids have a complex radiant structure with the center of activity being located just north of the star Betelgeuse at maximum. The Orionids are associated with Comet Halley and, like the η-Aquarids, display a plateau-like maximum. This can vary from year to year but is generally from October 20 to 25. The Orionid maximum occurs on October 21 with a ZHR that is usually in the range of 20 to 30 meteors per hour. Orionids are best observed during the latter part of the night when the radiant altitude rises above 20°. They are observable in both hemispheres and all possible Orionid meteors should be plotted unless the ZHR exceeds 10. Thereafter, classified counts may be taken.

Table 7 – Radiant positions of the Orionids.

Date	α	δ	Date	α	δ
Oct 10	80°	+14°	Oct 25	98°	+15°
Oct 15	86°	+15°	Oct 30	104°	+16°
Oct 20	92°	+15°			

9. Draconids

The October Draconids reach a sharp predicted maximum at 10^h UT. The Draconids can only be seen from the northern hemisphere and provide extremely variable rates from the ZHR 0 to storm proportions. Situated at a radiant of $\alpha = 262°$ an $\delta = +54°$, the Draconids should be monitored from October 8 to 11 to see if there are any unusual outbursts of activity and to determine the structure of the stream. Intending observers should plot all stream members seen unless the ZHR rises above 10 when classified counts may be taken. They should have their center of field of view located no more than 40° from the radiant position. The diameter of the Draconid radiant is 5°. The geocentric velocity of the Draconids equals $V_\infty = 20$ km/s.

10. Taurids

This shower is broken up into several substreams, the most important of which are called the Northern and the Southern Taurids respectively. The Taurids have one of the longest periods of activity known and last from September 13 through to November 25. They reach a broad maximum in late October and early November. The maximum of November 3 (Southern Taurids) and November 13 (Northern Taurids) given in the radiant list were derived from radio meteor and photographic meteor orbital elements and not visual observations. The latter give an uncertain picture. At maximum, Taurid activity is often very erratic with rates ranging from 1–2 meteors per hour to as high as 10 or 15 meteors per hour.

In September and October, the Taurids are best observed during the middle and latter parts of the night. They are noted for their many fireballs. These are frequently yellow and orange in color, but all of the other colors are also well represented. This together with their relatively low geocentric velocity means that they can be recorded more easily on film than most other showers.

Since they have a great longevity of activity, the Taurids have parts of their activity period moon-free and others greatly affected by the Moon. They can be easily seen from both hemispheres. When observing the Taurids, all possible shower members should be plotted. In order to distinguish meteors from the both branches the center of field of view should be located between 20° and 40° east or west of the radiant at the same declination.

In September the most favorable center of field of view is around $\alpha = 0°$ and $\delta = +10°$ to $+15°$. This way, κ-Aquarid, Southern Piscid, Northern Taurid and Southern Taurid radiants can all be observed simultaneously. In October the most favorable field of view is located at $\alpha = 80°$ and $\delta = +20°$ which enables both the Taurid radiants together with the Orionid, σ-Orionid and the ε-Geminid radiant to be monitored at the same time. The *IMO* is particularly looking to obtain Taurid ZHR profiles and to investigate the population index during the 1993 Taurid watch.

Table 8 – Radiant positions of the Taurids.

Date	Taurids North		Taurids South	
	α	δ	α	δ
Sep 20	29°	+16°	25°	+10°
Sep 30	37°	+17°	29°	+10°
Oct 10	41°	+18°	36°	+10°
Oct 20	46°	+19°	41°	+11°
Oct 30	51°	+20°	48°	+13°

11. ε-Geminids

The ε-Geminid meteor shower is active from October 14 to 27 with a maximum of 5 meteors per hour on October 20. As with the Orionids, Moon conditions are favorable in 1993 and the shower is to be targeted for investigation by the *IMO*.

The ε-Geminids can be seen during the last few hours before sunrise in both hemispheres where they often produce fast blue or white trained meteors. The ε-Geminids have angular velocities similar to those of the Orionids. Given the closeness of the radiants great care needs to be taken in separating ε-Geminids from Orionids. All possible ε-Geminids should be plotted. Observers are advised to have their field located around $\alpha = 80°$–$90°$ and $\delta = +10° - +20°$.

Telescopic Observers' Notes, September–October 1993

Malcolm J. Currie

Following a quiet first half of 1993 with few data submitted, the main finding being confirmation of activity from the θ-Herculids on May 28–29, the latter half of the year looks full of promise for telescopic observers. Besides the excitement, if not fever, surrounding the Perseids, the remainder of the year should not be seen as an anticlimax. The lunar cycle favors all the major showers except the Ursids. So I hope that the recent interest telescopic meteors generated by the Perseids will propel a growing team of telescopic observers to more discoveries about faint meteors.

The gnomonic charts are in regular production now. They come in seven sets, each with a different field of view and limiting magnitude, to span the spectrum of instrumentation used by observers. At present each set comprises 164 field centers for investigation of the most prominent showers and to look for "new" ones. Should you wish to participate in the Telescopic Commission's program, please write to me giving details of your binocular or telescope (aperture, magnification, field of view) and which shower you wish to observe, and I shall send you the appropriate charts, and details of observational method if you are a new observer. Why do you not give telescopic observing a try?

Forthcoming events

Following the feast of August meteors, the post-prandial period is usually neglected. Yet September is one of the best months of the year for telescopic observers. "Wait a moment, that cannot be right. Where is the major shower?" I hear you ask. You are correct... there is none. So what is the reason? Faint-meteor activity is dominated by the sporadic background, except perhaps at the peak of a few showers, and during September sporadic rates are at their highest. Also in mid-northern latitudes the weather is often fine and the nights mild. Beside the sporadics, there are several fascinating minor showers in the Auriga-Perseus-Cassiopeia region that can grip one's attention as on a given night one never knows quite what to expect.

All these streams have high inclinations, and produce swift-moving ($v_\infty \approx 65$ km/s) meteors. At least one is believed to have substreams present; according to Gary Kronk's analysis [1] from radio and photographic data, the *δ-Aurigids* have at least four filaments. Recent visual observations [2] had suggested that this shower was of long duration, starting sometime in early September and lasting through most of October. However, using additional data and RADIANT for analysis, Jürgen Rendtel [3] concludes that the early activity is due to another lesser-known shower—the *September Perseids*—radiating from around $\alpha = 55°$ and $\delta = +46°$ in mid-September. On September 13, 1990, visual observations also found a distinct radiant at $\alpha = 72°$ and $\delta = +53°$, though not evident in 1991. Contrast this with telescopic observations at around the same time which probably show some September Perseids, but more interestingly a strong radiant at $\alpha = 43°$ and $\delta = +49°$ and another possible one 13° further west. Also during the first half of September, there are the *β-Cassiopeids* comprising very faint meteors. In 1971, Michael Groocock found a strong telescopic shower from a compact radiant at $\alpha = 31°$ and $\delta = +57°$ ($\lambda_\odot = 205°$) during mid-October that has since failed to come under the spotlight to my knowledge. So all in all we have a complex of radiants during September and October whose activity dates and radiant parameters are at best poorly determined and at worst unknown. Observations by all methods are badly needed over a number of years to describe the properties of these showers, and to investigate if any are interrelated. Telescopic observers should concentrate on accurate plotting using at least three field centers to reduce radiant occlusions. It should be possible to disentangle the substreams, even ones only a few degrees apart. Try to observe both in September and October's dark time. Since the radiants have a low elevation during the evenings, watches after midnight local time are particularly valuable.

Now I make my annual plea for observations of the *Piscids*. The high population index and low velocity suggests that this weak shower is suitable for telescopic work, yet only a few possible Piscids are recorded in the telescopic archives. This may be due to a genuine lack of small particles in the shower, or because of a lack of observations. It has a diffuse radiant which might conceal sub-components, but in the first instance I should like to know whether or not the shower is present at telescopic magnitudes. I would urge observers, especially those further south, to use the time before the Auriga-Perseus showers attain observable elevations to look for members of this shower in the dark skies that coincide with its visual maximum. Given a careful choice of field centers it is possible to look for *κ-Aquarids* simultaneously. Again this is a shower of which little is known. It too is expected to have a high proportion of faint meteors, and it has an extremely low velocity, which should help identify any κ-Aquarids from the sporadic background.

Moving to October, it is always worth checking the *Draconids* for enhanced activity. The moon is absent during the evening while the radiant has a high altitude. Previous enhanced activity has always been noted for the high proportion of faint meteors.

The *Orionid* shower is probably the most fascinating of the year because of its complicated radiant structure that can be resolved by telescopic plots. See [4,5] for details. Moonlight only interferes after October 22, so there is a chance to follow the fluctuating numbers from the different branches in the week before the textbook maximum—a period for which we have comparatively few data. Remember that the radiant does not attain a decent elevation until after midnight.

There are several minor showers during October. The *ε-Geminids* are synchronic with and resemble the Orionids. These very fast meteors were first seen by telescopic observations in Czechoslovakia [6] during the mid-1960s. The shower had an activity index one tenth of that of the Orionids, so it does require many observers to look on a given night to yield a sufficient total for analysis, something that has not happened in recent years.

The *Taurids* are active weakly during the whole of October. Although not rich in telescopic meteors, this is compensated by their low angular speeds and characteristic long paths. You can compare the radiant shapes of the shower's two components from telescopic observations with a small binocular. It is important to select field centers carefully taking into account the daily motion of the radiants. One arrangement is four fields: a pair to the east and another to the west of the radiants, and each pair comprises centers about 5°–10° north and south of the ecliptic.

References

[1] G.W. Kronk, "Meteor Showers: A Descriptive Catalogue", Enslow, 1988, pp. 185–188.

[2] J. Rendtel, "Radiants in the Per-Aur Region between August and October", in *Proceedings IMC*, Violau, 1990, pp. 37–41.

[3] J. Rendtel, "Radiants and Orbits of Delta Aurigids and September Perseids", in *Proceedings IMC*, Smolenice, 1992, pp. 67–73.

[4] M.J. Currie, "Telescopic Observers' Notes: Nov–Dec 1990", *WGN* 18:5, October 1990, pp. 180–182.

[5] R. Koschack, P. Roggemans, "The 1990 Orionids", *WGN* 19:4, August 1990, pp. 115–130.

[6] V. Znojil, "Frequency Occurrence of Small Particles in Meteor Showers II. Orionids, ε Geminids", *Bull. Astr. Inst. Czech.* 19, 1968, pp. 307–315.

Progress in Meteor Science

Articles in this section have been formally refereed by at least one professional and one experienced, knowledgeable amateur meteor worker, and deal with global analyses of meteor data, methods for meteor observing and data reduction, observations with professional equipment, or theoretical studies.

Global Analysis of the 1991 and 1992 Perseids

Ralf Koschack, Rainer Arlt, and Jürgen Rendtel

A detailed analysis of the 1991 and 1992 Perseids is given based on 45010 and 9701 Perseids respectively. The double maximum was observed in both years, the first peak being much higher than in previous years with ZHR $\approx$ 350. In 1991 the two maxima were observed at $\lambda_{\odot 1} = 139.^\circ580 \pm 0.^\circ005$ (eq. 2000.0) and $\lambda_{\odot 2} = 140.^\circ00 \pm 0.^\circ10$, and in 1992 at $\lambda_{\odot 1} = 139.^\circ50 \pm 0.^\circ04$ and $\lambda_{\odot 2} = 140.^\circ06 \pm 0.^\circ10$. A new method to derive comparable spatial number densities for unusually high activity was applied using meteors with magnitudes $m \leq 3.5$. This modified algorithm gave densities of $\rho(m \leq 3.5) = 63 \pm 5$ particles per 10^9 km^3 for 1991 and $\rho(m \leq 3.5) \approx 100 \pm 25$ particles per 10^9 km^3 for 1992.

1. Introduction

The Perseids have become one of the most interesting meteor showers recently, with the rediscovery of their parent comet, P/Swift-Tuttle, in 1992. Japanese observers recorded an unexpectedly strong pre-maximum peak in 1991 [1], and a similar outburst was observed in 1992 as well.

Here we attempt to analyze the shower displays from visual data. The 1991 event was well monitored with about 45 000 Perseids recorded by 268 observers whereas the maximum in the following year was heavily interfered with by the Full Moon. For 1992, the *Visual Meteor Data Base (VMDB)* of the *IMO* recorded some 9700 Perseids seen by 179 observers. The authors are grateful to all the amateurs which contributed to this comprehensive analysis.

As all the analyzing methods have been explained in detail in recent issues of this journal, please refer to [2] for the general determination of the spatial number densities and to [3] and [4] for modifications in the procedures which are also valid for this analysis. As usual, all solar longitudes mentioned refer to equinox 2000.0.

2. The 1991 Perseids

Observational data for the outburst period

The August period traditionally is the best covered observational season of the year. Below, we list the observers who have contributed to the analysis together with their *IMO* code and the effective time spent on Perseid watches.

Dinand Alkema (ALKDI, $2^h.17$), Peter Aneca (ANEPE, $12^h.02$), Georgi Antonov (ANVGE, $4^h.70$), Rainer Arlt (ARLRA, $37^h.28$), Mauro Bachini (BACMA, $1^h.78$), Paolo Bachini (BACPA, $2^h.58$), Robert Bacon (BACRO, $3^h.00$), Pierre Bader (BADPI, $12^h.93$), Kremena Baltova (BALKR, $15^h.44$), Sandro Baroni (BARSA, $4^h.50$), Marc Bastiaens (BASMA, $4^h.41$), Alessio Bechini (BECAL, $6^h.65$), Gary Becker (BECGA, $4^h.83$), Luis R. Bellot (BELLU, $39^h.05$), Lance Benner (BENLA, $4^h.16$), Paul Bensing (BENPA, $29^h.28$), Ragnar Bödefeld (BODRA, $36^h.94$), Peter Brown (BROPE, $18^h.27$), Marina Brozovic (BROMA, $22^h.13$), Elsy Bullaert (BULEL, $2^h.40$), Branko Burmaz (BURBR, $4^h.40$), Jon Butcher (BUTJO, $5^h.00$), Miguel Camarasa (CAMMI, $19^h.31$), Francisco Campos (CAMFR, $4^h.65$), Franco Canepari (CANFR, $7^h.25$), Oscar Cervera García (CEROS, $3^h.58$), Stephan Christopher (CHRST, $3^h.40$), Yang Chunping (CHUYA, $5^h.52$), Johan Claes (CLAJO, $2^h.82$), Koen Clement (CLEKO, $1^h.83$), Sabine Clement (CLESA, $3^h.17$), Peter Cornille (CORPE, $2^h.83$), Tim Couillard (COUTI, $1^h.88$), Haakon Dahle (DAHHA, $2^h.94$), Peter Dalakov (DALPE, $4^h.94$), Luigi D'Argliano (DARLU, $1^h.17$), Peter David (DAVPE, $1^h.60$), Mark Davis (DAVMA, $4^h.00$), Bart de Pontieu (DE BA, $11^h.82$), Marc Desruelles (DESMA, $3^h.25$), Rachel Devore (DEVRA, $1^h.00$), Vincent Devore (DEVVI, $0^h.86$), Jean Deweerdt (DEWJE, $10^h.93$), José Vicente Díaz Martinez (DIAJO, $19^h.94$), Atanas Dimitrov (DIMAT, $8^h.10$), Georg

Authors' addresses: R. Koschack, Hochwaldstr. 12 A131, D-02763 Zittau, Germany; R. Arlt, Berliner Str. 41, D-14467 Potsdam, Germany; J. Rendtel, Gontardstr. 11, D-14471 Potsdam, Germany.

WGN, the Journal of the International Meteor Organization, Vol. 21, No. 4, August 1993, pp. 152–167.

Dittié (DITGE, 2h63), Tommaso Dorigo (DORTO, 19h76), Kathrin Düber (DUBKA, 12h32), Kenneth Eakins (EAKKE, 6h00), Maurizio Eltri (ELTMA, 3h08), Jean-Baptiste Feldmann (FELJE, 4h50), David Barba Fernandez (FERDB, 1h08), Raul Fernandez (FERRA, 5h16), Eric Ford (FORER, 3h00), Massimo Forte (FORMA, 4h00), Yasunori Fujiwara (FUJYA, 1h75), Michael Funke (FUNMI, 6h12), Kai Gaarder (GAAKA, 10h50), Mario Gaitano (GAIMA, 8h63), John Gallagher (GALJO, 37h47), Ivanka Getsova (GETIV, 23h30), Stefano Giovanardi (GIOST, 6h63), George W. Gliba (GLIGE, 4h07), Daniel Glomski (GLODA, 3h12), Luc Gobin (GOBLU, 4h98), Victor Gonzalez (GONVI, 17h70), Roberto Gorelli (GORRO, 5h33), Valentin Grigore (GRIVA, 14h25), Andrey I. Grishchenyuk (GRIAI, 20h36), Guido Guidotti (GUIGU, 8h81), Marc Gyssens (GYSMA, 3h25), Robert Haas (HAARO, 8h76), Mark Hamilton (HAMMA, 2h91), Teemu Hankamäki (HANTE, 3h23), Torsten Hansen (HANTO, 7h02), Jung Han-Sub (HANJU, 1h43), Takema Hashimoto (HASTA, 5h76), Roberto Haver (HAVRO, 6h69), Robert Hays (HAYRO, 5h25), Lars Trygve Heen (HEELA, 15h48), Udo Henning (HENUD, 7h20), Gunar Hering (HERGU, 1h20), Katleen Hermans (HERKA, 2h25), Veerle Herrygers (HERVE, 2h06), Trond Erik Hillestad (HILTR, 4h36), Wolfgang Hinz (HINWO, 2h00), Sinichiro Isii (ISISI, 4h34), Daiyu Ito (ITODA, 0h95), Kiyoshi Izumi (IZUKI, 1h25), Katrin Jentzsch (JENKA, 10h97), Anne Jokinen (JOKAN, 4h77), Kurt Jonckheere (JONKU, 6h22), Adam Jones (JONAD, 4h65), C. Kaat (KAACH, 1h30), Dmitrij Karkach (KARDM, 17h00), Marko Kautto (KAUMA, 4h24), Junji Kawamura (KAWJU, 2h75), Norihito Kawamuro (KAWNO, 3h91), Tosio Kawimura (KAWTO, 8h35), Stephan Ker (KERSP, 39h86), Mark Kidger (KIDMA, 13h47), Timo Kinnunen (KINTI, 13h66), H. Kitano (KITHI, 3h00), André Knöfel (KNOAN, 34h69), Bernhard Koch (KOCBE, 4h55), Korado Korlević (KORKO, 7h70), Ralf Koschack (KOSRA, 44h02), Nobuyuki Kosiyama (KOSNO, 3h67), Andreas Krawietz (KRAAN, 12h70), Rhena Krawietz (KRARH, 8h37), Gotfred M. Kristensen (KRIGO, 15h85), Taiiti Kurosawa (KURTA, 3h33), Kristine Larsen (LARKR, 4h58), Alberto Latini (LATAL, 3h65), Jean-Christophe Lernould (LERJE, 3h18), Anna S. Levina (LEVAN, 20h10), Inge Leyssens (LEYIN, 0h83), Janet Lindemann (LINJA, 0h95), Massimo Lotti (LOTMA, 2h83), Peter Lozanov (LOZPE, 10h61), Vladimir Lukić (LUKVL, 8h34), Robert Lunsford (LUNRO, 21h75), Hartwig Luthen (LUTHA, 1h02), Ismo Luukkonen (LUUIS, 3h22), Massimo Macuccio (MACMA, 1h17), Veikko Mäkelä (MAKVE, 8h47), Katuhiko Mameta (MAMKA, 24h27), Krasimir Manov (MANKR, 19h86), Enrico Mariani (MAREN, 2h73), Francisco A. Marin (MARFR, 1h00), Manel Marin (MARMN, 3h09), Tony Markham (MARTO, 3h19), Yukihisa Matumoto (MATYU, 4h33), Guiseppe Mazza (MAZGI, 2h00), Alastair McBeath (MCBAL, 22h58), Javier Méndez Álvarez (MENJA, 1h43), Stanimir Metchev (METST, 8h33), Wouter Meuleman (MEUWO, 2h60), Milka Miletic (MILMI, 6h02), Svetoslav Mincov (MINSV, 8h25), Edmond Miroen (MIRED, 3h25), Koen Miskotte (MISKO, 18h04), Julia Miteva (MITJU, 8h05), Sirko Molau (MOLSI, 14h09), T. Morita (MORTO, 0h83), Dina Moro (MORDI, 2h00), Naomi Muto (MUTNA, 3h50), N. Nakajima (NAKNO, 2h66), Atanas Nikolov (NIKAT, 17h92), Mirko Nitschke (NITMI, 11h07), N. Nogami (NOGNA, 1h55), Kunio Nose (NOSKU, 2h08), Vesna Obradović (OBRVE, 7h46), Masayuki Oka (OKAMA, 2h40), Sharon O'Neill (ONESH, 1h97), Kazuhiro Osada (OSAKA, 2h00), Xavier Otazu (OTAXA, 0h79), Kostadin Petkov (PETKO, 17h47), Dragana Petkovic (PETDR, 6h80), Alan Pevec (PEVAL, 29h98), Alessandro Pieri (PIEAL, 8h58), Glenn Piper (PIPGL, 6h00), Dulce Plasencia (PLADU, 2h10), Ghislain Plesier (PLEGH, 18h29), Jose Fco Ponce (PONJE, 7h18), Lilia Porozhanova (PORLI, 7h20), Nenad Radakovic (RADNE, 3h17), Stefano Raffaelli (RAFST, 5h42), Leo Rajala (RAJLE, 10h43), Pia Rämä (RAMPI, 2h02), Ina Rendtel (RENIN, 42h95), Jürgen Rendtel (RENJU, 45h22), Francisco Reyes Andrés (REYFR, 15h96), Tomas Rezek (REZTO, 1h30), Daniel Rhone (RHODA, 5h00), Diane Rhone (RHODI, 0h92), Janko Richter (RICJA, 8h23), Bauke Rispens (RISBA, 22h29), Paul Roggemans (ROGPA, 42h80), Liu Ruixiang (RUILI, 2h67), Julian Ruiz Ortega (RUIJU, 3h75), Roope Ruotsalainen (RUORO, 3h88), Toru Sagayama (SAGTO, 5h10), Kotaro Sakuma (SAKKO, 7h82), Hiromi Sato (SATHI, 2h33), Tatuo Sato (SATTA, 7h42), Patric Scharff (SCHPA, 5h48), Mary Schmal (SCHMR, 0h95), Richard Schmude (SCHRI, 1h25), Thomas Schreyer (SCHTH, 13h77), Daan Schroyens (SCHDA, 3h37), Don Scott (SCODO, 2h51), René Scurbecq (SCURE, 5h86), Takashi Sekiguchi (SEKTA, 3h65), Oleg Semenov (SEMOL, 23h12), Gregory Shanos (SHAGR, 5h00), Yasuo Shiba (SIBYA, 5h94), Markku Sihvonen (SIHMA, 2h53), Godfrey Sill (SILGO, 5h66), Brian Simmons (SIMBR, 1h33), Karl Simmons (SIMKA, 4h30), Stephen Simmons (SIMST, 3h59), Wanda Simmons (SIMWA, 5h88), Wendy Simmons (SIMWE, 2h99), Torsten Simon (SIMTO, 5h37), Y. Sindo (SINYO, 6h00), Alexander Smetanko (SMEAE, 18h30), Doug Smith (SMIDO, 1h96), James N. Smith (SMIJN, 11h34), Bert Smits (SMIBE, 3h25), Ulrich Sperberg (SPEUL, 5h25), Snezana Stanimirovic (STASN, 5h13), Siegfried Stapf (STASI, 15h47), Plamen Stoichev (STOPL, 3h18), Enrico Stomeo (STOEN, 2h95), Stefan Ströbele (STRST, 4h24), Dmitryi Suchov (SUCDM, 23h06), David Swann (SWADA, 3h00), Richard Sweetsir (SWERI, 1h00), Richard Taibi (TAIRI, 12h91), A. Takagi (TAKAT, 1h00), Syouiti Tanaka (TANSY, 1h00), Ouyang Tianjing (TIAOU, 0h92), M. Toda (TODMA, 5h92), Stanimir Todorov (TODST, 5h49), Hiroyuki Tomioka (TOMHI, 0h98), Morten Tønnesen (TONMO, 2h70), Sebastia Torrell (TORSE, 5h86), Tuomas Törrönen (TORTU, 5h50), Josep M. Trigo Rodriguez (TRIJO, 39h94), Masayoshi Ueda (UEDMA, 0h58), Satosi Uehara (UEHSA, 4h62), Yoshiaki Uyama (UYAYO, 0h75), Erwin van Ballegoy (VANER, 10h97), Jacques Vandaele (VANJA, 1h78), Hendrik Vandenbruaene (VANHE, 6h08), Jan Vandenbruaene (VANJN, 6h17), Mireille Vanheerentals (VANMR, 4h20), Pierre van Mechelen (VANPI, 2h42), Jeroen van Wassenhove (VANJE, 11h81), Claudio Veliz (VELCL,

1^h.00), Valentin Velkov (VELVA, 14^h.18), Cis Verbeeck (VERCI, 7^h.17), Daniel Verde (VERDA, 17^h.25), Iliyan Vulchev (VULIL, 5^h.15), Frank Wächter (WACFR, 1^h.10), Sabine Wächter (MORSA, 18^h.59), Bruce Watson (WATBR, 4^h.75), Noel White (WHINO, 4^h.24), Vaya Willemen (WILVA, 2^h.25), Roland Winkler (WINRO, 15^h.89), Jean-Marc Wislez (WISJE, 6^h.42), Tracy Lynn Wit (WITTR, 1^h.38), Steffen Witzschel (WITST, 2^h.79), Zhou Xingming (XINZH, 4^h.75), Yasuo Yabu (YABYA, 20^h.50), S. Yanagi (YANSI, 5^h.50), Panayot Yanazov (YANPA, 7^h.12), Stanislav Žabić (ZABST, 5^h.11), Han Zhiyong (ZHIHA, 6^h.85), Danijela Živkovic (ZIVDA, 12^h.34), Michael Zschoche (ZSCMI, 2^h.25).

In order to analyze the rapid variations in activity during an outburst, summary reports giving meteor numbers for 1-hour intervals are not useful. To achieve maximal time resolution for the rates and the population index, both ZHR data and magnitude distributions for the shower should be reported for intervals of about 10 minutes duration. On special request, the following observers provided the data for the outburst period August 12, 1991, 15^h00^m–19^h00^m UT, in the required format and according to the *IMO* standards:

D. Karkach (KARDM), N. Kosiyama (KOSNO), A. Levina (LEVAN), A. Smetano (SMETA), Y. Yabu (YABYA)

These five observers were able to provide data for 10-minute intervals. The use of 1-hour intervals would result in high statistical weights being achieved , however, at the expense of a considerable *systematic* underestimation of the real peak activity as well since the outburst's peak activity lasts for much less than 1 hour. The analysis of the outburst period $\lambda_\odot = 139°.50$–$139°.70$ is based entirely on the data obtained by these observers.

The profile of the population index r

As shown in [2] and recent shower analyses [4,5], the population index r is the fundamental quantity needed to permit further analyses. The method used for the determination of the r-profile has been described in [2] and very recently in [4].

First, the r-profile of the "regular" activity period, excluding the outburst period, has been determined. All individual r-values have been computed from the magnitude distributions and finally the sliding average procedure, including outlier rejection, has been applied to obtain a profile (for details of the procedure, cfr. [2,4]).

For the pre-maximum period, $\lambda_\odot = 130°$ to $\lambda_\odot = 138°$, a sampling period of $2°.0$ width shifted by $1°.0$ was chosen. For the maximum period (excluding outburst data), $\lambda_\odot = 138°.0$–$141°.0$, a sampling period of $1°.0$ width shifted by $0°.5$ was possible, and for the post maximum period, $\lambda_\odot = 141°$–$146°$, the sampling period was $2°.0$ shifted by $1°.0$. The resulting profile is shown in Table 1 and Figures 1 and 2. There is a minimum of $r \approx 2.0$ around $\lambda_\odot = 135°$. After this, the population index increases to $r = 2.20$–2.25 around $\lambda_\odot = 136°$–$138°$. The core of the stream, between $\lambda_\odot = 139°.0$–$140°.3$, is characterized by a slight minimum of $r = 2.10$–2.15. After the maximum there is a steady increase of r.

In order to detect possible short-term time variations in the population index during the outburst, magnitude distributions for intervals of about 40 minutes were used. For each of these magnitude distributions, the population index was computed. For this computation, only those magnitude classes at least 3 magnitudes brighter than the limiting magnitude were used. The reason for this restriction is discussed in the paragraph on spatial number densities. We attempted to obtain an r-profile of the outburst period, but there was no significant variation in r over this period. The average $r = 2.15$ for the outburst does not significantly differ from the values before and after (see Table 1 and Figure 2). *This means the mass distribution of the filament which caused the outburst does not differ from that of the "regular core" of the stream.*

This finding is in contradiction to observers' reports (e.g., [1]) of an increase in the number of bright meteors. We must remember that when the activity increases significantly, such as during an outburst, and the population index remains constant, the number of bright meteors increases, but the ratio of faint meteors to bright meteors stays the same. It is not possible to conclude from a reported increase in bright meteors that a decrease in the population index or mass distribution index has also occurred. Qualitative reports do not help in reliably evaluating these quantities. The analysis of the magnitude distributions is necessary.

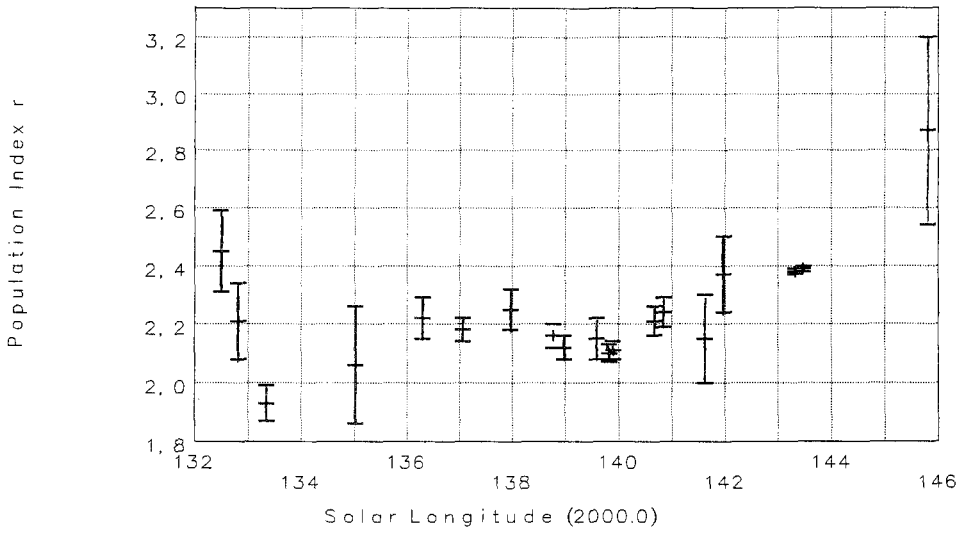

Figure 1 – The r-profile of the 1991 Perseids. The error bars correspond to the 67% confidence interval.

Table 1 – Profile of the population index r for the 1991 Perseids derived from the magnitude distributions of the observers listed in the Introduction.

$\lambda_\odot$ (2000.0)	Date (UT)	r	Per	$\overline{\text{lm}}$
132.49	Aug 05.2	2.45 ± 0.14	235	6.40
132.81	Aug 05.5	2.21 ± 0.13	337	6.62
133.34	Aug 06.0	1.93 ± 0.06	192	6.83
135.02	Aug 06.8	2.06 ± 0.20	259	6.61
136.30	Aug 09.1	2.22 ± 0.07	912	6.43
137.06	Aug 10.0	2.18 ± 0.04	1035	6.46
137.96	Aug 10.9	2.25 ± 0.07	567	6.50
138.78	Aug 11.7	2.16 ± 0.04	2807	6.53
138.97	Aug 12.0	2.12 ± 0.04	2703	6.47
139.59	Aug 12.6	2.15 ± 0.07	989	5.72
139.82	Aug 12.8	2.10 ± 0.03	11157	6.24
139.90	Aug 12.9	2.11 ± 0.03	11738	6.21
140.67	Aug 13.7	2.21 ± 0.05	3496	5.97
140.84	Aug 13.8	2.24 ± 0.05	2579	5.96
141.62	Aug 14.6	2.15 ± 0.15	406	6.19
141.97	Aug 15.1	2.37 ± 0.13	547	6.30
143.32	Aug 16.4	2.38 ± 0.01	178	6.22
143.47	Aug 16.6	2.39 ± 0.01	146	6.15
145.80	Aug 19.0	2.87 ± 0.33	91	6.05

The ZHR-profile

Firstly, all individual ZHRs meeting the following criteria were computed:

1. The limiting magnitude must be better than 5.0;
2. The radiant elevation must be at least 20°;
3. The correction factor for field obstruction F must be smaller than 1.2; and
4. The total correction factor $C_{\text{lm}} \times F \times C_z$ must be smaller than 5.0 (C_{lm} being the correction factor for limiting magnitude and C_z being the zenith correction factor).

In this way, only observations carried out under good circumstances have been used for further analysis. For the outburst period, ZHRs were computed for intervals of about 20 minutes.

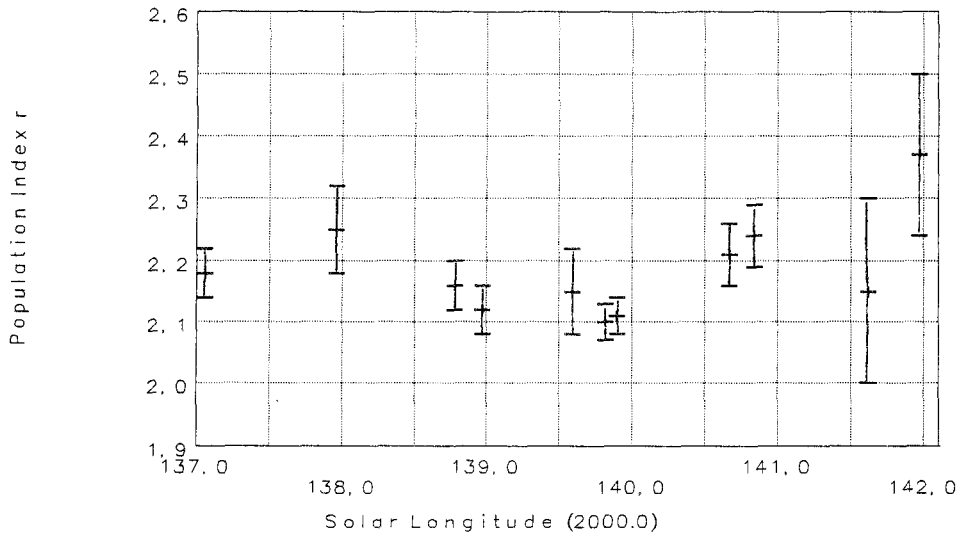

Figure 2 – The r-profile of the 1991 Perseids. Details of Figure 1 for the maximum.

To compute the relative perceptions of the individual observers according to [3,6], the periods shown in Table 2 have been chosen. Problems with this method have been discussed in [4]. All individual ZHRs have been recomputed using these perceptions. For some observers, it was not possible to compute the perception coefficients due to a lack of data during the intervals of Table 2. Their ZHRs were not perception-corrected.

Table 2 – Intervals for computation of observers' perception

$\lambda_\odot$	Sampling interval	Shift
130°–137°	3°	1°.5
139°.7–140°.0	0°.5	0°.25
140°.4–141°.0	0°.5	0°.25

To obtain a ZHR profile, the sliding average procedure with outlier rejection [4] was applied. The data of the sampling periods can be found in Table 3. For the period between $\lambda_\odot = 139°.5$ and $\lambda_\odot = 139°.7$, only the data obtained by the selected five observers were used.

Table 3 – Intervals of the sliding average procedure for computation of the ZHR profile.

$\lambda_\odot$	Sampling interval	Shift
110°–137°	2°.0	1°.0
137°–139°.5	0°.3	0°.15
139°.50–139°.59	0°.01	0°.005
139°.59–139°.70	0°.02	0°.01
139°.7–140°.0	0°.08	0°.04
140°.0–142°.0	0°.2	0°.1
142°–146°	1°.0	0°.5
146°–153°	2°.0	1°.0

The resulting ZHR profile is shown in Figures 3, 4, and 5; numeric data can be found in Table 4. In Figure 4, the double maximum is obvious. The second ("regular") maximum occurred at $\lambda_\odot = 140°.0 \pm 0°.1$ with ZHR ≈ 120 exactly at the same solar longitude as in 1989 [3]. The peak of the outburst is reached at $\lambda_\odot = 139°.580 \pm 0°.005$ with ZHR ≈ 350. The full width at half maximum (FWHM) of the outburst is $\Delta\lambda_\odot = 0°.06$ or 1.4 hours.

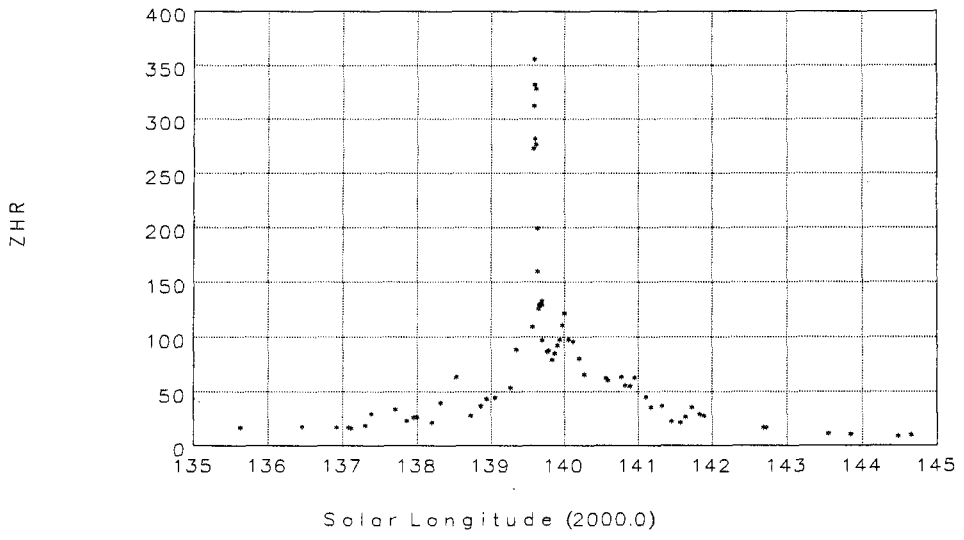

Figure 3 – ZHR-profile of the 1991 Perseids. For the error margins, we refer the reader to Table 4. Error bars were left out for reasons of clarity.

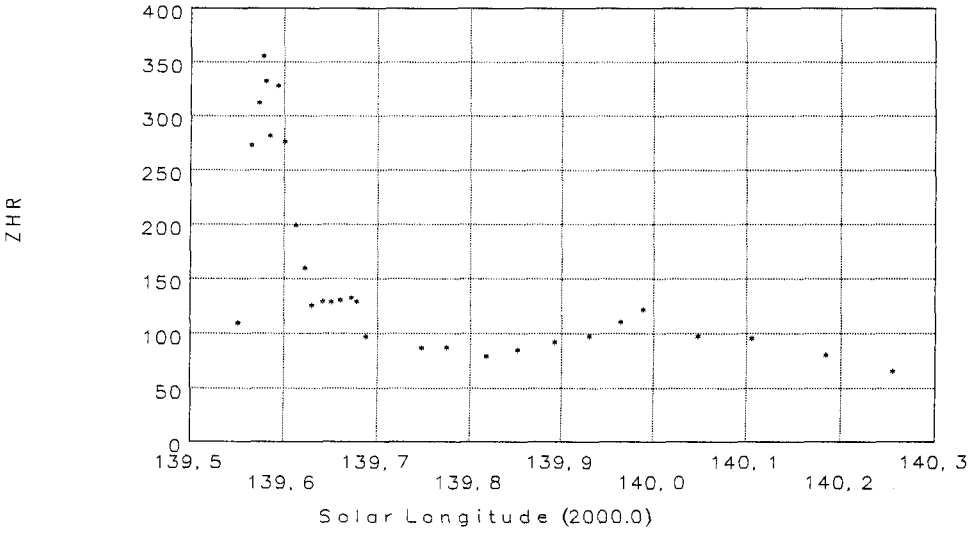

Figure 4 – ZHR-profile of the 1991 Perseids at times near the two peaks.

Spatial number densities

The conversion of the observed ZHR into the spatial number density is based on the perception probabilities of visual observers determined for "normal" activity [2]. If the activity (i.e., the visible meteor rate) becomes very high, a larger portion of faint meteors will be missed, i.e., the perception probabilities particularly for faint meteors decrease. Using the higher "standard" perception probabilities for the conversion of the ZHR into spatial number densities would result in number densities which are too small. In [7], it was shown that the effect starts to become significant for ZHRs of 120–150 onwards. With a maximum ZHR of about 350, the effect is expected to be considerable.

In [7], a method for obtaining number densities of very high activity from visual observations was proposed. It is reasonable to assume that the perception probabilities of brighter meteors are much less affected than those of fainter meteors. The magnitude distributions for the outburst period confirm this assumption. It is obvious that the magnitude classes fainter than magnitude +3 are heavily affected. Therefore it is appropriate to use only the brighter meteors for the analysis, for the case of the outburst under study those of magnitude +3 and brighter.

In the standard conversion procedure from ZHR to spatial number density, the true ZHR of meteors brighter than magnitude 6.5, $\mathrm{ZHR}_{\mathrm{true}}(m \leq 6.5)$, is an intermediate product of the

calculation. In this variation of that procedure, we have to calculate the true ZHR of meteors of magnitude class +3 or brighter, $\mathrm{ZHR}_{\mathrm{true}}(m \leq 3.5)$ for the outburst period. (Note that the magnitude class +3 consists of the meteors of magnitude +2.5 and +3.5). We achieve this result using the magnitude distributions given for short intervals. The observed meteor numbers for each magnitude class m, $n(m)$, is converted to the true number of meteors for this magnitude class $\varphi(m)$ by using the corresponding perception probabilities $p(\mathrm{lm} - m)$ given in [2]:

$$\varphi(m) = \frac{n(m)}{p(\mathrm{lm} - m)}.$$

The quantity $\varphi(m)$ refers to the effective field of a visual observer of 52°.5 radius [2]. The true cumulative number of meteors brighter than magnitude +3.5, $\Phi(+3)$, results from

$$\Phi(+3) = \sum_{m=-\infty}^{+3} \varphi(m).$$

Finally we find

$$\mathrm{ZHR}_{\mathrm{true}}(m \leq 3.5) = \frac{F \times C_z}{T_{\mathrm{eff}}} \Phi(+3).$$

The spatial number density of meteors brighter than +3.5 absolute magnitude, $\rho(m \leq 3.5)$, results from

$$\rho(m \leq 3.5) = \frac{\mathrm{ZHR}_{\mathrm{true}}(m \leq 3.5)}{A_{red} \times 3600 \times v_\infty} \qquad (*)$$

with $A_{\mathrm{red}} = 37\,200\mathrm{km}^2 \times (r - 1.3)^{-0.748}$ (cfr. [2], especially the erratum note on p. 118).

To this point, we have explained the theory behind the method. In practice, one problem encountered is that the magnitude distributions may be affected by systematic errors such as preference for certain magnitude classes. To reduce the influence of such errors, the following procedure has been applied.

The true cumulative number of meteors increases exponentially with the magnitude:

$$\Phi(m) = C \times r^m.$$

For each magnitude distribution, the parameters r and C were determined by linear regression:

$$\log \Phi(m) = m \times \log r + \log C.$$

The regression interval was chosen as follows:

- *brightest magnitude class* m_{max}*:* first magnitude class with $\Phi(m) \geq 3$; and
- *faintest magnitude class* m_{min}*:* faintest magnitude class taken into consideration for this analysis, i.e., $m_{\mathrm{min}} = +3$.

For the computation of $\mathrm{ZHR}_{\mathrm{true}}(m \leq 3.5)$, the raw observed value of $\Phi(+3)$ was not used, but rather the value for $Phi(+3)$ resulting from the regression.

To analyze the outburst period $\lambda_\odot = 139°.5$–$139°.7$ with this method, exactly the same data was used as for the ZHR analysis but split into intervals of about 20 minutes duration. For each interval, the value of $\mathrm{ZHR}_{\mathrm{true}}(m \leq 3.5)$ was computed. To obtain a profile, the same sliding average procedure using the same parameters (cfr. Table 3) as for the ZHR profile was applied. The resulting profile of $\mathrm{ZHR}_{\mathrm{true}}(m \leq 3.5)$ is shown in Figure 5. Then $\rho(m \leq 3.5)$ was computed according to equation (*) for each point of the profile.

The value of $\rho(m \leq 6.5)$ based on the ZHR was computed according to [2] for the whole activity period. The limiting magnitude offset $\Delta\mathrm{lm}$ of the standard observers was $\Delta\mathrm{lm} = +0.168 \pm 0.033$. To compare the results of the standard method based on the ZHR and the method based on the value of $\mathrm{ZHR}_{\mathrm{true}}(m \leq 3.5)$ for the outburst period $\lambda_\odot = 139°.5$–$139°.7$, the value of $\rho(m \leq 6.5)$ resulting from the former method was converted to $\rho(m \leq 3.5)$ with the following formula:

$$\rho(m \leq 3.5) = \rho(m \leq 6.5) \times r^{3.5-6.5}.$$

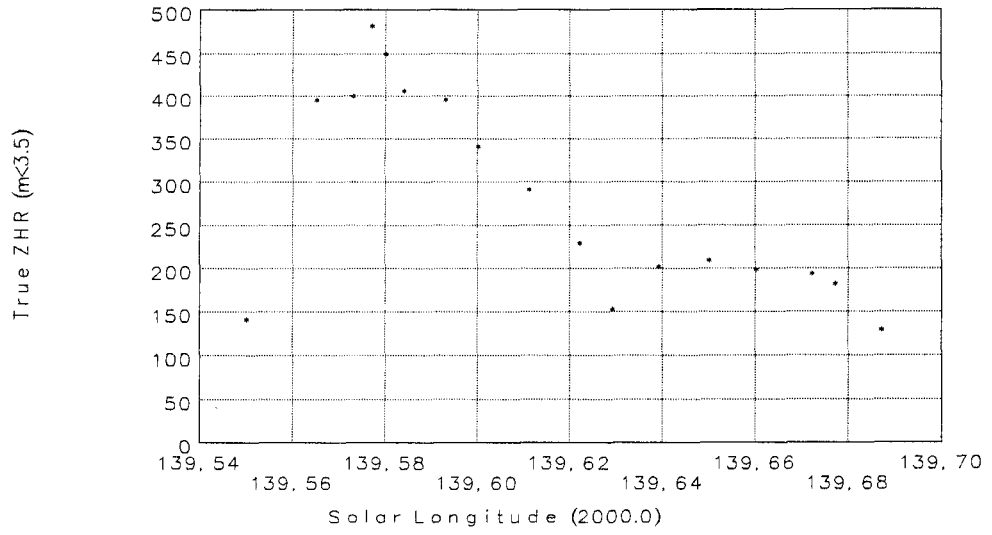

Figure 5 – True ZHR of meteors brighter than +3.5, $\mathrm{ZHR}_{\mathrm{true}}(m \leq 3.5)$, for the outburst period.

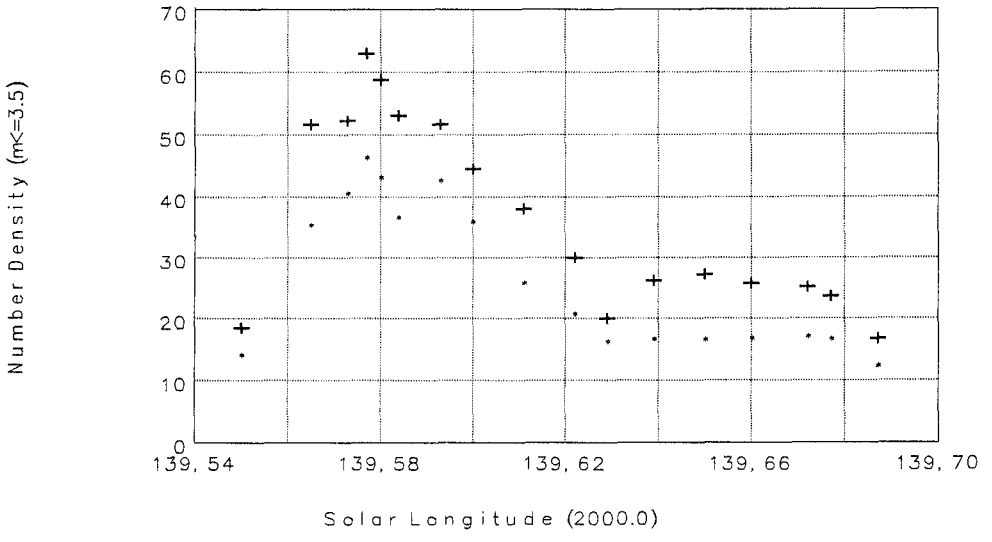

Figure 6 – Spatial number density (particles per 10^9 km^3) of meteoroids producing meteors of magnitude at least +3.5 absolute magnitude, $\rho(m \leq 3.5)$. The results based on the ZHR obtained in the standard way are plotted as dots; the results based on the value of $\mathrm{ZHR}_{\mathrm{true}}(m \leq 3.5)$ are plotted as crosses.

The values of $\rho(m \leq 3.5)$ resulting from both methods are plotted in Figure 6. It can be seen that particularly for the period of the highest activity the values based on the ZHR in the standard way are considerably smaller than those based on the value of $\mathrm{ZHR}_{\mathrm{true}}(m \leq 3.5)$. This difference is due to the effect described at the beginning of this paragraph and demonstrates the applicability of the method described here for the analysis of outburst-like activity.

In the following tables and diagrams all results of the outburst period $\lambda_\odot = 139°.5–139°.7$ are based on the value of $\mathrm{ZHR}_{\mathrm{true}}(m \leq 3.5)$. To complete the profile of $\rho(m \leq 6.5)$ for the outburst period, the values of $\rho(m \leq 3.5)$ for this period were converted into $\rho(m \leq 6.5)$ by

$$\rho(m \leq 6.5) = \rho(m \leq 3.5) \times r^{6.5-3.5}.$$

This conversion is not very reliable as the magnitude range 3.5–6.5 was not analyzed for the outburst period. Hence, the values of $\rho(m \leq 6.5)$ for the period $\lambda_\odot = 139°.5–139°.7$ in Table 4 should be treated with caution.

On the other hand, conversion of $\rho(m \leq 6.5)$ based on the ZHR in the standard way into $\rho(m \leq 3.5)$ is correct since the ZHR does indeed take the corresponding magnitude range into consideration.

Figures 7 and 8 show the double maximum of the 1991 Perseids in terms of the spatial number densities $\rho(m \leq 6.5)$ and $\rho(m \leq 3.5)$. The latter shows a maximum of $\rho(m \leq 3.5) = 63 \pm 5$ particles per 10^9 km^3. Since the population index does not vary significantly during the maximum period the shape of the number density profiles of different magnitude ranges is almost identical.

The numeric data for the whole activity period of the 1991 Perseid meteor stream can be found below in Table 4.

Table 4 – Numeric data for the 1991 Perseid activity period. All error margins correspond to the 67% confidence interval. In this table, s is the mass index, $\rho_{6.5}$ the number density (particles per 10^9 km^3) for meteors brighter than +6.5, and $\rho_{0.4}$ the number density of particles of at least 1 mg. The relations between these quantities are described in [2]. Note that for the outburst period $\lambda_\odot = 139°.5$–$139°.7$ the spatial number densities are not based on the corresponding ZHR values found in this table.

$\lambda_\odot$ (2000.0)	r	s	Interv.	Per	$\overline{\text{lm}}$	ZHR	$\rho_{6.5}$	$\rho_{0.4}$
113.84	2.19 ± 0.39	1.78	3	3	5.70	1.4 ± 1.0	2.2 ± 2.6	0.2
114.54	2.19 ± 0.39	1.78	7	7	6.10	1.3 ± 0.8	2.1 ± 2.1	0.2
115.39	2.19 ± 0.39	1.78	6	5	6.29	1.5 ± 1.2	2.4 ± 2.7	0.2
116.83	2.19 ± 0.39	1.78	6	7	6.26	2.1 ± 0.6	3.4 ± 2.8	0.3
117.50	2.19 ± 0.39	1.78	11	25	6.19	3.1 ± 0.7	4.9 ± 4.2	0.4
118.16	2.19 ± 0.39	1.78	8	20	6.15	2.8 ± 0.9	4.5 ± 3.9	0.4
119.25	2.19 ± 0.39	1.78	4	10	6.54	1.9 ± 0.7	3.0 ± 2.5	0.3
119.67	2.19 ± 0.39	1.78	2	8	6.78	2.6 ± 0.2	4.2 ± 3.0	0.4
120.69	2.19 ± 0.39	1.78	1	0	5.25	0.0 ± 0.0	0.0 ± 0.0	0.0
123.58	2.19 ± 0.39	1.78	1	2	5.00	7.2 ± 0.0	11.5 ± 11.7	1.0
124.19	2.19 ± 0.39	1.78	2	3	5.00	4.3 ± 4.3	6.9 ± 9.8	0.6
125.14	2.19 ± 0.39	1.78	2	2	5.15	2.9 ± 0.1	4.6 ± 4.6	0.4
125.48	2.19 ± 0.39	1.78	1	1	5.40	3.8 ± 0.0	6.1 ± 5.8	0.5
129.20	2.19 ± 0.39	1.78	4	12	6.63	5.1 ± 1.1	8.1 ± 6.2	0.7
129.87	2.19 ± 0.39	1.78	15	74	6.51	7.2 ± 0.9	11.5 ± 8.8	1.0
130.51	2.21 ± 0.38	1.79	18	118	6.39	9.6 ± 1.0	15.9 ± 11.9	1.4
132.04	2.37 ± 0.22	1.86	33	188	6.33	9.3 ± 0.8	20.6 ± 8.2	1.4
132.76	2.16 ± 0.12	1.77	59	484	6.49	10.3 ± 0.5	15.5 ± 4.2	1.4
133.64	2.01 ± 0.10	1.70	72	682	6.42	11.6 ± 0.5	12.4 ± 3.4	1.5
134.59	2.02 ± 0.15	1.70	86	792	6.28	13.7 ± 0.7	15.1 ± 5.9	1.7
135.62	2.14 ± 0.13	1.76	114	1387	6.34	17.5 ± 0.6	25.2 ± 7.6	2.4
136.44	2.19 ± 0.07	1.78	132	1589	6.30	18.1 ± 0.5	28.9 ± 5.5	2.6
136.90	2.19 ± 0.04	1.78	66	666	6.22	17.2 ± 0.8	27.4 ± 4.3	2.5
137.06	2.18 ± 0.04	1.78	28	395	6.18	17.2 ± 1.7	26.9 ± 4.8	2.4
137.09	2.18 ± 0.04	1.78	34	444	6.22	16.6 ± 1.4	26.0 ± 4.4	2.4
137.28	2.19 ± 0.05	1.78	11	152	6.36	19.3 ± 2.5	30.8 ± 6.3	2.8
137.37	2.19 ± 0.05	1.78	6	137	6.37	30.6 ± 8.1	48.8 ± 15.1	4.4
137.69	2.20 ± 0.06	1.79	3	34	5.74	34.2 ± 16.5	55.6 ± 28.7	4.9
137.84	2.21 ± 0.06	1.79	27	363	6.39	24.1 ± 2.5	40.0 ± 8.0	3.5
137.94	2.25 ± 0.09	1.81	78	1731	6.37	27.1 ± 1.1	48.5 ± 10.3	4.0
137.98	2.27 ± 0.10	1.82	64	1560	6.35	27.2 ± 1.2	50.5 ± 11.4	4.1
138.18	2.29 ± 0.11	1.83	18	280	6.13	22.2 ± 2.8	42.8 ± 11.7	3.3
138.30	2.26 ± 0.10	1.81	16	387	5.96	40.2 ± 9.0	73.3 ± 23.9	6.0
138.51	2.23 ± 0.08	1.80	15	381	6.08	64.1 ± 10.0	110.5 ± 28.4	9.4
138.71	2.17 ± 0.05	1.77	34	362	6.11	28.7 ± 2.5	44.0 ± 8.1	4.1
138.85	2.14 ± 0.04	1.76	105	2383	6.28	37.6 ± 1.6	54.1 ± 8.4	5.2
138.93	2.13 ± 0.04	1.76	127	4136	6.38	44.1 ± 1.4	62.2 ± 9.5	6.1
139.04	2.12 ± 0.04	1.75	66	2322	6.34	44.8 ± 2.3	61.8 ± 9.8	6.1
139.25	2.11 ± 0.04	1.75	32	1064	6.07	54.3 ± 7.1	73.3 ± 14.8	7.4
139.33	2.11 ± 0.03	1.75	16	784	6.09	88.9 ± 14.5	120.1 ± 25.8	12.0

Table 4 – (continued).

$\lambda_\odot$ (2000.0)	r	s	Interv.	Per	$\overline{\text{Im}}$	ZHR	$\rho_{6.5}$	$\rho_{0.4}$
139.53	2.11 ± 0.03	1.75	1	64	6.50	118.3 ± 0.0	159.8 ± 21.9	16.0
139.55	2.15 ± 0.07	1.76	3	46	5.82	109.8 ± 6.6	183.4 ± 41.4	17.4
139.57	2.15 ± 0.07	1.76	5	191	5.73	273.3 ± 24.3	511.9 ± 118.3	48.5
139.57	2.15 ± 0.07	1.76	5	224	5.73	312.5 ± 33.5	517.9 ± 123.3	49.0
139.58	2.15 ± 0.07	1.76	3	163	6.13	356.3 ± 28.2	624.1 ± 138.5	59.1
139.58	2.15 ± 0.07	1.76	5	224	5.89	332.5 ± 25.2	582.7 ± 124.6	55.2
139.58	2.15 ± 0.07	1.76	2	61	5.55	282.2 ± 23.0	526.6 ± 111.7	49.9
139.59	2.15 ± 0.07	1.76	5	231	5.88	328.4 ± 64.1	512.3 ± 148.6	48.5
139.60	2.15 ± 0.07	1.76	10	398	5.88	277.0 ± 36.1	441.9 ± 105.5	41.8
139.61	2.15 ± 0.07	1.76	8	224	5.98	199.5 ± 9.1	377.0 ± 77.5	35.7
139.62	2.15 ± 0.07	1.76	10	235	5.78	160.2 ± 13.9	297.3 ± 69.9	28.2
139.63	2.15 ± 0.07	1.76	4	90	5.67	126.0 ± 12.6	198.6 ± 41.5	18.8
139.64	2.14 ± 0.06	1.76	7	155	5.84	129.9 ± 7.6	256.7 ± 50.9	24.7
139.65	2.14 ± 0.06	1.76	7	174	5.88	129.1 ± 4.2	266.6 ± 51.3	25.6
139.66	2.14 ± 0.06	1.76	4	101	5.90	130.7 ± 6.9	252.1 ± 51.1	24.2
139.67	2.14 ± 0.06	1.76	4	135	5.95	133.4 ± 12.0	246.3 ± 49.5	23.7
139.68	2.14 ± 0.06	1.76	4	132	5.95	129.5 ± 14.4	231.2 ± 51.7	22.2
139.69	2.13 ± 0.05	1.76	1	20	5.50	97.3 ± 0.0	161.6 ± 28.1	15.8
139.75	2.10 ± 0.03	1.74	22	1006	6.48	87.6 ± 3.9	115.7 ± 16.7	11.8
139.77	2.10 ± 0.03	1.74	46	2228	6.45	87.8 ± 2.6	116.0 ± 16.3	11.8
139.82	2.10 ± 0.03	1.74	74	3579	6.31	79.6 ± 2.8	105.2 ± 15.0	10.7
139.85	2.11 ± 0.03	1.75	95	5292	6.31	85.8 ± 2.1	115.9 ± 16.3	11.6
139.89	2.11 ± 0.03	1.75	90	5877	6.33	92.4 ± 2.1	124.8 ± 17.5	12.5
139.93	2.11 ± 0.03	1.75	81	6313	6.35	97.8 ± 2.7	132.1 ± 18.6	13.3
139.96	2.12 ± 0.03	1.75	53	4439	6.30	110.7 ± 4.4	152.8 ± 22.0	15.1
139.99	2.12 ± 0.03	1.75	17	1311	6.22	121.9 ± 7.8	168.2 ± 25.8	16.6
140.05	2.13 ± 0.03	1.76	18	1359	6.26	97.8 ± 6.3	137.9 ± 21.1	13.4
140.11	2.13 ± 0.03	1.76	39	2107	6.14	96.0 ± 4.9	135.3 ± 20.1	13.2
140.18	2.15 ± 0.04	1.76	31	1172	5.97	81.2 ± 6.0	119.4 ± 20.2	11.3
140.25	2.15 ± 0.04	1.76	11	501	6.12	66.0 ± 6.2	97.0 ± 17.3	9.2
140.55	2.19 ± 0.05	1.78	15	375	6.11	62.9 ± 4.4	100.3 ± 17.7	9.0
140.58	2.20 ± 0.05	1.79	19	493	6.11	60.7 ± 4.0	98.7 ± 17.3	8.7
140.76	2.22 ± 0.05	1.80	39	1253	6.11	63.7 ± 3.7	107.7 ± 18.5	9.2
140.82	2.23 ± 0.05	1.80	73	2622	6.09	56.3 ± 3.0	97.1 ± 16.5	8.2
140.88	2.24 ± 0.06	1.81	57	2435	6.16	55.5 ± 3.3	97.5 ± 17.8	8.1
140.94	2.23 ± 0.07	1.80	20	1036	6.38	63.1 ± 4.8	108.8 ± 21.5	9.2
141.10	2.21 ± 0.09	1.79	5	182	6.10	45.9 ± 7.0	76.1 ± 20.6	6.6
141.17	2.20 ± 0.09	1.79	4	98	5.88	36.2 ± 7.7	58.9 ± 18.5	5.2
141.32	2.19 ± 0.10	1.78	2	43	6.21	37.3 ± 17.8	59.5 ± 31.8	5.3
141.44	2.17 ± 0.13	1.77	2	13	5.93	23.0 ± 32.9	35.2 ± 51.6	3.2
141.56	2.16 ± 0.14	1.77	5	43	5.78	22.4 ± 9.6	33.6 ± 18.5	3.1
141.63	2.17 ± 0.15	1.77	9	82	6.17	27.5 ± 2.5	42.1 ± 14.8	3.9
141.72	2.23 ± 0.14	1.80	14	262	6.29	36.0 ± 2.6	62.1 ± 19.0	5.3
141.83	2.29 ± 0.14	1.83	21	486	6.25	29.8 ± 1.7	57.4 ± 16.8	4.5
141.88	2.32 ± 0.14	1.84	12	292	6.31	28.3 ± 1.8	57.5 ± 16.3	4.3
142.68	2.38 ± 0.07	1.87	26	315	6.14	17.3 ± 2.0	38.9 ± 8.2	2.7
142.71	2.38 ± 0.06	1.87	28	331	6.13	17.3 ± 2.0	38.9 ± 7.9	2.7
143.54	2.42 ± 0.03	1.88	12	81	6.03	11.5 ± 2.8	27.6 ± 7.8	1.8
143.84	2.46 ± 0.05	1.90	17	91	5.98	10.7 ± 2.5	27.3 ± 7.7	1.7
144.47	2.60 ± 0.15	1.95	20	77	5.95	9.0 ± 1.9	28.2 ± 9.6	1.5
144.65	2.64 ± 0.18	1.97	17	84	5.96	10.1 ± 1.9	33.4 ± 11.8	1.7
145.54	2.83 ± 0.30	2.04	20	112	6.18	7.7 ± 1.6	32.4 ± 14.5	1.3
145.63	2.84 ± 0.31	2.04	18	89	6.25	6.8 ± 1.8	29.0 ± 13.9	1.2
145.99	2.87 ± 0.33	2.05	1	1	6.10	2.2 ± 0.0	9.7 ± 4.2	0.4
146.33	2.87 ± 0.33	2.05	4	11	6.15	4.9 ± 0.7	21.6 ± 9.7	0.8
147.11	2.87 ± 0.33	2.05	10	20	6.15	2.9 ± 0.9	12.8 ± 6.7	0.5
147.96	2.87 ± 0.33	2.05	9	19	6.16	2.7 ± 1.0	11.9 ± 6.7	0.5

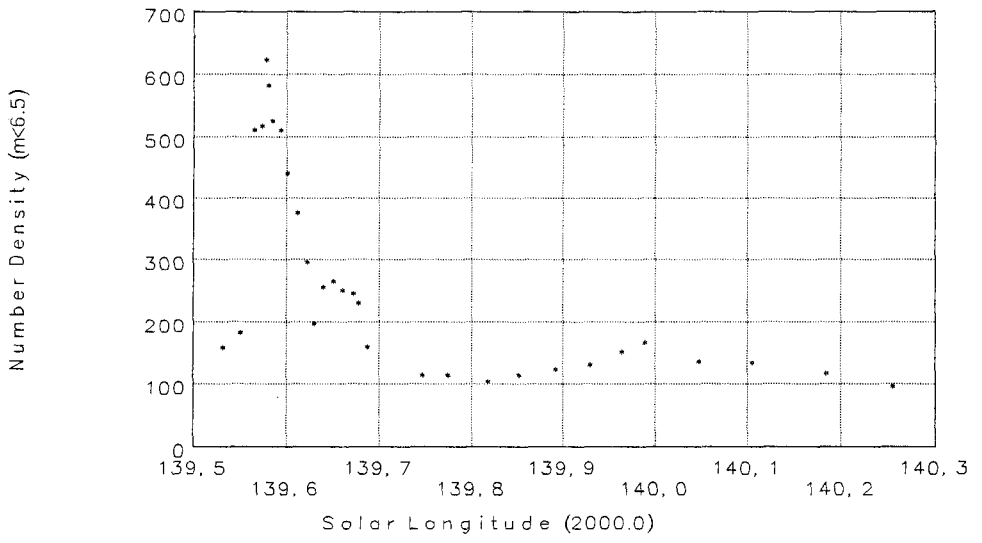

Figure 7 – Spatial number density (particles per 10^9 km^3) of particles causing meteors of at least +6.5 absolute magnitude, $\rho(m \leq 6.5)$.

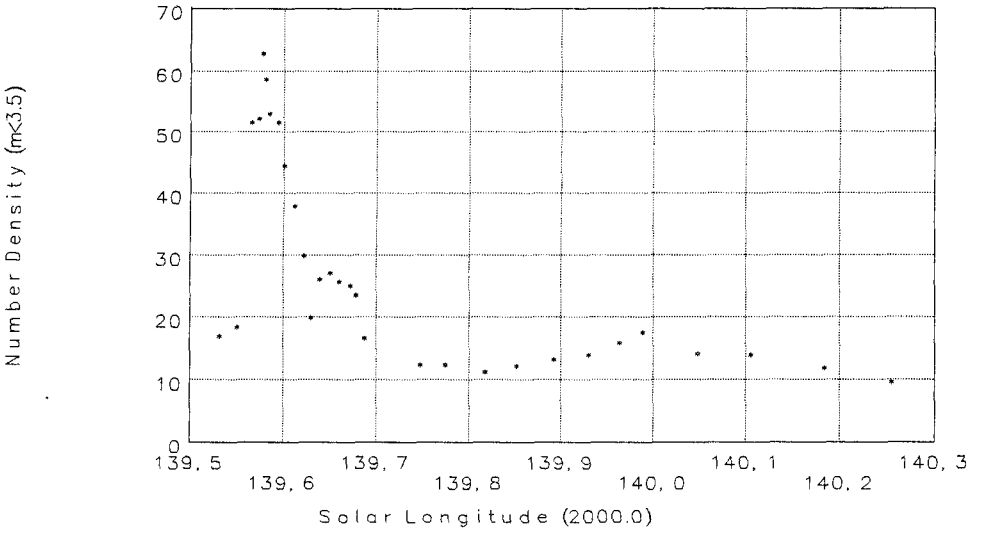

Figure 8 – Spatial number density (particles per 10^9 km^3) of particles causing meteors of at least +3.5 absolute magnitude, $\rho(m \leq 3.5)$.

3. The 1992 Perseids

Due to interference from the Full Moon during the maximum period of the Perseids in 1992, the amount of data from August 1992 is much smaller than in an average year. Below, we list the observers having contributed to the analysis together with their *IMO* code and the effective time spent on Perseid watches.

Ben Apeldoorn (**APEBE**, $3^h.78$), Rainer Arlt (**ARLRA**, $4^h.07$), Slavomir Babnic (**BABSL**, $25^h.22$), Luc Bastiaens (**BASLU**, $8^h.02$), Marc Bastiaens (**BASMA**, $6^h.35$), Mario Bellavance (**BELMA**, $8^h.01$), Luis R. Bellot (**BELLU**, $7^h.91$), Orlando Benítez Sánchez (**BENOR**, $15^h.05$), Paul Bensing (**BENPA**, $11^h.79$), Felix Bettonvil (**BETFE**, $15^h.23$), Ragnar Bödefeld (**BODRA**, $11^h.23$), Michael Bonnes (**BONMI**, $4^h.19$), Vanja Brčić (**BRCVA**, $2^h.59$), Peter Brown (**BROPE**, $9^h.56$), William Burmeister (**BURWI**, $4^h.25$), Dominico Carbajo (**CARDM**, $2^h.35$), Koen Clement (**CLEKO**, $3^h.62$), Jorge Cuadrado (**CUAJO**, $2^h.66$), Albert de Clerck (**DE AL**, $1^h.98$), Niek de Kort (**DE NI**, $2^h.91$), Werner Depoorter (**DEPWE**, $3^h.80$), Carl de Pooter (**DE CA**, $1^h.48$), Marta Dikova (**DIKMA**, $7^h.30$), Kathrin Düber (**DUBKA**, $20^h.39$), Jiří Erlebach (**ERLJI**, $3^h.50$), Ján Fabricius (**FABJA**, $3^h.93$), Andrea Friebel (**FRIAN**, $4^h.20$), Michael Funke (**FUNMI**, $2^h.10$), Martin Furuhed (**FURMA**, $1^h.89$), Marija Gajić (**GAJMA**, $8^h.02$), Jaroslav Gerboš (**GERJA**, $12^h.82$), Tom Giguere (**GIGTO**, $3^h.00$), George W. Gliba (**GLIGE**, $4^h.00$), Roel Gloudemans (**GLORO**, $14^h.01$), Jeffrey D. Gortatowsky (**GORJE**, $1^h.42$), Valentin Grigore (**GRIVA**, $13^h.65$), Antoine Grima (**GRIAN**, $5^h.92$), Erwin Guetens (**GUEER**, $4^h.99$),

José Luis Guixeras Romero (GUIJO, $0^h.94$), Teemu Hankamäki (HANTE, $1^h.00$), Torsten Hansen (HANTO, $14^h.72$), Takasi Hasegawa (HASET, $1^h.00$), Takema Hashimoto (HASTA, $5^h.74$), Robert Hays (HAYRO, $6^h.00$), Udo Henning (HENUD, $1^h.70$), Michael Hlusik (HLUMI, $4^h.55$), David Holman (HOLDA, $8^h.63$), Oomi Iiyama (IIYOO, $10^h.09$), Daiyu Ito (ITODA, $2^h.99$), Kiyoshi Izumi (IZUKI, $1^h.00$), Katrin Jentzsch (JENKA, $9^h.20$), Carl Johannink (JOHCA, $3^h.00$), Anne Jokinen (JOKAN, $6^h.20$), Stanislav Kaniansky (KANST, $18^h.29$), Aram Karalič (KARAR, $2^h.17$), John H. King (KINJO, $4^h.50$), Timo Kinnunen (KINTI, $2^h.00$), James E. Kirby (KIRJA, $2^h.00$), André Knöfel (KNOAN, $8^h.65$), Bernhard Koch (KOCBE, $14^h.82$), Kyozaburo Komatusaki (KOMKY, $3^h.73$), Vladimir Kordik (KORVL, $14^h.40$), Korado Korlević (KORKO, $1^h.83$), Ralf Koschack (KOSRA, $6^h.16$), Detlef Koschny (KOSDE, $5^h.42$), Nobuyuki Kosiyama (KOSNO, $1^h.94$), Jan Kysely (KYSJA, $6^h.36$), Inge Leyssens (LEYIN, $1^h.40$), Ruda Linke (LINRU, $1^h.00$), Vladimir Lukić (LUKVL, $8^h.74$), Robert Lunsford (LUNRO, $26^h.06$), Kouji Maeda (MAEKO, $2^h.59$), Veikko Mäkelä (MAKVE, $2^h.08$), Katuhiko Mameta (MAMKA, $8^h.81$), Nevena Marić (MARNE, $5^h.02$), Tony Markham (MARTO, $6^h.76$), Jan Masiar (MASJA, $13^h.20$), Damir Matković (MATDA, $5^h.36$), Yukihisa Matumoto (MATYU, $8^h.21$), Alastair McBeath (MCBAL, $16^h.41$), Stefan Meister (MEIST, $10^h.50$), Stanimir Metchev (METST, $5^h.92$), Ivo Micek (MICIV, $5^h.53$), Vedran Mirko (MIRVE, $0^h.93$), Koen Miskotte (MISKO, $20^h.91$), Hidekatu Mizoguchi (MIZHI, $3^h.64$), Sirko Molau (MOLSI, $21^h.23$), Michael Morrow (MORMI, $7^h.00$), Alfonso Murias Núñez (MURAL, $6^h.94$), Marko Myllyniemi (MYLMA, $3^h.60$), Tomas Nasku (NASTO, $5^h.53$), Sandra Niedermair (NIESA, $3^h.00$), Atanas Nikolov (NIKAT, $22^h.98$), Markku Nissinen (NISMA, $2^h.76$), Mirko Nitschke (NITMI, $19^h.50$), Kunio Nose (NOSKU, $1^h.71$), Daniel Ocenas (OCEDA, $9^h.14$), José Ortega (ORTJO, $1^h.26$), Kazuhiro Osada (OSAKA, $3^h.79$), Urška Pajer (PAJUR, $2^h.07$), Michael A. Pelizzari (PELMI, $0^h.92$), A. Petrenko (PETA , $2^h.15$), Milan Pohořalý (POHMI, $2^h.50$), Lilia Porozhanova (PORLI, $4^h.64$), Jože Prudič (PRUJO, $1^h.02$), Petar Radovan (RADPE, $1^h.00$), Mateja Raič (RAIMA, $2^h.17$), Leo Rajala (RAJLE, $6^h.89$), Pia Rämä (RAMPI, $6^h.50$), Ljubinko Ranković (RANLJ, $4^h.02$), Daniela Rapava (RAPDA, $4^h.67$), Martin Rapava (RAPMA, $11^h.09$), Pavol Rapavy (RAPPA, $6^h.75$), Thomas Rattei (RATTH, $3^h.75$), Jürgen Rendtel (RENJU, $17^h.28$), Francisco Reyes Andrés (REYFR, $1^h.76$), Miroslav Řezníček (REZMI, $2^h.75$), Daniel Rhone (RHODA, $1^h.00$), James Riggs (RIGJA, $13^h.62$), Bauke Rispens (RISBA, $2^h.72$), Maria Rocio (ROCMA, $2^h.39$), Miguel Rodriguez (RODMI, $2^h.33$), Tom Roelandts (ROETO, $7^h.67$), Tuomo Roine (ROITU, $2^h.43$), Tony Royal (ROYTO, $5^h.75$), Stefan Ruzicka (RUZST, $7^h.30$), Blanka Ruzickova (RUZBL, $2^h.82$), Toru Sagayama (SAGTO, $1^h.98$), Pablo Santos (SANPA, $2^h.55$), Hiromi Sato (SATHI, $3^h.51$), Koetu Sato (SATKO, $5^h.45$), Tatuo Sato (SATTA, $6^h.08$), Nicholas K. Sauter (SAUNI, $2^h.25$), Adrian Sava (SAVAD, $8^h.61$), Patric Scharff (SCHPA, $6^h.86$), Stefan Scholz (SOLST, $3^h.20$), Takashi Sekiguchi (SEKTA, $1^h.45$), Francisco Sevilla (SEVFR, $2^h.46$), Gregory Shanos (SHAGR, $3^h.54$), I. Shekhedrov (SHEI , $6^h.41$), Yasuo Shiba (SIBYA, $2^h.04$), E. Shortova (SHOE , $6^h.02$), Brian Shulist (SHUBR, $5^h.00$), Godfrey Sill (SILGO, $11^h.00$), Kzuaki Siotani (SIOKA, $7^h.55$), Kenji Sirayanagi (SIRKE, $1^h.32$), Juraj Škvarka (SKVJU, $4^h.40$), Alexander Smetanko (SMEAE, $2^h.04$), James N. Smith (SMIJN, $10^h.59$), Ulrich Sperberg (SPEUL, $7^h.57$), Siegfried Stapf (STASI, $17^h.49$), Plamen Stefanov (STEPL, $2^h.75$), Chris Stephan (STECR, $5^h.62$), Tuyla Stickelman (STITU, $3^h.00$), Robert Stine (STIRO, $1^h.00$), Marta Svancarova (SVAMR, $8^h.95$), David Swann (SWADA, $13^h.25$), Tomáš Sýkora (SYKTO, $6^h.20$), Richard Taibi (TAIRI, $8^h.79$), Tony Tanti (TANTO, $3^h.17$), Hiroyuki Tomioka (TOMHI, $4^h.13$), Tuomas Törrönen (TORTU, $4^h.33$), Manuela Trenn (TREMA, $8^h.72$), Josep M. Trigo Rodriguez (TRIJO, $2^h.85$), Dragana Urošević (URODR, $4^h.83$), Yoshiaki Uyama (UYAYO, $0^h.93$), Mireille Vanheerentals (VANMR, $2^h.71$), Frank Ventura (VENFR, $2^h.42$), Cis Verbeeck (VERCI, $6^h.38$), Thomas Voigt (VOITH, $14^h.26$), Burkhard Wiche (WICBU, $11^h.71$), Jean-Marc Wislez (WISJE, $2^h.51$), Nikolai Wünsche (WUNNI, $7^h.34$), Yasuo Yabu (YABYA, $4^h.83$), Chen Yu (YU CH, $0^h.91$), George Zay (ZAYGE, $25^h.92$), Peter Zimnikoval (ZIMPE, $4^h.50$), Danijela Živkovic (ZIVDA, $3^h.99$), Miroslav Znášik (ZNAMI, $9^h.05$).

Calculations of the r-profile do not permit short temporal resolution graphs for the maximum as the outburst around 19^h UT on August 11 are not covered sufficiently. Therefore, we decided to determine a profile with about one value for r per day which is given in Table 5. As expected, the result turned out to be smooth and unspectacular. Figure 9 shows the r-graph which was used to interpolate the population index needed for ZHR calculations.

A first attempt to determine the ZHR profile did not take the perception coefficients of the observers into account as the number of intervals was rather small. With several reports still coming in during the creation of this analysis (about 2500 Perseids) we decided to re-calculate the r-profile as well as the rates. Two periods shown in Table 6 yielded the perception values for 101 observers which were used for further analysis.

The ZHR profile consists of five averaged periods as shown in Table 7. The high pre-maximum activity in 1991 is also found in 1992. The smallest interval near the new peak is some 2 hours, which is reasonable considering the very few observations made during the outburst. Figure 10 shows the ZHR profile found in accordance with the resolution sizes given in Table 7.

Table 5 – The population index r for the 1992 Perseids.

$\lambda_\odot$ (2000.0)	Date (UT)	r	Per	$\overline{\text{lm}}$
124.20	Jul 26.9	1.74 ± 0.57	23	6.08
125.34	Jul 28.0	1.97 ± 0.18	73	6.30
126.52	Jul 29.3	2.15 ± 0.20	124	6.25
127.13	Jul 29.9	2.22 ± 0.40	74	6.10
130.02	Aug 01.9	2.30 ± 0.13	106	6.32
130.26	Aug 02.2	2.23 ± 0.10	167	6.25
130.62	Aug 02.5	2.13 ± 0.16	61	6.15
132.89	Aug 05.0	2.22 ± 0.07	287	6.09
133.24	Aug 05.5	2.26 ± 0.06	509	6.13
134.20	Aug 06.3	2.43 ± 0.08	409	6.23
135.30	Aug 07.5	2.48 ± 0.08	282	6.30
136.36	Aug 08.6	2.21 ± 0.14	281	6.29
137.31	Aug 09.5	2.09 ± 0.09	340	6.23
138.03	Aug 10.3	2.06 ± 0.10	248	6.07
139.56	Aug 12.0	2.05 ± 0.05	2324	5.16
139.65	Aug 12.1	2.08 ± 0.05	2359	5.12
140.50	Aug 12.9	2.24 ± 0.42	83	5.13

Table 6 – Intervals for computation of observers' perception

$\lambda_\odot$	Sampling interval	Shift
131°–137°	2°	1°
139°.6–140°.5	0°.4	0°.2

Table 7 – Periods of the sliding averages for the 1992 ZHR profile.

$\lambda_\odot$	Sampling interval	Shift
110°.0–138°.0	2°.0	1°.0
138°.0–139°.2	1°.0	0°.5
139°.2–139°.6	0°.08	0°.04
139°.6–140°.5	0°.2	0°.1
140°.5–153°.0	2°.0	1°.0

The young peak was resolved in 2-hour intervals shifted by one hour. Figure 11 magnifies the maximum part with slightly smaller peak intervals (0°.06 shifted by 0°.03 during $\lambda_\odot$ = 139°.2–139°.6). The annual maximum with a rate of 93 occurred at $\lambda_\odot = 140°.06 \pm 0°.1$. The best peak time which can be estimated is $\lambda_\odot = 139°.50 \pm 0°.04$ though the maximum value found here does not represent the maximum activity as the peak may be smaller than the 1.5-hour intervals used. The *mean* maximum value is about 240. The actual 30 to 50-minutes observing periods around $\lambda_\odot$ = 139°.5 have ZHRs between 312 and 374. Surprisingly, these six rates are fairly consistent, although the unfavorable circumstances during the peak would suggest a variety of high values.

Due to the small amount of data, we can only estimate the magnitude of the spatial number density at the peak. As with the 1991 analysis, we can find a number density from magnitude distributions obtained by observers watching near the new peak.

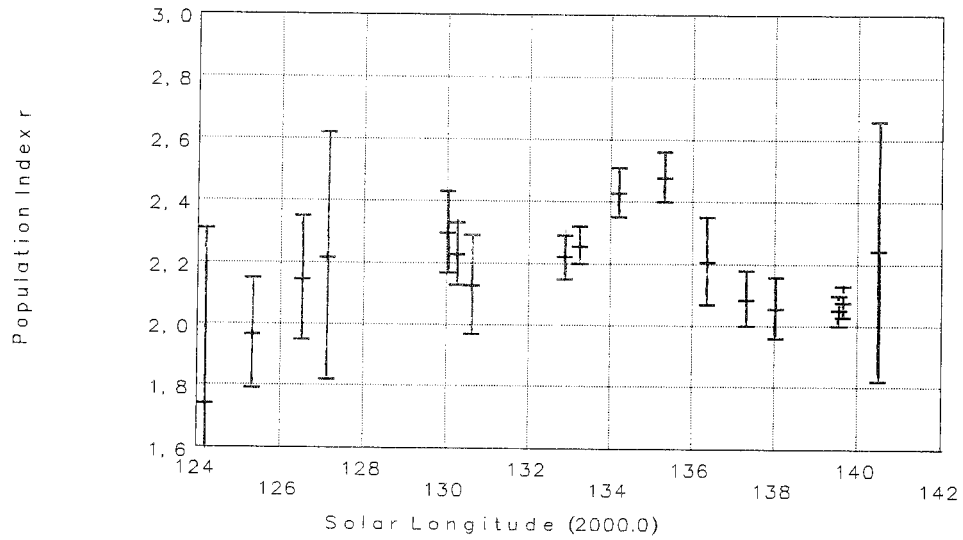

Figure 9 – The r-profile of the 1992 Perseids. The error bars correspond to the 67% confidence interval.

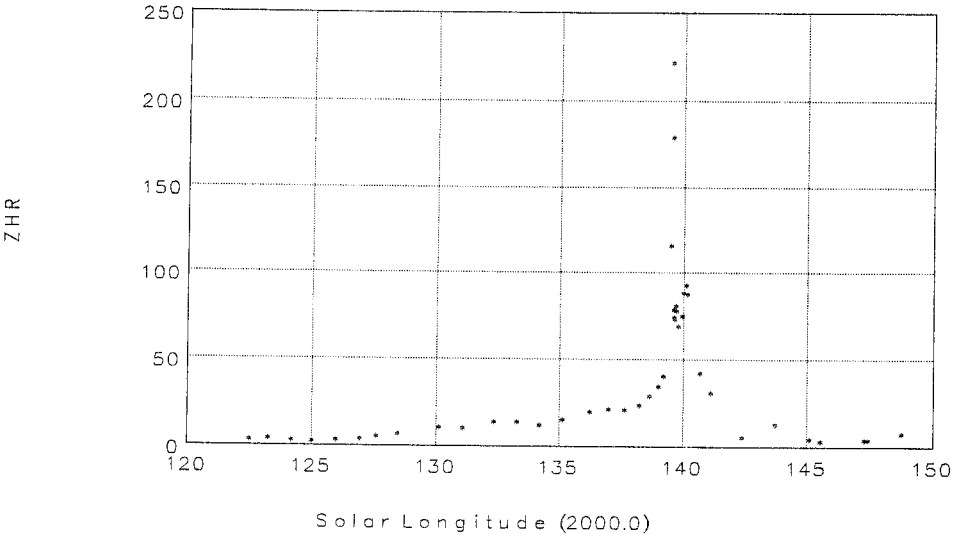

Figure 10 –Profile of the ZHRs of the 1992 Perseids. The averages correspond to different periods which are listed in Table 7.

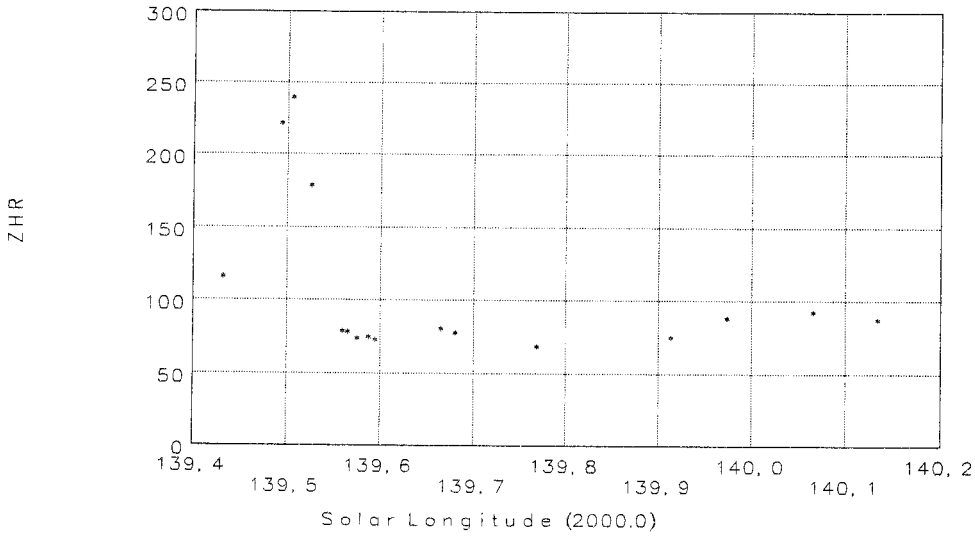

Figure 11 –The ZHR-profile of the 1992 Perseids around the maximum.

Table 8 - Numeric data for the 1992 Perseid activity period. All error margins correspond to the 67% confidence interval. For the explanation of the quantities, see Table 4.

$\lambda_\odot$ (2000.0)	r	s	Interv.	Per	$\overline{\text{lm}}$	ZHR	$\rho_{6.5}$	$\rho_{0.4}$
119.26	1.74 ± 0.57	1.55	4	1	5.84	0.5 ± 0.4	0.2 ± 0.4	0.0
119.71	1.74 ± 0.57	1.55	9	3	5.75	0.8 ± 0.4	0.3 ± 0.7	0.1
120.07	1.74 ± 0.57	1.55	5	2	5.65	1.1 ± 0.6	0.4 ± 1.0	0.1
122.47	1.74 ± 0.57	1.55	4	4	5.76	3.5 ± 4.8	1.2 ± 3.4	0.2
123.22	1.74 ± 0.57	1.55	16	28	5.70	4.3 ± 1.2	1.5 ± 3.6	0.3
124.14	1.78 ± 0.49	1.58	30	51	5.99	3.2 ± 0.5	1.3 ± 2.4	0.2
124.97	1.89 ± 0.31	1.64	47	82	6.05	2.9 ± 0.4	1.6 ± 1.6	0.2
125.94	2.05 ± 0.21	1.72	63	145	6.04	3.5 ± 0.4	2.8 ± 1.6	0.3
126.90	2.18 ± 0.31	1.78	77	238	6.02	4.3 ± 0.5	4.4 ± 3.1	0.4
127.56	2.23 ± 0.36	1.80	68	269	6.00	5.8 ± 0.7	6.5 ± 5.0	0.6
128.43	2.26 ± 0.27	1.81	31	145	6.06	7.3 ± 1.1	8.6 ± 5.0	0.7
130.08	2.24 ± 0.15	1.81	30	285	6.14	10.7 ± 1.3	12.2 ± 4.5	1.0
131.02	2.19 ± 0.13	1.78	41	361	6.10	10.6 ± 0.7	11.1 ± 3.7	1.0
132.30	2.20 ± 0.10	1.79	70	666	5.96	14.2 ± 0.5	15.1 ± 4.3	1.3
133.25	2.29 ± 0.07	1.83	102	928	6.01	14.2 ± 0.4	17.5 ± 4.2	1.4
134.15	2.39 ± 0.07	1.87	86	715	6.14	12.5 ± 0.5	17.9 ± 4.3	1.2
135.09	2.42 ± 0.09	1.88	55	610	6.20	15.5 ± 0.7	23.2 ± 5.9	1.5
136.19	2.26 ± 0.11	1.81	45	746	6.22	20.2 ± 0.7	23.8 ± 6.8	1.9
136.95	2.14 ± 0.12	1.76	37	655	6.14	21.4 ± 1.0	20.5 ± 6.6	2.0
137.59	2.08 ± 0.10	1.73	14	213	5.95	21.3 ± 3.2	18.2 ± 6.1	1.9
138.18	2.06 ± 0.09	1.72	7	91	5.60	23.6 ± 6.7	19.3 ± 7.9	2.1
138.60	2.06 ± 0.08	1.72	19	247	5.64	29.1 ± 3.4	23.8 ± 7.1	2.6
138.94	2.05 ± 0.07	1.72	14	208	5.73	34.6 ± 5.3	27.8 ± 8.2	3.0
139.15	2.05 ± 0.06	1.72	3	64	5.76	40.7 ± 23.3	32.7 ± 20.2	3.6
139.43	2.05 ± 0.05	1.72	1	25	5.50	116.1 ± 0.0	93.2 ± 20.6	10.2
139.49	2.05 ± 0.05	1.72	6	329	5.68	221.9 ± 48.1	178.1 ± 54.9	19.5
139.53	2.05 ± 0.05	1.72	10	417	5.73	179.5 ± 41.9	144.1 ± 46.0	15.8
139.57	2.06 ± 0.05	1.72	16	283	5.49	78.8 ± 19.5	64.6 ± 21.4	7.0
139.58	2.06 ± 0.05	1.72	13	272	5.62	74.3 ± 8.0	60.9 ± 14.9	6.6
139.59	2.06 ± 0.05	1.72	2	89	6.00	73.4 ± 13.7	60.1 ± 17.1	6.5
139.67	2.08 ± 0.06	1.73	52	1125	5.30	81.0 ± 2.7	69.1 ± 16.8	7.2
139.68	2.08 ± 0.06	1.73	63	1286	5.32	78.2 ± 2.3	66.7 ± 16.2	7.0
139.77	2.10 ± 0.10	1.74	23	371	5.27	69.2 ± 4.9	61.4 ± 20.4	6.3
139.91	2.13 ± 0.16	1.76	13	288	5.16	75.1 ± 3.8	70.6 ± 33.0	6.9
139.97	2.14 ± 0.19	1.76	9	270	5.10	88.4 ± 4.1	84.6 ± 45.8	8.1
140.07	2.16 ± 0.22	1.77	5	162	5.31	93.0 ± 5.7	92.3 ± 54.3	8.6
140.13	2.17 ± 0.25	1.77	2	48	5.63	87.7 ± 7.6	88.7 ± 55.2	8.2
140.64	2.24 ± 0.42	1.81	8	133	5.16	42.6 ± 3.6	48.6 ± 50.2	4.1
141.10	2.24 ± 0.42	1.81	11	142	5.24	31.1 ± 5.1	35.4 ± 36.4	3.0
142.37	2.24 ± 0.42	1.81	4	10	5.38	5.8 ± 2.1	6.6 ± 7.0	0.6
143.69	2.24 ± 0.42	1.81	4	16	5.21	13.0 ± 6.8	14.8 ± 17.0	1.2
145.07	2.24 ± 0.42	1.81	6	9	5.30	4.8 ± 1.9	5.5 ± 5.9	0.5
145.53	2.24 ± 0.42	1.81	5	5	5.48	3.4 ± 1.8	3.9 ± 4.3	0.3
147.26	2.24 ± 0.42	1.81	16	24	5.68	4.1 ± 0.9	4.7 ± 4.5	0.4
147.40	2.24 ± 0.42	1.81	16	26	5.74	4.3 ± 1.0	4.9 ± 4.7	0.4
148.71	2.24 ± 0.42	1.81	3	8	6.36	7.9 ± 4.1	9.0 ± 8.7	0.8

The value corresponding to the short period around $\lambda_\odot = 139°.50$ with ZHR ≈ 350 is most roughly $\rho(m \leq 3.5) \approx 100 \pm 25$ particles per 10^9 km^3 based on 361 Perseids of 7 observers. This value is somewhat higher than the maximum number density in Figure 8, suggesting activity was in fact heightened in 1992 though the display lost its strikingness with the poor observing conditions. Table 8 summarizes the ZHRs and spatial number densities of the 1992 Perseids. The densities during the peak do not represent the actual activity as they are based on meteors down to magnitude 6.5. A lot of faint meteors may be lost below the perceptive limits of the observer due to the large number of bright meteors. Moreover, since limiting magnitudes in 1992 were very low (lm = 4.3–5.2), even meteor numbers of magnitude class +3 will be affected. Therefore, the spatial number densities $\rho(m \leq 3.5)$ may still be underestimated.

4. Conclusions

Both the 1991 and the 1992 Perseids show a clear double peak with very similar shape. A strong outburst of short duration with rates over 200 is followed by a broad maximum; this feature is common to other Perseid analyses made over the last decades. This old maximum occurred at $\lambda_\odot = 140\overset{\circ}{.}0 \pm 0.1$ in 1991 and at $\lambda_\odot = 140\overset{\circ}{.}1 \pm 0.1$ in 1992, the difference between both values being statistically insignificant. The same longitude was found in [3] for the 1989 Perseids, and the 1988 Perseids showed the highest activity at $\lambda_\odot = 140\overset{\circ}{.}2 \pm 0.1$ [6]. In both years, a second maximum of similar activity was observed about 12 hours before these given times.

However, a straightforward comparison of values obtained from analyses back to 1988 is difficult, because of the method developed which has different applications to different sets of data. The new peak at $\lambda_\odot = 139\overset{\circ}{.}580 \pm 0.005$ in 1991 and at $\lambda_\odot = 139\overset{\circ}{.}50 \pm 0.04$ in 1992 can be definitely related to freshly ejected material from Comet P/Swift-Tuttle which was rediscovered in September 1992. The enhanced activity before the regular peak in the previous years since 1988 may represent the first traces of the material ejected during the last perihelion passage of the comet and still being close to the comet.

The difference between the peaks in 1991 and 1992 is about $-2^h \pm 1^h$, though the maximum ZHRs are very similar with values of 350. The calculation of the spatial number densities of such peaks is complicated in that a considerable number of fainter meteors may go unnoticed during the observation. Therefore, a modified algorithm for number densities for high activity was applied, cutting the meteor number by $m \leq 3.5$. The resulting number densities are about 60 particles per 10^9 km^3 in 1991 and roughly 100 particles per 10^9 km^3 in 1992. Note that the 1992 values are extremely uncertain because of the unfavorable conditions during the entire maximum period.

Predictions for the 1993 activity seem to promise extremely high ZHRs as we will observe the stream just after the comet has passed the orbital node. The Earth passes this intersection at 1^h UT on August 12, 1993. This is the most probable time for a short and very high activity peak. Bearing in mind that the Perseids peaked 2 hours earlier in 1992 than in the preceding year, one might tend to extrapolate this shift to 1993 resulting in an outburst time between 22^h and 23^h UT on August 11. However, a meteor storm of very recently ejected material will more likely occur at the node of the comet's orbit.

References

[1] Roggemans P., Gyssens M., Rendtel J., "One-Hour Outburst of the 1991 Perseids Surprises Japanese Observers!", *WGN* 19:5, October 1991, pp. 181–184.

[2] Koschack R., Rendtel J., "Determination of Spatial Number Density and Mass Index from Visual Meteor Observations", *WGN* 18:2 and 18:4, 1990, pp. 44–58, 118–140; Erratum note on p. 118.

[3] Koschack R., Roggemans P., "The 1989 Perseid Meteor Stream", *WGN* 19:3, June 1991, pp. 87–98.

[4] Rendtel J., Arlt R., Brown P., "The 1991 Geminid Meteor Shower", *WGN* 21:1, February 1993, pp. 19–28.

[5] Koschack R., Roggemans P., "The 1990 Orionids", *WGN* 19:4, August 1991, pp. 115–130.

[6] Roggemans P., "The 1988 Perseid Meteor Stream and Observers' Perception Coefficients", *WGN* 17:5, October 1989, pp. 189–193.

[7] Koschack R., "Determination of the Flux Density for High Activity up to Meteor Storms Based on Visual Observations", in *Proceedings of the IMC*, Smolenice, Slovakia, July 1992, pp. 55–58.

Received June 1993; revised July 1993; accepted August 1993

An Unusual Meteor Cluster Observed by Image-Intensified Video

P.A. Piers and R.L. Hawkes

A cluster of 5 near-simultaneous, parallel meteors was detected with an image-intensified video system on October 18, 1985. The detailed analysis of the video frames suggests that each of the 5 main objects was in turn composed of at least 4 smaller meteoroids. The spatial spread of the 5 main objects was about 4.0 km, while the temporal spread (for similar positions) was only about 0.1 s. The small fragments which resulted from clustering of the main bodies were generally confined to an area of a few hundred meters, consistent with differential aerodynamic lag. The radiant and angular speed could be consistent with a separated fragment of Comet Biela, but we do not regard this as probable. The radiant is not consistent with any of the major fall showers. The clustering mechanism observed here could produce very high apparent rates in a small field of view system with poor time resolution (such as a CCD "exposure"), and therefore one should be cautious in suggesting meteor outbursts on the basis of such data.

1. Introduction

Groupings of several near-simultaneous shower meteors have occasionally been reported by visual and telescopic observers. For example, S.J. Perry [1] reported regarding the 1872 Bielid storm *A very peculiar feature of the display was the parallel motion of many stars that became visible at the same time. Thus at 9:16 five burst out close to γ Andromedae, and traveled eastward together; at 9:25 four went together from γ Andromedae to the Pleiades.* Describing the same storm, A.S. Herschel [2] reports *...two or three bright meteors apparently running a race with each other in parallel courses side by side or pursuing each other upon the same path was frequently observed...* The famous meteoric procession of February 9, 1913 [3] in which swarms of meteors (several at a time) covered a path of approximately 8000 km in total length is another well-documented case of meteor clusters. The total number of meteoroids involved in the 1913 procession is uncertain, but one observer with opera glasses estimated it at 10 groups, each group consisting of 20 to 40 individual meteors. Telescopic observers have also occasionally reported near-simultaneous meteors, with the analysis by Hoffleit [4] suggesting that as many as 16% of faint telescopic meteors may be double, although other telescopic meteor observations have yielded very few "double" meteors. Studies of visual and radar meteor rates have come to varying conclusions regarding whether the times of occurrence of shower meteors are random. Most radar meteor based studies [5,6,7,8] conclude that there is no significant clustering. However, it might be argued that radar is not an ideal technique for identification of near-simultaneous parallel meteor trains, which could be confused as single long enduring echoes. Also, two parallel meteor ionization trains will not both meet the specular reflection requirement if the trains are significantly separated.

Low Light Level Television (LLLTV) would seem a near-ideal tool for detection of meteor clustering, since there is no bias (except possibly the relatively small fields of view) against cluster detection and the rates are relatively high permitting meaningful statistics. Over the past two decades we have recorded many hundreds of hours of LLLTV observations, with about 200 hours of data having been at least partially analyzed. We have occasionally detected two parallel meteors with a relatively short time interval, and are planning a detailed study of the time distribution of television meteors. However, recent analysis of some video tapes recorded in 1985 has revealed a cluster of at least 5 near-simultaneous meteors. To our knowledge this is the first cluster recorded by video means, and we therefore deem it worthy of detailed reporting. Even during a strong shower, only rarely are two television meteors recorded with time intervals of less than 1 s. For example, during our LLLTV observations of the Perseid shower on August

Author's address: Physics, Engineering, and Geology Department, Mount Allison University, Sackville, New Brunswick, E0A 3C0, Canada.

WGN, the Journal of the International Meteor Organization, Vol. 21, No. 4, August 1993, pp. 168–174.

12-13, 1991, we recorded 187 meteors in a 6 hour period. In only one case did two meteors fall within a 1.0 s interval of each other. Therefore this near-simultaneous occurrence of at least 5 meteors is indeed unusual. Furthermore, there is a strong suggestion that each of the 5 meteors are themselves clusters of several smaller fragments.

One of our initial reasons for writing this paper was to suggest an alternative explanation for the "outburst" on November 5, 1991, recorded by the CCD camera on the Canada-France-Hawaii Telescope [9]. With a system lacking fine time resolution (such as a CCD or photographic time exposure) a single meteor cluster could not be differentiated from a meteor outburst. Subsequently, a non-meteoric explanation for the CCD evidence of the event on November 5, 1991, has been published [10].

Before giving a detailed description of this cluster event, we wish to briefly address potential non-meteoric explanations. Our sensitive LLLTV cameras do routinely record many satellites and airplanes, and, at certain times of the year and observing locations, various insects, bats and birds. Both insects and bats fly highly non-linear paths, and can be immediately discounted. Airplanes are also easily recognized, and too slow for the observed event. We considered the possibility of small fragments of space debris, but the angular speeds observed are a factor of 2 higher than for probable satellite orbits. Migrating birds flying in formation frequently appear as somewhat linear images with roughly uniform speeds (although usually even the high flight of migrating birds is somewhat non-linear and non-uniform in speed). Blokpoel [11] has reviewed available data including typical heights and ground speeds for night-time migration of various species of birds in different locations, while Richardson [12] provides data specific to the maritime provinces of Canada and fall migration. Radar suggests that night-time migration of waterfowl are typically at heights of 750 m to 2200 m, and that typical speeds are 11 to 25 m/s. Shorebirds frequently fly at much greater heights of 3000 to 6000 m. Given our observing elevation angle of about 68°, and assuming the statistically probable aspect ratio, we obtain the following relation for the apparent angular speed ω (in degrees per second) as a function of the speed v (in meters per second) and height h (in meters): $\omega = 51v/h$. For a waterfowl with $v = 18$ m/s and $h = 610$ m, we obtain an apparent angular speed of about 1°.2/s, which is consistent with the sorts of angular speeds observed when birds are detected with our cameras. For a typical shorebird, the angular speed would be 0°.2/s. Even in an optimum high-speed scenario (25 m/s at 300 m height) the apparent angular speed is 4°.2/s. Considering our measured cluster angular speed of 9°.0/s (see below) we consider it improbable that the cluster is a flock of migrating birds.

2. Observations

The data were recorded on a single-station ISIT video camera (RCA TC1040) using a 50 mm objective lens which resulted in a field of view of approximately 9° by 13° (the limiting stellar magnitude was about +9). Observations were performed from Sackville, New Brunswick, Canada (64°22′22″ W, 45°53′33″ N), with the observing field centered at roughly 68° elevation and 149° azimuth.

The cluster was observed at $2^{h}01^{m}20^{s}$ UT on October 18, 1985. There were at least 5 main objects, which we will refer to by letter designations A through E. Unfortunately, all 5 objects traversed the top right corner of the field of view, and therefore complete light curves are not available for any of the meteors. Meteors A and B appeared almost simultaneously, and traveled together at equal speeds. The transverse separation of paths A and B was about 0°.5. Approximately 0.37 s after the appearance of A, object C appeared, above and to the right of objects A and B, and a 4th meteor D appeared another 0.10 s later. Note that the times when the different fragments reached corresponding positions were within about 0.1 s, however. Meteor C was roughly 1°.2 displaced from path B, while D was displaced by a further 0°.2. Meteors C and D had more of their flight path cut off by the edge of the field of view. A 5th meteor, E, appeared, but so close to the corner that only a few frames are available.

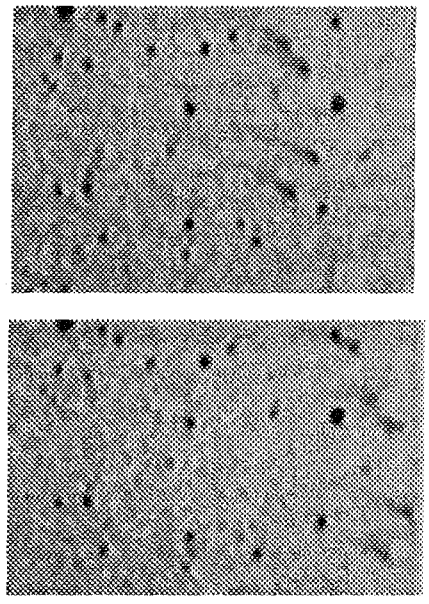

Figure 1 – The appearance of the cluster in two video images separated by 1/6 s. In the top photo, 4 of the meteors are traveling to the right and downward (about 35° angle), while all 5 meteors are visible in the bottom image.

We show in Figure 1 a portion of two of the digitized video images. The field printed here is about 6°.3 wide. The bright star at the top edge is α And (magnitude 2.1) while the second bright star (on the right hand side) is ψ Peg (4.6). The meteor cluster travels to the right and downward on the right hand side of the pictures. The top image shows fragments *A*, *B*, *C*, and D, while all 5 fragments are visible in the bottom image. These two images are 10 video fields (1/6 s) apart. The meteor images are about +6 in apparent luminosity.

The data were originally recorded on Beta III video tape. A RasterOps 24stv board in a Macintosh IIci computer was used for video digitization. We employed $320 \times 240 \times 8$ bit mode for this work. Unfortunately, repeated viewing of the tape prior to digitization degraded the quality of the images on some frames. The original video signal was NTSC interlaced composite video, and we digitized both even and odd fields (therefore the time resolution is 1/60 s). For various reasons, a few fields were not available for analysis, and we provide in Table 1 below the circumstances for each meteor. A count of 1 in the field number corresponds to 1/60 s.

Table 1 – Video field information. Each NTSC field is 1/60 s. "Angle" is the angle subtended between the beginning and end for that meteor, and speed is the apparent angular speed in degrees per second (the average for the 5 objects is 9°.02/s ± 0°.17/s).

Met.	Begin	End	Missing	Interval	Angle	Speed
A	1	47	3, 11, 21, 43	0.767 s	6°.92	9°.02/*s*
B	1	45	3, 11, 21, 23, 43	0.733 s	6°.49	8°.85/*s*
C	22	47	43	0.417 s	3°.78	9°.06/*s*
D	28	46	38, 39, 43	0.300 s	2°.66	8°.87/*s*
E	41	51	43, 48	0.167 s	1°.55	9°.28/*s*

The data in Table 1 may be combined with those of Figure 2 to calculate the positions of the meteors at corresponding times.

A bilinear interpolation 3× scaling on each image was performed prior to measurement. The digital image processing software NIH Image 1.42 was used for measurement of positions of the meteors and 13 local reference stars (10 to 12 on some frames).

We used the procedures outlined by Hawkes et al. [13] for reduction of the measurements to obtain the equatorial coordinates (epoch 2000.0).

The average apparent measurement error (based on deviation of reference stars) was 0°.019, which translates to an unbiased expected error of 0°.030. The extreme corner position (leading to greater nonlinearities and the impossibility of using reference stars on all sides of the meteor images) means that the real error is probably greater, particular near the beginning and end of each trail. Furthermore, we cite below evidence that each object is in fact a cluster of smaller grains, with apparent sizes for each collection of particles being of the order of 0°.14. This made the measurement of fiducial positions difficult, and one might regard the real errors in the measured positions as being of the order of ±0°.1.

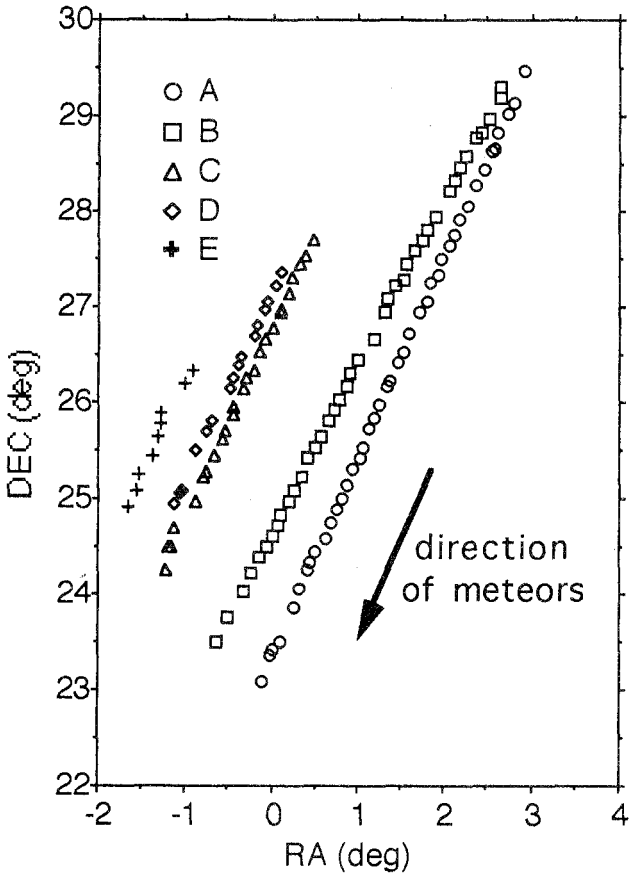

Figure 2 – Subsequent positions of the main cluster centers.

We show in Figure 2 a plot in right ascension and declination space (epoch 2000.0) of the 5 meteors. In such a plot, meteor motion is from top right to bottom left, whereas in the actual field of view of our camera (Figure 1), apparent meteor motion was from left to right, and downward.

A cursory examination of Figure 2 suggests that paths *A* and *B* are divergent, implying either a shower radiant very near the field of view, or some sort of explosive break-up near the Earth. A closer examination of the individual frames suggests another possibility—that trail *B* is in fact a composite of a number of shorter meteor trails, each of which is straight and parallel to the other trails. The later segments are further to the left (in the plot of Figure 2) and this gives the composite trail its apparent orientation. Indeed upon close examination it appears that each of objects *A* through *E* is a composite of at least 2 to 7 smaller particles. At times, these trails demonstrate significant changes within time intervals as short as 0.03 s. For example, in Figure 3 we show a magnified contour plot of the *B* object (magnified 15×) in video fields 34 and 36. We have used the elevation and a probable height of about 90 km to derive a 100 m scale which is shown. Field 34 shows two main and distinct objects, while field 36 (only 1/30 s later) shows a complex pattern with as many as 4 separate meteors (the scale and orientation of both images is the same).

The identification of the number of separate objects is very subjective, but we present in Table 2 the range in numbers given by several independent observers for the better defined frames.

Table 2 – Number of individual fragments apparent in each video image.

Field	*A*	*B*	*C*	*D*	*E*
16	4	3			
18	3–4	3			
20	2–3	3			
24	4–5	3–4	1–3		
26	3–4	3–4	5		
28	4–6	2			
30	4	4	2	4–5	
32	4	3	5–6	3–4	
34	3–5	2	4–6	2–3	
36	4–5	4	4–5	3–4	
38	2–3	5–7	4	3–5	
40		4–5	3–4	2–3	
44	4	4–6	6–7	4–6	4
46	4–5	3–4	4	4	4
48					5

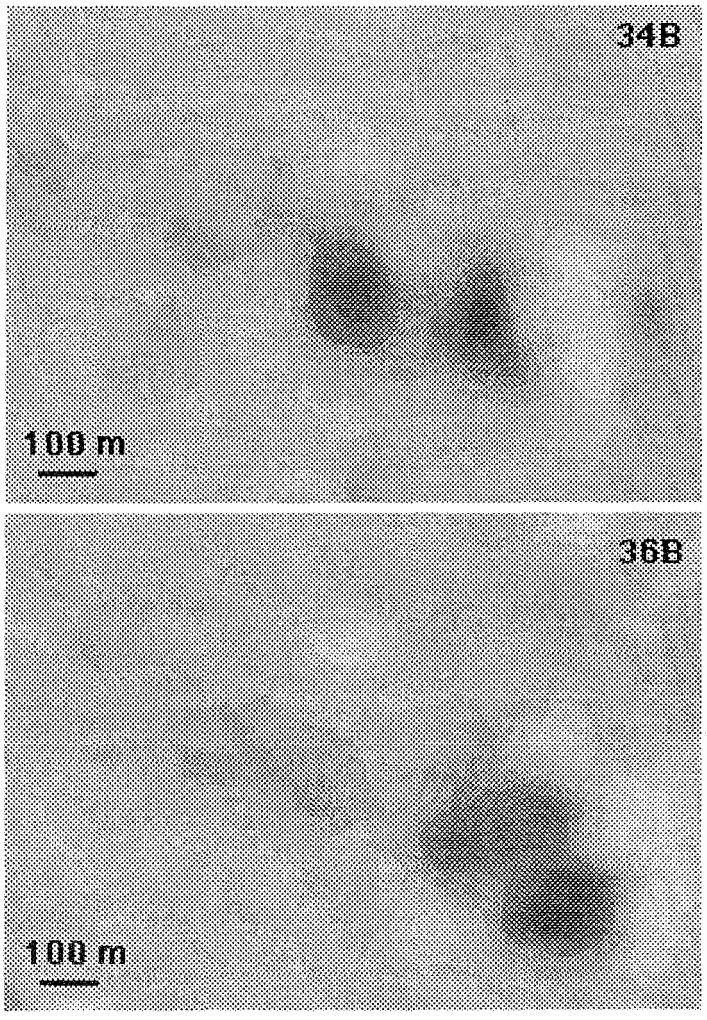

Figure 3 – A magnified (15×) view of video fields 34 and 36 for object *B*. These two images are separated by only 1/30 s, yet show distinct differences as a result of further clustering.

Another indication that the objects are composite combinations of smaller particles is the spatial dimensions of the objects. With image-intensified video detectors, point sources are bloomed to have apparent spatial spread. We measured the peak pixel intensity value and the width of the image for a number of reference stars in our digitized video frames. For those stars which did not saturate the system, we calculated a second order polynomial fit of apparent width to intensity, and then used this to predict the size for each of our meteor images. In most cases the actual dimensions (measured transverse to the trail) of the objects were significantly greater, as illustrated in Table 3.

Table 3 – Width of meteor images transverse to trail (pixels in 3× magnified image).

Meteor	Measured	Predicted	Fraction greater than predicted
A	11.6	8.9	35/44
B	11.0	8.4	36/44
C	10.4	7.3	21/26
D	10.4	5.8	18/18
E	9.0	5.7	8/10

A detailed analysis of the sizes of these constituent grains is beyond the scope of this paper. An upper limit for the mass of each of the main segments would be roughly 10^{-6} kg, but the rapid changes in appearance suggest clusters of smaller grains perhaps a factor of 10 or more smaller than this.

3. Discussion

It is natural to ask whether this cluster is a member of any of the major meteor streams. One of our initial inclinations was that this cluster might be related to the Bielid (Andromedid) Complex, whose radiant has shifted substantially during the past two centuries [14]. That shower is noted for "grouped" meteors, and it was suggested that it could have been the cause of the event on November 5, 1991 [14]. With only single station observations it is not possible to uniquely identify the radiant and orbit. However, since time information is available from the video record, it is possible to considerably narrow the range of potential radiants. It can be shown that the angle α between the viewing direction and the radiant is given by

$$\alpha = \sin^{-1}\left(\frac{2H\,\mathrm{tg}(\beta/2)}{v\tau\sin e}\right)$$

where H is the height of the meteor, e the elevation angle, β the angle subtended by the meteor in time τ, and v the geocentric speed of the meteor. If we assume an apparent geocentric speed of 20 km/s for the Bielid shower [15], and a height of 88 km for meteors of this speed based on two station television data [16], we obtain a value for α of about 47°. Even though the Bielid radiant is complex and broad due to several close approaches to Jupiter, and has moved considerably with time [14], we conclude that the apparent direction and angular speed of these meteors is inconsistent with the Bielid radiant. Should Comet Biela have been fragmented by collision with the Leonid Stream [17], it is possible that one component of Biela would have been significantly diverted by the high speed collision, and have a radiant consistent with the cluster's apparent angular speed and direction. We regard this scenario as possible but unlikely. We tested the other possible fall showers, but no matches were found.

It is reasonable to ask whether the spatial dimensions of the observed clusters are consistent with lag values expected due to differential aerodynamic deceleration [18]. The few hundred meter dimensions (see, e.g., Figure 3) are clearly of the right order of magnitude. The rapid temporal variations, even in the mid to early part of the trail, suggest that the constituent grains are probably quite small.

Two grains of different sizes, even if released into identical initial orbits, will over time separate due to differential radiation effects. The fact that such effects occur rather rapidly compared to the life-times of shower meteoroids accounts for the small number of "grouped" meteors observed. A detailed theoretical modeling is beyond the scope of this paper, but we would point out that some reasonable estimates on the sizes of the fragments would permit an estimate of the time since release. The two most distant observed objects are separated by just over 4 km.

Acknowledgments

Our Mount Allison video-based meteor research program is supported by the Natural Sciences and Engineering Research Council of Canada, and one of the authors (P.A. Piers) was supported by a NSERC Undergraduate Research Award. We are grateful to Dr. J. Jones of the University of Western Ontario who provided on loan the camera which was used for these observations. We acknowledge the Canadian Wildlife Service for assistance with determining migratory bird flight information. We thank an anonymous referee for several excellent suggestions.

Note

We have recorded 47 digitized images of the cluster procession in the form of a 2.5 MB Macintosh digital QuickTime movie. These data are available to other researchers who might be interested in further investigation of this event (contact R.L. Hawkes).

References

[1] Perry S.J., "Meteoric shower", *Nature* 7, 1872, p. 84.

[2] Herschel A.S., "The recent star shower", *Nature* 7, 1873, pp. 185–188.

[3] Chant C.A., "An extraordinary meteoric display", *J. R. Astr. Soc. Can.* 7, 1913, pp. 142–215.

[4] Hoffleit D., "Cosmic double meteors", *Harvard Coll. Observ. Circular* 420, 1937.

[5] Bowden K.R.R., Davies J.G., "The time distribution of meteors", *J. Atmosph. Terr. Phys.* 8, 1957, pp. 62–66.

[6] McCrosky R.E., "Variations from a Poisson distribution of meteors recorded by radar techniques", *Bull. Astron. Inst. Czech.* 8, 1957, pp. 1–4.

[7] Poole L.M.G., "Time distribution of Perseid meteors", *Bull. Astron. Inst. Czech.* 16, 1965, pp. 364–368.

[8] Porubčan V., "On the grouping of meteors in meteor streams", *Bull. Astron. Inst. Czech.* 19, 1968, pp. 316–323.

[9] Brown P., Asher D., Steel D., "The strong meteor display of November 5, 1991", *WGN* 20, 1992, pp. 28–31.

[10] Jenniskens P., Cailloux M., de Lignie M., Kuiper J., "No meteor outburst on November 5, 1991", *WGN* 20, 1992, pp. 28–31.

[11] Blokpoel H., "Bird Hazards to Aircraft", Clarke, Irwin, and Co. and the Canadian Wildlife Service, 1976.

[12] Richardson W.J., "Autumn migration and weather in eastern Canada: a radar study", *American Birds* 26, pp. 10–17.

[13] Hawkes R.L., Mason K.I., Fleming D.E.B., Stultz C.T., "Analysis procedures for two station television meteors", in *Proc. International Meteor Conference 1992*, D. Očenáš and P. Zimnikoval, eds., *IMO*, 1993, pp. 28–43.

[14] Roggemans P., "Letters to *WGN*", *WGN* 20, 1992, pp. 55–57.

[15] Lovell A.C.B., "Meteor Astronomy", Oxford Univ. Press, 1954.

[16] Sarma T., Jones J., "Double-station observations of 454 TV meteors", *Bull. Astron. Inst. Czech.* 36, 1985, pp. 9–24.

[17] Babadzhanov P.B., Wu Z., Williams I.P., Hughes D.W., "The Leonids, Comet Biela and Biela's associated meteoroid stream", *Mon. Not. R. Astr. Soc.* 253, 1992, pp. 69–74.

[18] Robertson M.C., Hawkes R.L., "Wake in faint television meteors", in *Asteroids, Comets, Meteors 1991*, A.W. Harris and E. Bowell, eds., Lunar and Planetary Institute, Flagstaff, AZ, 1991, pp. 517–520.

Received February 1993; revised June 1993; accepted June 1993

Ongoing Meteor Work

Meteor Observations on August 10-11, 1863

Donald W. Olson and Russell L. Doescher, Southwest Texas State University

A review is given of meteor observations made on the night of August 10-11, 1863, at locations in Greece, Poland, Italy, Germany, Belgium, France, England, the United States, and Cuba.

1. Introduction

The meteor observing season in August of 1863 was the first following a passage of Comet P/Swift-Tuttle, as is the case again in August of 1993. To find out what happened in 1863, the authors searched through scientific and popular journals of the day and were able to locate published reports of meteor observations at more than 50 stations on August 10-11, 1863. The 1863 encounter with the meteor stream produced an unusually rich display: a spectacular fireball appeared over northern Italy, groups of observers counted more than 200 meteors per hour in Europe, and group rates exceeded 300 meteors per hour in North America.

2. Observations in Greece on August 10–11, 1863

Johann Friedrich Julius Schmidt (1825–1884), director of the Athens Observatory and a famed lunar observer, was traveling on August 10-11, 1863. He observed the shower maximum from a steamship in the Ionian Sea between Corfu and Ithaca. Schmidt reported the following:

> *Three or four of the larger meteors went down below the horizon of the sea and disappeared there all at once, leaving behind long brilliant fiery paths reflected in the water. Others were remarkable for their beauty and the unusual duration of their trains, which often persisted for 12 to 20 seconds.* [1]

From his position on the ship he could *survey 40% of the visible hemisphere of the heavens.* With this view, Schmidt counted 64 meteors from 21^h to 22^h, 111 meteors from 22^h07^m to 23^h07^m, 105 meteors from 23^h08^m to 0^h08^m, 113 meteors from 1^h to 2^h, and 76 meteors from 3^h01^m to 4^h01^m, expressed in Vienna time. Schmidt saw one great fireball which exploded with a red flash in the southwest at 22^h04^m as the ship was passing the island of Paxoí. [1]

3. Observations in Poland on August 10–11, 1863

Franciszek Karlinski (1830–1906), director of the observatory in Cracow, reported 23 meteors seen between 22^h and 23^h and 136 meteors from 23^h to midnight on August 10, 1863. [2]

4. Observations in Italy on August 10–11, 1863

Caterina Scarpellini (1808–1873) observed at Rome, and contributed many reports to scientific journals throughout the 1850s and 1860s, including a description of the great Leonid storm in November of 1866. On the night of August 10-11, 1863, she watched the falling stars from the Capitoline Observatory, located in a tower overlooking the ancient Roman Forum. Her observing report included the times of appearance for 197 bright meteors (194 of 1st, 2nd, and 3rd magnitude, along with three fireballs) noted from about 20^h to 1^h, local time. She described each of these bright meteors in detail, giving the stars nearest the beginning and end of the path. Most of the activity came near the end of the observing session, with 126 bright meteors logged in the last two hours. However, she acknowledged that many other meteors were missed, in part because they were coming so swiftly. Had she tried to include all the fainter meteors of that night, the *number would have been no less than a myriad, impossible to count.* [3]

Elsewhere in Rome, Father Angelo Secchi (1818–1878) directed the meteor count at the Roman College Observatory. Secchi, best known for his work on stellar spectroscopy, reported 31 meteors logged between 20^h45^m. and 21^h45^m, local time, on August 10, 1863. [4]

In northern Italy, at about 21^h30^m on August 10, 1863, J. Joseph Bianconi saw a spectacular fireball with a long-enduring train:

> *A superb bolide burst forth last night, the 10th of August... I was observing the falling stars from the top of my house located in the countryside along the Torrente Samoggia, a mountain stream halfway between Bologna and Modena. At nine hours and a half, the bolide appeared a small distance to the east of the polar star; it directed its course towards the constellation of the Great Bear, and it disappeared within that of Arcturus... it took on a dazzling brilliance and its light, which was white at first, then became an azure violet of a marvelous beauty, accompanied by an extremely strong luminosity... its disk, at the maximum of its incandescence, equaled one-sixth of the lunar disk... the train, at first straight and later bent and serpentine, remained visible for about three minutes. Not any sound manifested itself to our ears: all was in silence. Our eyes were enchanted by the beauty of this spectacle... The people who were on the roads saw the entire countryside illuminated. More strongly than that of the moon, the brilliant light of this bolide cast very distinctly the shadows of trees and of the surrounding objects.* [5]

Observers over much of northern Italy saw the spectacular fireball of August 10, 1863. Giulio Casoni observed it at Bologna [6]. According to Bernhard von Wüllerstorf-Urbair at Venice, the great fireball's track began in Corona Borealis and continued to Scorpius [7]. Based on the observed parallax, triangulation indicated that the fireball first appeared about 100 km above the Earth's surface and disappeared at a height of about 30 km. The direction of motion indicated that this was a shower member [7].

5. Observations in Germany on August 10–11, 1863

Eduard Heis (1806–1877), a professor at Münster and a famed observer of meteors and the zodiacal light, organized the count in Germany. According to Heis, the August meteor season was *extraordinarily rich* in 1863:

> *The several observers commanded every direction of the compass and the zenith. The observers themselves drew the paths on the prepared maps, while the secretary noted the time in Münster mean time (to the nearest second), the magnitude, and other details. On the 10th of August the falling stars followed so quickly one after another that those fainter than third or fourth magnitude could no longer be reckoned in the count. Each time a falling star was seen simultaneously by two or more observers, it was noted down only once. Remarkable were the extremely bright trains of the falling stars on the 10th of August and their long duration.* [8]

Even counting only the brighter meteors, the rate at Münster reached 166 meteors per hour between 23^h and midnight on August 10, 1863. [2]

Heis had sent out requests to other schools to participate in the count, and he later published detailed reports from nine other stations located in and around Westphalia. Of these, Headmaster Neuhaus and his students at Gaesdonk reported the highest rates, with 105 meteors counted from 21^h17^m to 22^h, 210 meteors from 22^h to 23^h, and 248 meteors from 23^h to 0^h09^m, on August 10-11, 1863 [2]. The result from the last interval is equivalent to 216 meteors per hour.

6. Observations in Belgium on August 10–11, 1863

The observations in Brussels were organized by Lambert Adolphe Jacques Quetelet (1796–1874), a noted meteor authority and the Secretary of the Royal Academy of Belgium. Quetelet himself watched one-third of the sky and counted 23 meteors from 21^h to 22^h and 33 meteors from 22^h to 23^h, local time. During the following hour he was succeeded by his son, Ernest Quetelet, and Charles Hooreman. Despite some interference from nearby trees and a building, those two observers were able to command a view of about two-thirds of the sky and recorded 112 meteors between 23^h and midnight. [9]

In Ghent, F.J.F. Duprez (1807–1884) noted that the *falling stars observed on the night of the 10th and the 11th of August were very numerous.* Duprez watched a clear part of the sky between the north-northeast and the southeast, equivalent to about one-sixth of the heavens. Even with this limited view, he was able to count 32 meteors between 22^h and 23^h and 73 meteors between 23^h and midnight, local time, on August 10, 1863. He added that *most had a center of emanation in the part of the sky occupied by the constellations of Cassiopeia and Perseus.* [10]

7. Observations in France on August 10–11, 1863

At Paris, a total of 739 falling stars were counted during an observing run of 5.75 hours, centered on midnight. After applying various correction factors, Rémi Armand Coulvier-Gravier (1802–1868) reported this as equivalent to 121.2 meteors per hour at midnight, local time. [11]

8. Observations in England on August 10–11, 1863

The *British Association for the Advancement of Science* published a report describing activity at eleven stations in England. The detailed tables published by the Association included 38 pages giving the time, magnitude, color, duration, position and direction, and other remarks for each bright meteor of August 10-11, 1863. [6]

Relatively little attention was paid to determining hourly rates. Instead, the focus of the British Association in 1863 was multiple-station work, in which *observations were made at the Greenwich and Cambridge Observatories, at Cranford and Euston Road Observatories, and at Hawkhurst, for determining the heights and velocities of the annual shooting-stars of this period.* The summary report concluded that the average height of first appearance of the meteors was about 81.6 miles (131 km) and that they typically disappeared at about 57.7 miles (93 km) above the surface of the Earth. The mean geocentric velocity was given as 34.3 miles per second (55 km/s). [6]

The observers at Hawkhurst, Kent, were John F.W. Herschel (1792–1871) and Alexander S. Herschel (1836-1907), the son and the grandson of William Herschel, the discoverer of Uranus. John Herschel later wrote that the *meteors observed on the 10th of August were magnificent, extremely numerous and very brilliant. Almost all left long luminous trains which diverged from a point near B Camelopardalis.* [12]

The Association Report for 1862–63 stated that the radiant was not far from the star γ Persei on August 10, 1863 [6]. The British Association also published another analysis which used 120 paths and determined that the position of the radiant was near the star k Persei on August 10-11, 1863 [7].

Several letters about the meteors appeared in *The Times of London.* Thomas Crumplen, of the Euston Road Observatory in London, wrote a letter while the shower was taking place on August 10, 1863, and described the observations up to 23^h:

> THE AUGUST METEORS ... *There has been a perfect shower of these strange bodies to-night, and from observations made here we estimate that they fell at least at the rate of 200 per hour. Of course it was absolutely impossible to record all seen, but all appeared to diverge from about one radiant.* [13]

A few days later, Crumplen added the following:

> THE AUGUST METEORS ... *There is reason to believe that this has been one of the finest displays for many years.* [14]

Another Times correspondent, W.S.B. at Taunton, gave the following account in a letter dated August 11, 1863:

> "FIERY TEARS" OF ST. LAWRENCE ... *Last night, a little after 10 o'clock, and within the space of a quarter of an hour or twenty minutes, I must have seen at least 200 shooting stars, some of considerable brilliancy.* [15]

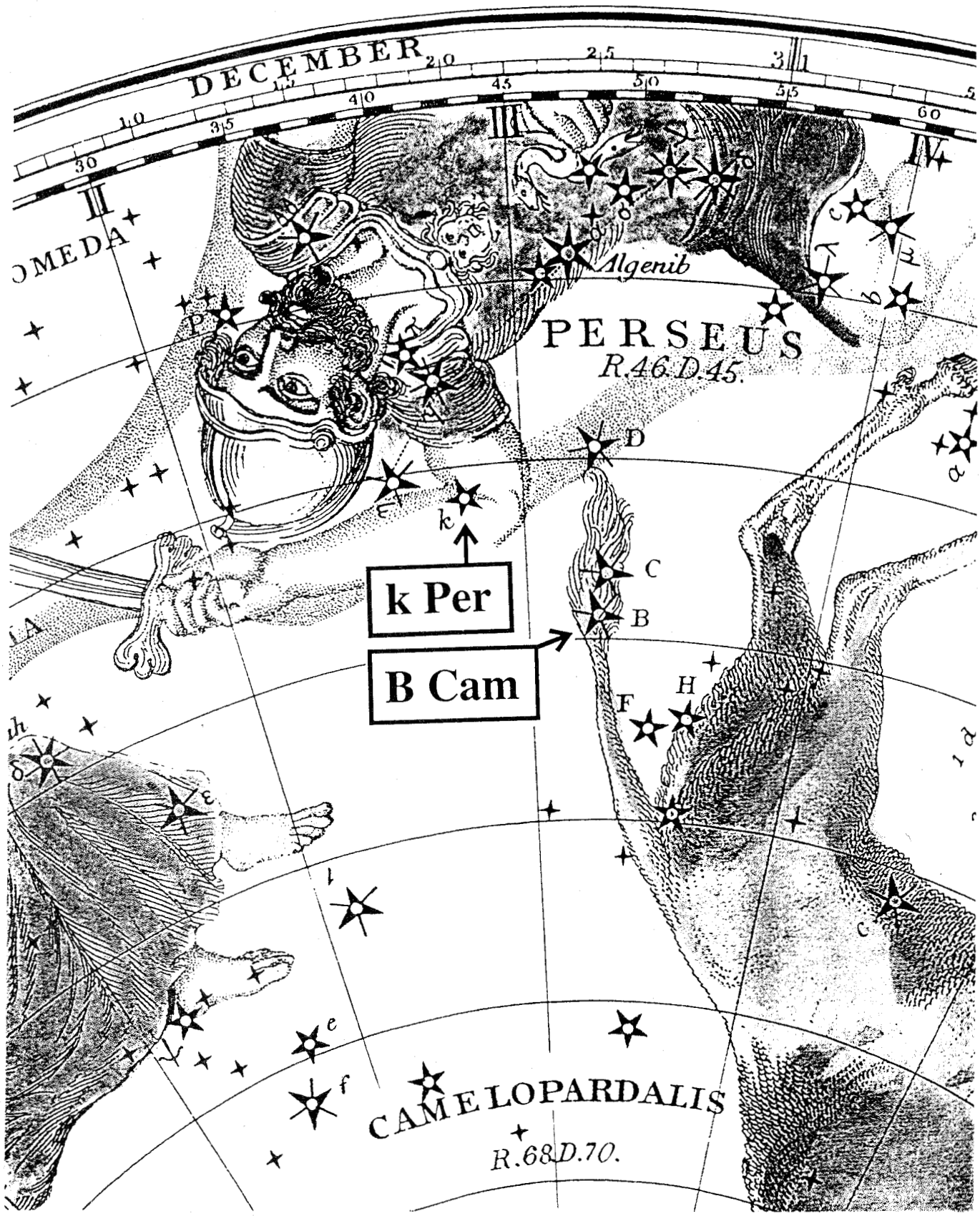

Figure 1 – On August 10-11, 1863, John Herschel placed the radiant near the star *B* Camelopardalis, shown on this 19th-century star chart. Another British analysis of meteor paths from that same night determined that the radiant was near the star *k* Persei.

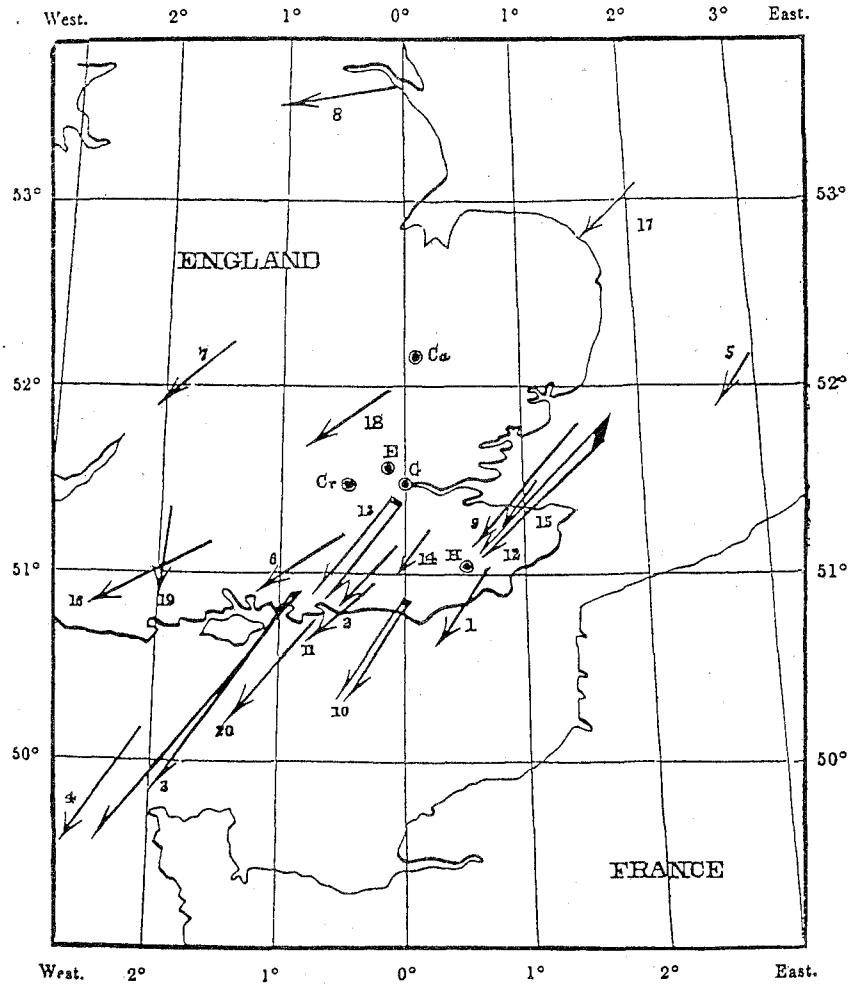

Figure 2 – This map appeared in the 1863 *British Association for the Advancement of Science Report* and shows trajectories of multiply-observed meteors, mostly Perseids.

W. Frank Lynn of Esher, in another letter dated August 11, 1863, stated the following:

> THE METEORS OF AUGUST 10 ... *Last night, at 10 minutes to 11 precisely, as I was proceeding home, my attention was attracted by a sudden blaze of light... caused by a large and most remarkable meteor, seemingly about one-sixth the diameter of the moon... I observed the same evening that the sky was full of smaller meteors of the ordinary description... so many, indeed, that scarce a minute passed without 12 or 14 being visible.* [15]

9. Observations in the United States on August 10–11, 1863

According to the American Journal of Science for 1863,

> *The Committee upon Periodical Meteors of the Connecticut Academy of Arts and Sciences have this year undertaken a more extended system of observations than in any year preceding... a stellar chart suited to observations at all times was prepared by Prof. H.A. Newton, of the Committee, and distributed to observers at various stations, together with instructions for observing at the August period.* [16]

The journal published reports from 19 stations in the Eastern and Central United States. [17]

For example, a group of 4 observers at Natick, Massachusetts, counted 164 meteors between 23^h and midnight, local time, on August 10, 1863. The multiple observers took care so that no meteors were counted twice. The Natick report stated that the radiant fell in the triangle between the stars η, γ, and τ Persei.

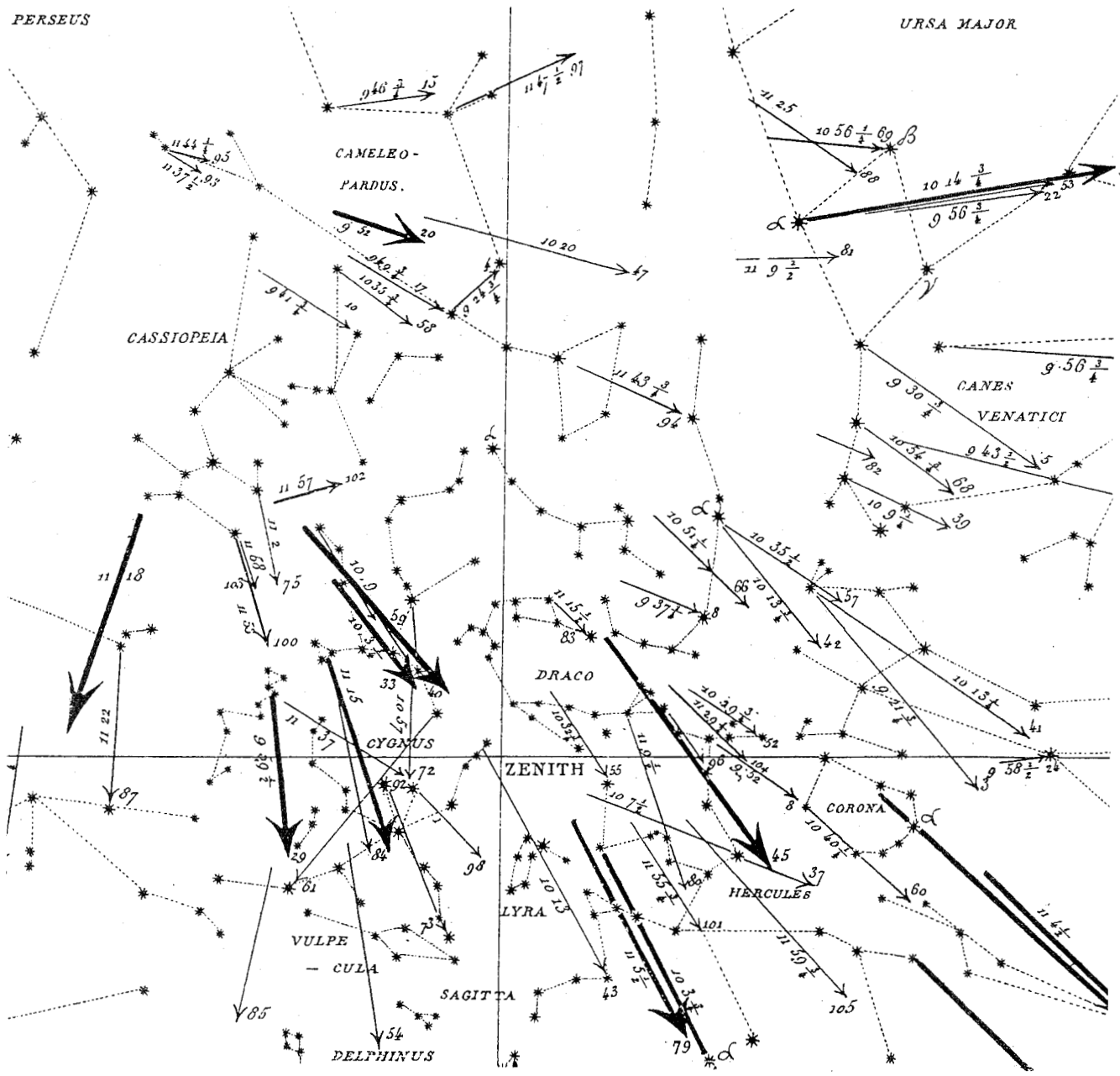

Figure 3 – This chart, which appeared in the *Bulletin de l'Académie Royale des Sciences* (Brussels) for 1863, is based on observations made at Hawkhurst, England, between 21^h18^m and midnight, local time, on August 10, 1863. The observers were John F.W. Herschel and Alexander S. Herschel.

Alexander C. Twining (1801–1884) was in the party at New Haven, Connecticut, where clouds interfered with the count on August 10, 1863. However, at 22^h25^m, local time, Twining saw a stationary meteor and used it to place the radiant *near the sword handle of Perseus*, which is traditionally figured near the Double Cluster, h and χ Persei.

A large observing group at Williamstown, Massachusetts, counted 162 meteors between 23^h and midnight, local time, on August 10, 1863. At Manchester, Maine, Joseph G. Pinkham and E. Pope Sampson counted 150 meteors between midnight and 1^h, local time, on August 11, 1863.

The group at Hartford, Connecticut, reported the strongest activity. Hubert Anson Newton (1830–1896) of Yale University personally directed this group, which included several associates from Yale. The six observers, *counting aloud to prevent duplication*, recorded 153 meteor flights during the half hour from 3^h10^m to 3^h40^m, local time, on August 11, 1863. The report states that the *moon, the clouds near the horizon, and the twilight somewhat diminished the number.* Nevertheless, the Hartford count for this half hour is equivalent to 306 meteors per hour.

10. Observations in Cuba on August 10–11, 1863

In Havana, Cuba, on the night of August 10-11, 1863, Andrès Poey watched the northern sky, while Ricardo Zenoz was charged with observing towards the south. The two observers tabulated 31 meteors between 23^h and midnight, 24 meteors from midnight to 1^h, 48 meteors from 1^h to 2^h, and 25 meteors from 2^h to 3^h, local time. Poey stated that the *great majority of the falling stars radiated from Cepheus and Cassiopeia.* [18]

11. Conclusion

It is likely that there are more reports to be discovered in the literature. The preceding accounts definitely show enhanced meteor activity on August 10-11, 1863, with group rates at some locations exceeding 200 and even 300 meteors per hour.

References

[1] Schmidt J.F.J., "Meteore im August und September 1863", *Wochenschrift für Astronomie*, October 7, 1863, pp. 314–317.

[2] Heis E., "Die Sternschnuppen der August-Periode 1863 in Westfalen und Umgegend", *Wochenschrift für Astronomie*, November 18, 1863, pp. 363–366.

[3] Scarpellini C., "Sur les étoiles filantes du 10 août 1863", *Bulletins de l'Académie Royale des Sciences*, 2nd series, 16, 1863, Brussels, pp. 297–305.

[4] Secchi A., "Sulle stelle cadenti del 10 Agosto 1863", *Bullettino meteorologico* 2, 1863, pp. 157–158, and *Les Mondes* 3, 1863, pp. 562–563.

[5] Bianconi J.J., "Sur un bolide qui a éclaté à Bologne, le 10 août 1863", *Bulletins de l'Académie Royale des Sciences*, 2nd series, 16, 1863, Brussels, pp. 313–314.

[6] Glaisher J. et al., "Report on Observations of Luminous Meteors, 1862-63", *Report of the British Association for the Advancement of Science*, 33rd meeting, 1864, pp. 209–339.

[7] Glaisher J. et al., "Report on Observations of Luminous Meteors, 1863-64", *Report of the British Association for the Advancement of Science*, 34th meeting, 1865, pp. 1–101.

[8] Heis E., "Die August Periode der Sternschnuppen", *Wochenschrift für Astronomie*, August 19, 1863, pp. 258–259.

[9] Quetelet L.A.J., "Observations des étoiles filantes, faites pendant la période du milieu du mois d'août 1863", *Bulletins de l'Académie Royale des Sciences*, 2nd series, 16, 1863, Brussels, pp. 286–295.

[10] Duprez F.J.F., "Étoiles filantes périodiques du 9 et du 10 août 1863, observées à Gand", *Bulletins de l'Académie Royale des Sciences*, 2nd series, 16, 1863, Brussels, pp. 295–297.

[11] Coulvier-Gravier R.A., "Résultats des observations d'étoiles filantes, faites durant le maximum des 9, 10, et 11 août, avec les résultats des jours qui l'ont précédé et suivi", *Comptes Rendus* 57, 1863, pp. 403–404.

[12] Herschel J.F.W., "Sur les étoiles filantes du 10 août 1863", *Bulletins de l'Académie Royale des Sciences*, 2nd series, 16, 1863, Brussels, p. 306.

[13] *The Times of London*, August 11, 1863.

[14] *The Times of London*, August 14, 1863.

[15] *The Times of London*, August 13, 1863.

[16] Twining A.C., "Observations of the August Meteors", *American Journal of Science*, 2nd series, 36, 1863, pp. 301–302.

[17] Newton H.A., "Summary of observations of shooting stars during the August period, 1863", *American Journal of Science*, 2nd series, 36, 1863, pp. 302–306.

[18] Poey A., "Étoiles filantes observées à la Havane du 24 juillet au 12 août, et remarques sur le retour périodique du mois d'août", *Comptes Rendus* 58, 1864, pp. 119–124.

The Occurrence of Sporadic-E and Noctilucent Clouds, and Correlations with Meteor and Auroral Activities, May to August, 1977–1991

Alastair McBeath

An analysis of 15 years of Sporadic-E and noctilucent cloud results is examined with especial regard to correlations with the occurrence of meteor and auroral activities. A complex pattern is revealed in which it seems probable major meteor shower maxima play an important role in providing input of metallic ions and solid dusty material. Possible broad-scale scenarios for the formation of Sporadic-E and noctilucent clouds are suggested.

1. Introduction

In the northern hemisphere, the radio propagation mode Sporadic-E is especially prevalent from May to August in most years, and often creates major interference problems for amateur radio meteoricists trying to observe three of the year's strongest "daytime" meteor streams active during June: the Arietids, ζ-Perseids and β-Taurids. The amateur literature contains many colloquial reports of possible associations between Sporadic-E and meteor showers, and this link is borne out by professional results too (e.g., [1]). Another radio propagation mode, Auroral-E, can be similar to Sporadic-E at times, which produces obvious problems of interpretation. The two are separate, but again, occasional references to a link can be found. Other observers have suggested, in a tentative way, the possibility that Sporadic-E and noctilucent clouds may have a common origin, while meteoric dust may well be a chief source of nuclei for noctilucent clouds. As far as the author is aware, however, no attempt has been made to look for possible correlations between all four phenomena, particularly over a number of years. This paper sets out to try to redress that situation. In the following four sections, all times and dates refer to a typical northern hemisphere (specifically British) site.

2. Sporadic-E (Es)

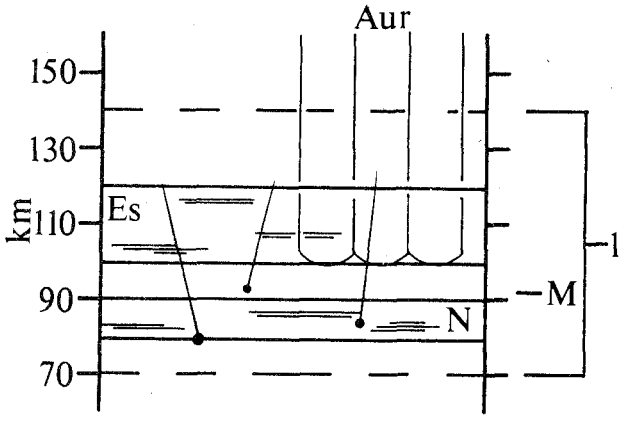

Figure 1 – Cross-section through part of the Earth's atmosphere, showing the regions of Es, NLC (N), meteor (the main region of meteor ablation is shown by three meteor trails; the zone numbered 1 gives the maximum limits of most visual meteor occurrence) and auroral (Aur—extends up to 1000 km) activity discussed in this paper. The letter M indicates the approximate height of the mesopause, which separates the lower mesosphere from the overlying thermosphere.

Sporadic-E (Es) occurs as a localized enhancement of the E-layer ionization, lying between approximately 100–120 km altitude (see Figure 1), sufficient to allow the propagation of HF and VHF radio signals. The enhanced regions are, on average, roughly 1 km thick, and occur as irregular sheets up to about 100 km in lateral extent. As the name suggests, the appearance of Es is quite unpredictable, although it is commonest from April to September, and two diurnal activity peaks are noticeable from longer time-series observations, at about 11^h30^m UT and about 17^h UT. Es is usually absent between approximately 0^h and 6^h UT each day, and from December to February [2]. Other recent data have indicated possible short and long-term repetitive patterns for Es displays of approximately 5–6 days and 5–6 years duration [3].

Ionized sheets of Es are believed to consist of metallic ions, probably largely of meteoric origin, which are thought to be able to form into dense patches through the action of wind shear and atmospheric internal gravity wave mechanisms.

Auroral ions may be able to form Es as well, especially when solar/auroral activity is high. References [2] and [4] have more details on Es formation theories.

In addition to the time constraints outlined above, the Es sheet has to be so-located that propagated communication will be possible—i.e., the sheet must lie roughly between the transmitting and receiving stations. Communication is possible in this way up to distances of about 4000 km or so, although this, and the actual detection of Es, are also somewhat frequency-dependent. At a relatively low VHF frequency, such as 50 MHz, Es occurs on virtually all days during the main May–August "season," and contact up to the maximum distance is possible. Near sunspot maximum, the E-layer may be sufficiently ionized that propagation can take place even in the absence of Es, however, albeit genuine Es events seem to be fewer at such times too. At higher VHF frequencies, Es numbers show a tendency to fall, and the contact range also diminishes, implying that a greater ion concentration is required to propagate these signals. At 144 MHz, for instance, Es events are rather less common, but those events which can be detected may well represent major peaks in Es formation, and therefore may correlate better with other activities. Even at 144 MHz, communication up to about 2500 km may be feasible.

Indeed, 144 MHz was the frequency selected for examining Es here, partly because major Es activity peaks are probably thus indicated (this is borne out by works such as [3]), but partly because UK data for this frequency from 1977–1991 were recently published by Toms [5]. Toms used results from various radio magazines and journals, primarily contributed by the amateur community, in compiling his work.

3. Noctilucent clouds (NLC)

Noctilucent clouds (NLC) are best observed from the Earth's surface, since they are physically and optically thin (typical cloud sheet thicknesses are of the order of approximately 1 km), and they are thus most readily seen against a relatively dark background. The daytime sky is too bright for them to be visible, but they can be observed in the sky's twilight arch on some nights from May to August, at sites between $\varphi \approx 50°$–$65°$, when the Sun lies between 6° and 12° below the horizon. The clouds shine by scattering direct sunlight, since they form at a far greater height (about 80–90 km, just below the mesopause—see Figure 1) than the more usual tropospheric clouds, whose maximum elevation is generally about 12 km.

NLC are composed of minute, reflective ice crystals. Water vapor, although not plentiful at these heights—estimates suggest about 3 ppm is reasonable—freezes rapidly once it condenses, as the air temperature at about 80–90 km is around 100–150 K, much colder than the regions adjacent to this layer. Water freezes at about 140 K at these heights. The actual condensation nuclei as determined from rocket flights through NLC fields appear to be of three main types: meteoric dust, metallic ions (probably of meteoric origin) and some volcanic dust/aerosols. Uncertainty remains as to the origin of all of these nuclei, due to the detection techniques employed, as NLC are extremely difficult to examine in situ [6]. In addition to [6], a further good, brief review of NLC is [7].

Visual observations of NLC made from UK sites using the method as described in [8] were extracted from annual reports of NLC activity [9–23] for this analysis. Negative nights, that is, nights on which two or more observers reported clear skies with no visible NLC, were also taken from those years' data which featured such notes.

4. Meteor activity

From Sections 2 and 3, it is clear that a number of meteoric by-products, whether dust or ions, are required to permit Es and NLC to form, at least in part. We need to consider here two main types of meteoric input, micrometeoroids and the normal meteor flux producing the vast bulk of objects observed.

Meteoroids of mass smaller than, say, 10^{-7} g decelerate so rapidly on entering the Earth's upper atmosphere that they cannot heat up enough to ablate, and thus probably form a significant

Auroral ions may be able to form Es as well, especially when solar/auroral activity is high. References [2] and [4] have more details on Es formation theories.

In addition to the time constraints outlined above, the Es sheet has to be so-located that propagated communication will be possible—i.e., the sheet must lie roughly between the transmitting and receiving stations. Communication is possible in this way up to distances of about 4000 km or so, although this, and the actual detection of Es, are also somewhat frequency-dependent. At a relatively low VHF frequency, such as 50 MHz, Es occurs on virtually all days during the main May–August "season," and contact up to the maximum distance is possible. Near sunspot maximum, the E-layer may be sufficiently ionized that propagation can take place even in the absence of Es, however, albeit genuine Es events seem to be fewer at such times too. At higher VHF frequencies, Es numbers show a tendency to fall, and the contact range also diminishes, implying that a greater ion concentration is required to propagate these signals. At 144 MHz, for instance, Es events are rather less common, but those events which can be detected may well represent major peaks in Es formation, and therefore may correlate better with other activities. Even at 144 MHz, communication up to about 2500 km may be feasible.

Indeed, 144 MHz was the frequency selected for examining Es here, partly because major Es activity peaks are probably thus indicated (this is borne out by works such as [3]), but partly because UK data for this frequency from 1977–1991 were recently published by Toms [5]. Toms used results from various radio magazines and journals, primarily contributed by the amateur community, in compiling his work.

3. Noctilucent clouds (NLC)

Noctilucent clouds (NLC) are best observed from the Earth's surface, since they are physically and optically thin (typical cloud sheet thicknesses are of the order of approximately 1 km), and they are thus most readily seen against a relatively dark background. The daytime sky is too bright for them to be visible, but they can be observed in the sky's twilight arch on some nights from May to August, at sites between $\varphi \approx 50°$–$65°$, when the Sun lies between 6° and 12° below the horizon. The clouds shine by scattering direct sunlight, since they form at a far greater height (about 80–90 km, just below the mesopause—see Figure 1) than the more usual tropospheric clouds, whose maximum elevation is generally about 12 km.

NLC are composed of minute, reflective ice crystals. Water vapor, although not plentiful at these heights—estimates suggest about 3 ppm is reasonable—freezes rapidly once it condenses, as the air temperature at about 80–90 km is around 100–150 K, much colder than the regions adjacent to this layer. Water freezes at about 140 K at these heights. The actual condensation nuclei as determined from rocket flights through NLC fields appear to be of three main types: meteoric dust, metallic ions (probably of meteoric origin) and some volcanic dust/aerosols. Uncertainty remains as to the origin of all of these nuclei, due to the detection techniques employed, as NLC are extremely difficult to examine in situ [6]. In addition to [6], a further good, brief review of NLC is [7].

Visual observations of NLC made from UK sites using the method as described in [8] were extracted from annual reports of NLC activity [9–23] for this analysis. Negative nights, that is, nights on which two or more observers reported clear skies with no visible NLC, were also taken from those years' data which featured such notes.

4. Meteor activity

From Sections 2 and 3, it is clear that a number of meteoric by-products, whether dust or ions, are required to permit Es and NLC to form, at least in part. We need to consider here two main types of meteoric input, micrometeoroids and the normal meteor flux producing the vast bulk of objects observed.

Meteoroids of mass smaller than, say, 10^{-7} g decelerate so rapidly on entering the Earth's upper atmosphere that they cannot heat up enough to ablate, and thus probably form a significant

fraction of the meteor dust flux in the atmosphere as a whole. These micrometeoroids are primarily of sporadic origin, although some may come from telescopic/radio or weak visual showers, and the flux can probably be roughly illustrated by a combined index of minor shower and sporadic activity.

Meteoroids whose mass exceeds the micrometeoroid level, up to about 10^{-2} g, which form the majority of such particles producing detectable meteors encountered by the Earth generally, ablate between heights of around 80–120 km above the surface (see Figure 1), although friable stone-type bodies, for example, may start to radiate at about 140 km altitude on occasion. The actual height depends on the meteoroid's physical and chemical structure, but particularly on its velocity [24,25]. Higher velocity particles normally begin and end their flight at a greater altitude than slower-moving ones. See Table 1.

Table 1 – Results of a survey of 15 visual meteor showers from [25], correlating velocity ranges in km/s with the mean beginning and end heights in km for the number of showers in each velocity bin.

Velocity range	Begin height	End height	Nr. of showers
11–31	99.4	82.4	5
32–51	100.8	86.5	6
52–71	118.8	95.0	4

Since meteor ablation produces a column of ions approximately 1 m in diameter and usually more than 10 km long [24]—using the 15 showers from Table 1, the mean atmospheric path length for these sources is about 18 km—this sets a number of parameters concerning where in the atmosphere shower meteors possessing certain characteristics may be expected to initially input most of their dust and/or ions. At times away from major shower maxima, mean values are liable to dominate, thanks to the overall superior abundance of randomly-distributed sporadic meteors over the lower activity of the minor streams. From May to August, an average of 6 visually or forward-scatter-radio detectable showers are active every day [27], for instance. This velocity-height factor may well thus only be of importance at a major shower peak, if then. Again, an index similar to that described above for micrometeoroids should usefully define the likely effect of all but the main shower peaks.

Based on *IMO* data, it was decided to include only those 26 showers which are believed to produce definite rates during May–August at the present time. These are essentially as detailed in [27]. Checking other streams lists (e.g., [28]) did not reveal any further potentially significant contributions, nor were any unusual, definite, one-off or extraordinary northern hemisphere shower returns uncovered during the period in question, with the exception of the Perseid returns of 1980, 1981, and 1991, when above-normal activity did take place. The showers selected for this analysis are detailed in Tables 2 and 3. Sporadic values used here were extracted from [29].

5. Aurorae

Auroral activity can be detected at times between 100 and 1000 km altitude, and it has long been suggested that heating of the atmosphere by aurorae directly above the region where NLC form, may cause the NLC ice-crystals to melt or sublimate, thus the cloud-field should dissipate. In recent years, however, a number of simultaneous NLC/auroral events have been observed, casting doubts on the reality of this effect.

Aurorae produce large amounts of ionization in the upper atmosphere, which can be dense enough to allow short-wave radio propagation by the Auroral-E mode [30], and may also give rise to ionization capable of producing Es sheets too. Radio amateurs have commented on difficulties in separating Es from Auroral-E on occasion, although Auroral-E propagation signal tones are normally considered unique. It is conceivable some ionization may aid NLC formation too, although this is unknown at present.

Table 2 – Visual meteor showers treated as significantly active, May–August. Details include the meteoroidal atmospheric velocities (V) in km/s, and the solar longitude, $\lambda_\odot$ (eq. 2000.0), active to (<), from (>) or between.

Shower	Activity	V	$\lambda_\odot$	Notes (from [25,26,27])
Virginids	Low	30	< 69°	Late activity from several sources
Sco/Sgr Complex	Low	~ 30	< 122°	10 minor maxima; best is α-Scorpids, $\lambda_\odot \approx 43°$
α-Bootids	Very low	20	< 52°	Late activity only
η-Aquarids	High	67	< 67°	Main peak in early May, $\lambda_\odot \approx 43°$
June Lyrids	Low/none?	30	80°– 90°	Occasional outbursts?
June Bootids	Low/none?	14	95°– 99°	Rarely strong; may no longer encounter Earth
Pegasids	Low?	70	105°–109°	Little studied
July Phoenicids	Very low	47	93°–116°	Stronger radio source; southerly radiant ($\delta = -45°$)
Piscis Austrinids	Low	35	107°–144°	Southerly radiant ($\delta = -30°$)
δ-Aquarids (S)	Moderate	42	106°–146°	Low activity other than near peak ($\lambda_\odot \approx 126°$); peak may vary, and is probably not sharp
α-Capricornids	Low	26	101°–152°	Weak shower
ι-Aquarids (S)	Very low	34	113°–152°	Very weak
δ-Aquarids (N)	Low	42	113°–152°	Ill-defined peak
Perseids	Very high	57	115°–151°	Activity high at $\lambda_\odot \approx 138°$–141°; good returns in 1980, 1981 (?), and 1991 (brief outburst)
κ-Cygnids	Low	23	131°–158°	Weak shower
ι-Aquarids (N)	Very low	36	> 139°	Very weak
π-Eridanids	Very low	59	> 147°	Very weak
α-Aurigids	Low	66	> 151°	Pre-peak phase
Piscids (S)	Low	26	> 143°	Early activity only

Table 3 – Same as Table 2, for radio showers.

Shower	Activity	V	$\lambda_\odot$	Notes (from [25,26,27])
ε-Arietids	Low		< 66°	Weak; Taurid Complex stream?
May Arietids	Low		44°– 76°	Weak
o-Cetids	Moderate		45°– 72°	Peak falls between $\lambda_\odot = 54°$–64° and may be irregular
Arietids	High	37	61°–100°	Peak rates good at $\lambda_\odot = 76°$–78°
ζ-Perseids	High	29	59°–103°	Sharp maximum around $\lambda_\odot = 79°$
β-Taurids	Moderate	30	75°–115°	Flat maximum from $\lambda_\odot = 94°$–100°; Taurid Complex stream
γ-Leonids	Low		> 142°	Weak

Radio and visual aurorae need not—in fact, often do not—occur simultaneously, but major storms will usually be capable of producing both, and thus both forms of aurora need to be considered in seeking correlations with Es and NLC, since positive or negative results would be of equal interest. Auroral data from UK mainland sites observed during May–August, 1980–1991, were obtained from [31–42] for use in this paper. Visual aurorae were detailed from [31] onwards, but radio observations were only recorded after this reference. Radio auroral frequencies were not stated for each event, but were between 50 and 144 MHz in all cases.

6. Analysis methods

Having collected the raw data from the sources given earlier, all items were processed to reduce their dates of occurrence to the nearest degree of solar longitude (eq. 2000.0). This was to allow the direct comparison of all the various observations without any calendrical problems. After this first stage was completed, a number of calculations were performed to give statistically useful information from the observations.

For Es and NLC, probabilities of occurrence were worked out for each one-degree interval of solar longitude over the entire 15-year period, stated as a percentage. Since the period length is fixed, and each interval will contain an integer value between 0-15, the percentage values end up as one of a set of figures from 0.0, 6.7, 13.3, 20.0, 26.7, 33.3, etc., up to 100.0. In practice, the percentage values should not then be taken literally, but they can be used to show which solar longitude, if any, are more likely to exhibit Es or NLC.

A further refinement was possible in the subsidiary 9-year period from 1983 to 1991 for NLC only, as during this time, routine negative dates, when NLC was not observed in clear skies, were reported. Here, it was practical to introduce a crude level of certainty indicator to each solar-longitude point having either definite positive, negative, or both, NLC sightings. Again, this "error" value was stated as a percentage, based on the number of years in each interval of solar longitude for which data were available. As before, these percentage figures cannot be taken as absolutes, but simply as probabilities. Although no negative Es dates were recorded, a set of Es percentage occurrence data were prepared from 1983 to 1991 too, for comparison with the NLC results. Negative Es observations are in any case very difficult to ascertain—see Section 11 below.

Next, the strength of each observed Es and NLC display was rated using a simple 1-2-3 scale, with "1" a weak, short-lived or faint event and "3" a major, extensive or bright display. The mean activity strength per unit solar longitude was then computed for the whole period from 1977–1991 using a negative NLC data point as equal to zero where this information was available.

Statistics on the numbers and strengths of displays per year were also produced, together with overall means and totals at this stage, along with tables of these figures per degree of solar longitude for each year.

The following step was to derive a rough mean index of meteor activity from May to August. It was decided that the best way to achieve this, in the absence of precise data for a sufficient length of time, and bearing in mind the arguments in Section 4 above, was to take the sporadic CHRs from [29], and add directly to that a rate of one meteor per hour per shower active during the appropriate solar-longitude intervals from [27]. Major shower peaks were then added in, using their most recently-obtained mean ZHR levels (primarily taken from [27]). Although a very crude method, this has the advantage that the overall likely meteor activity can at least be indicated from this index, and important showers can be judged relative to one another. It is clear from radio work (e.g., [43]) that daylight showers during June are probably responsible for one of the most active spells of meteor activity in the whole year. This is well-illustrated by Figure 11.19 in [44, p. 11.18], itself based on 24-hour back-scatter radio counts obtained by Millman, which indicates that meteor rates from $\lambda_{\odot} = 76°$–$86°$ (eq. 1950.0) are exceeded only briefly by Geminid peak counts in December from the whole year. June and July are the most active months for radio meteors, judging by these results. Recent *IMO* forward-scatter radio work also shows these general points [45]. The implication is that there may well be other showers active during June and July which have not been identified at present, or that the daytime shower maxima may be more sustained than expected. It is even possible that Es and meteor-scatter radio propagation modes are overlapping or being confused with one another to produce the observed patterns. With these uncertainties, the qualified use of the index described above was felt advisable.

After this, auroral activity, both visual and radio, were reduced to the correct solar longitudes and visual displays were allocated a strength number using the same criteria as outlined for Es and NLC displays earlier. Radio auroral strengths were not stated in the sources used, so a measure for them was not possible. As before, annual totals and means were computed at this stage too.

The final step in the analysis was to plot these results out as graphs, which are given, with other details, in the following four sections.

7. Overall display probabilities

Figure 2 shows the probabilities of Es and NLC displays during 1977–1991, together with a superimposed graph of the crude meteor activity index.

Several points are immediately apparent. Firstly, both the Es and NLC distributions are very uneven, and neither run the full length of the May–August period, in particular seeming to peter out after $\lambda_\odot \approx 144°$ or so. The "spiky" nature of occurrence shown by both graphs strongly suggests that whatever mechanisms actually cause Es or NLC, they are not often capable of sustaining either beyond a matter of hours or so. Intervening tropospheric clouds may account for some of these features with NLC, but cannot be employed as an explanation for the Es distribution.

With Es, if mid-summer insolation of the atmosphere is a primary source of the ionization, a symmetrical distribution about the solstice ($\lambda_\odot = 90°$), or with a peak after that event if the ionization needs time to build up, might be expected. This is not what is seen. The center of Es activity overall falls at $\lambda_\odot \approx 93°$, only slightly displaced from the solstice, but the occasions when Es is consistently more likely all fall before this time. The main phase seems to run from $\lambda_\odot \approx 66°$–$100°$, with a moderately strong secondary phase from $\lambda_\odot \approx 105°$–$119°$. Lesser activity runs between $\lambda_\odot \approx 45°$–$64°$ (very sporadically) and $\lambda_\odot \approx 122°$–$150°$ (rather more reliably, especially between $\lambda_\odot \approx 122°$–$135°$).

As NLC are chiefly observed due to scattered sunlight in the mid-summer twilight arch of the sky, it might be supposed that if NLC were equally likely to be present on any occasion, again a symmetrical pattern about the solstice should be seen. Once more, this is far from the case found here. The central solar longitude for all NLC occurrences is actually at $\lambda_\odot \approx 99°$, while the main phase of NLC activity runs from $\lambda_\odot \approx 74°$–$134°$. All the nights most likely to yield NLC occur after the summer solstice, except one, and that gives the highest probability of all (around 73%). It actually takes place at $\lambda_\odot \approx 90°$ itself. This may be due to greater observer activity—particularly of the more casual observers—on the northern hemisphere's shortest "night" (i.e., period of darkness), however, rather than any genuine peak in NLC formation. Two other phases are apparent in the NLC graph, from $\lambda_\odot \approx 45°$–$71°$ (strongest) and $\lambda_\odot \approx 137°$–$149°$ (very weak), both producing generally lower likelihoods of NLC events. These divisions, for Es and NLC, are somewhat arbitrary, but do seem to indicate real patterns.

There is no clear instant correlation between Es, NLC and meteor activity, although the peaks of the Arietids, ζ-Perseids, β-Taurids and Southern δ-Aquarids all happen near times of greater Es and NLC probability. The o-Cetid maximum also coincides with a peak in NLC occurrence at $\lambda_\odot \approx 59°$. Further discussion of this subject is given under Section 11 below.

8. Display probabilities, 1983–1991

Figure 3 shows Es and NLC display probabilities for the period during which routine negative-date NLC data were recorded. An approximate measure of the reliability of the various NLC features is obtained as a result, although the Es points are plotted simply for comparison. Even so, the Es results are consistent with those for the full period.

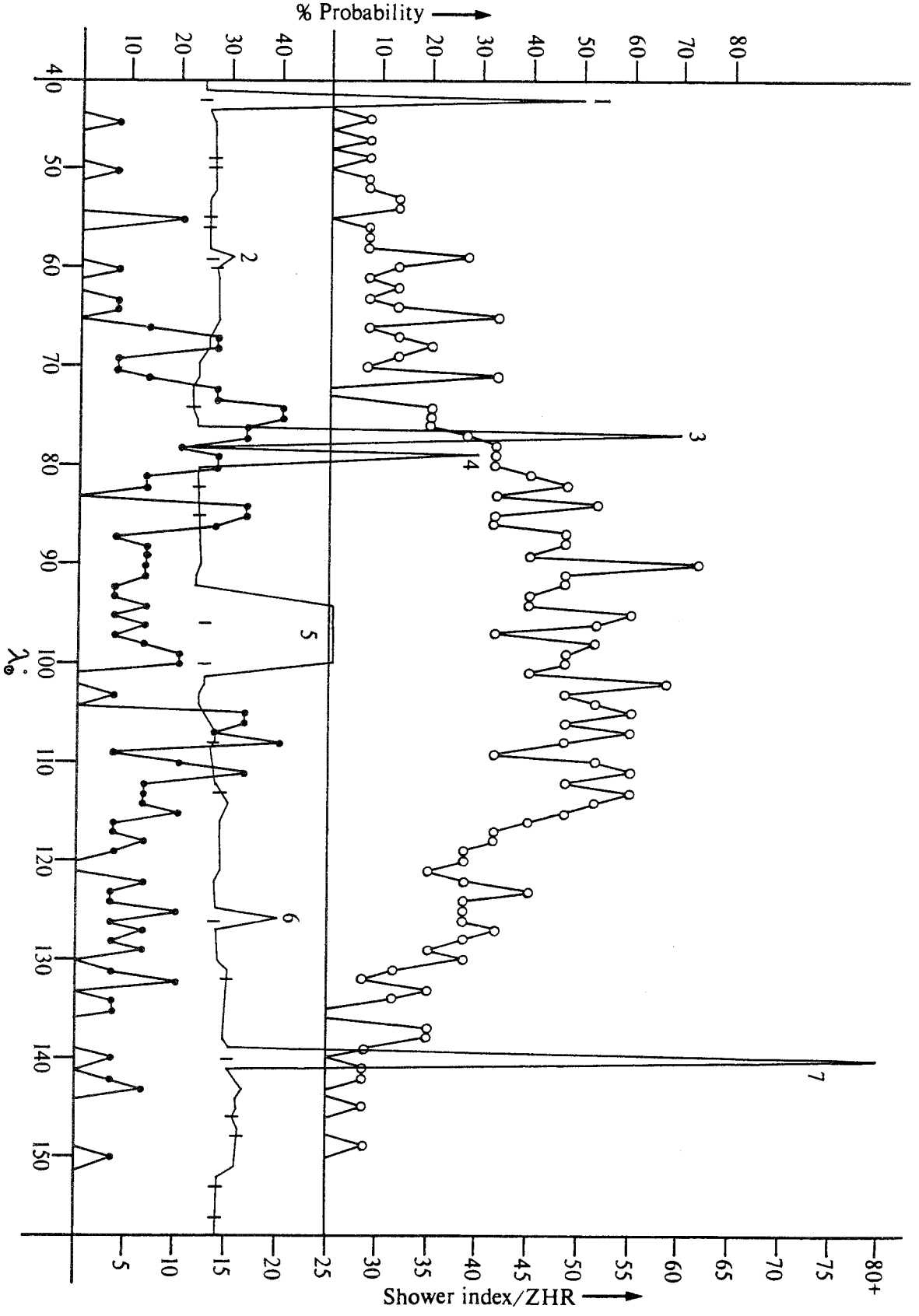

Figure 2 – Es (lower—filled circles) and NLC (upper—open circles) display probabilities, 1977–1991. An approximate meteor activity index (thin line—ticks indicate minor shower maxima) has been added to help show up possible correlations. The major shower peaks are (1) η-Aquarids, (2) o-Cetids, (3) Arietids, (4) ζ-Perseids, (5) β-Taurids, (6) Southern δ-Aquarids, and (7) Perseids.

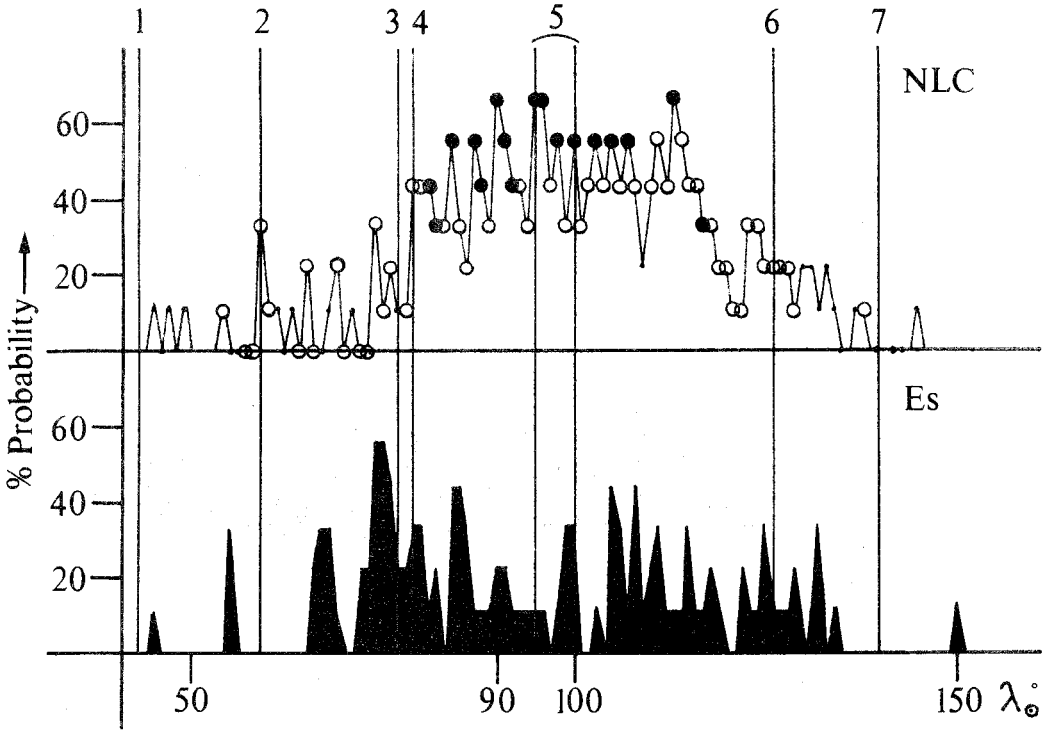

Figure 3 – Es (lower—filled line) and NLC (upper) display probabilities, 1983–1991, giving rough values for the certainty involved with each NLC data point (only). Filled circles carry a 67%+ probability of producing the observed percentage of displays, open circles between 33% and 66%, dots less than 33%, and blank points indicate no data available. Note that this applies equally to occasions with and without NLC present, so also shows up which times are less likely to yield NLC. Major meteor shower peaks are also illustrated.

Similar trends are found to Figure 2. The Es center here is at $\lambda_\odot \approx 95°$, while the NLC mid-point is at $\lambda_\odot \approx 99°$. Main activity phases run from $\lambda_\odot \approx 66°$–$100°$ and $\lambda_\odot \approx 74°$–$134°$ respectively, with lower activity beyond these ranges. Again, a strong secondary Es phase occurs between $\lambda_\odot \approx 105°$–$119°$, while all the most likely times for NLC fall at or after the solstice. Note that the prominence of the solstice peak has diminished to equal the better other NLC peaks. Since these results, featuring the negative night reports, are probably the most reliable information on NLC overall, this may well be significant.

Correlations between the *o*-Cetids, ζ-Perseids, and β-Taurids and greater NLC probabilities seem reasonable, and Es peaks are not far from the Arietid, ζ-Perseid, β-Taurid, and Southern δ-Aquarid maxima too.

In all, these NLC data tend to support the reliability of the entire 1977–1991 period results, implying that the peaks, troughs and general patterns found can be regarded as correct, at least to a first approximation.

9. Display strengths, 1977–1991

Figure 4 gives the Es and NLC display strengths per unit solar longitude. The NLC strengths are moderated by the factoring-in of negative occasions (strength = 0), but both graphs must be viewed in the light of the display probabilities shown in Figure 2. A single strength 3 display on one date, for example, can give a highly anomalous result, as clearly shown by the Es peak at $\lambda_\odot = 140°$, which took place at the unusually high Perseid maximum of 1991. Es data, where negative events were not recorded, are especially prone to this problem.

The strongest activity is likely before the solstice for Es, although the highest peak (ignoring that at $\lambda_\odot = 140°$) falls at $\lambda_\odot \approx 108°$, coincident with the greatest occurrence probability in the secondary phase, noted in Section 7 above.

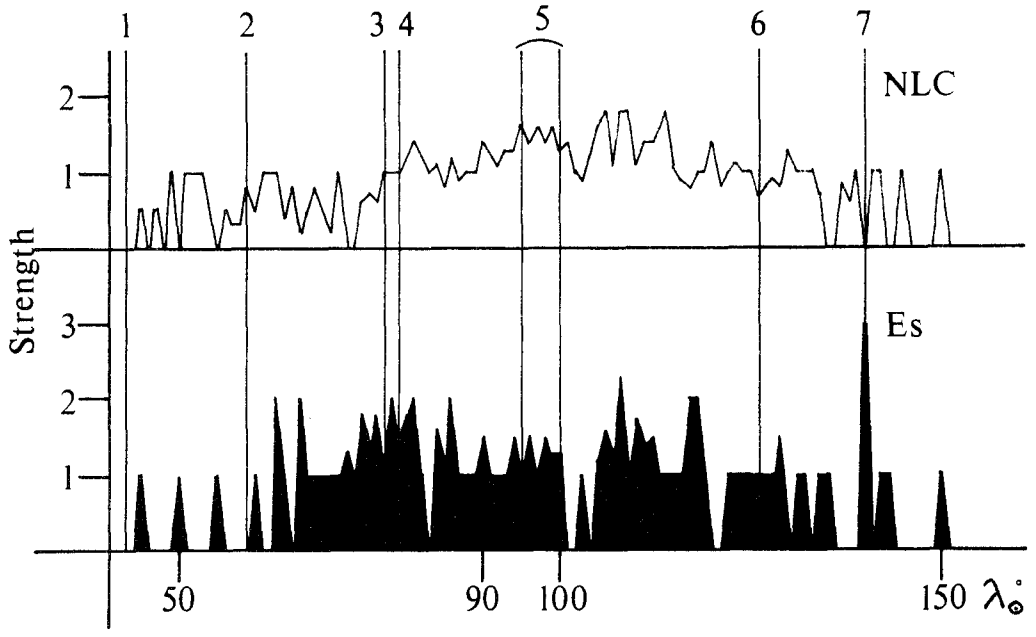

Figure 4 – Es (lower—filled line) and NLC (upper) mean display strengths per degree of solar longitude, 1977–1991. Negative nights (strength = 0) have been applied to the NLC results only. The main meteor shower maxima are shown too.

NLC strengths seem to consistently, if irregularly, increase with time, until $\lambda_\odot \approx 114°$, when a relatively rapid fall-off starts to happen. The brightest displays seem to take place about 1° of solar longitude later than the most probable dates for NLC occurrence. Note also the coincidence of stronger displays with the extended β-Taurid maximum from $\lambda_\odot \approx 93°$–$101°$.

Table 4 gives the annual breakdown of numbers of display strengths for Es and NLC.

Table 4 – Breakdown of numbers of Es and NLC display strengths per year, 1977–1991. Overall percentages (%) are given too, as are the mean numbers per year (N).

Year	Es				NLC			
	1	2	3	Total	1	2	3	Total
1977	5	3	0	8	29	16	3	48
1978	14	2	0	16	22	8	6	36
1979	2	1	0	3	20	5	3	28
1980	2	3	0	5	13	7	1	21
1981	7	3	1	11	25	7	2	34
1982	5	1	1	7	18	5	1	24
1983	17	4	1	22	12	2	2	16
1984	5	2	1	8	9	2	1	12
1985	10	4	0	14	9	3	2	14
1986	9	2	0	11	26	3	3	32
1987	23	7	2	32	26	3	0	29
1988	7	3	3	13	20	9	2	31
1989	3	0	3	6	29	8	1	38
1990	9	3	0	12	16	4	2	22
1991	5	0	1	6	17	6	0	23
Total	123	38	13	174	291	88	29	408
%	72.2	23.6	4.2		71.3	21.6	7.1	
N	7.4	2.4	0.4	10.3	19.4	5.9	1.9	27.2

The mean display strength for Es was 1.37, while for NLC, this figure was 1.36 (not allowing for strength = 0—i.e., negative date—events). These figures and the total percentages of each display strength are remarkably similar, suggesting the possibility that some form of genuine link is present, although this is insufficient evidence on its own to support such a link. As we might predict, bright or strong displays are relatively uncommon, compared to the medium-weak events. The mean numbers of each strength class of display are also interesting, as the NLC figures are roughly three to four times higher than those for Es in each category (class 3, having the smallest number of events, is not unexpectedly slightly adrift from this pattern, but not by too large a margin). This pattern is not as obvious in most individual years.

Figure 5 plots graphically the mean display strengths per year. Neither line shows a great variation from the mean, the somewhat greater deviation for the Es results due presumably to their lower overall numbers. There is a very slight suggestion of a gradually lessening mean strength for NLC displays, compared to a slight indication of an increase in the mean Es strength over the entire fifteen year period.

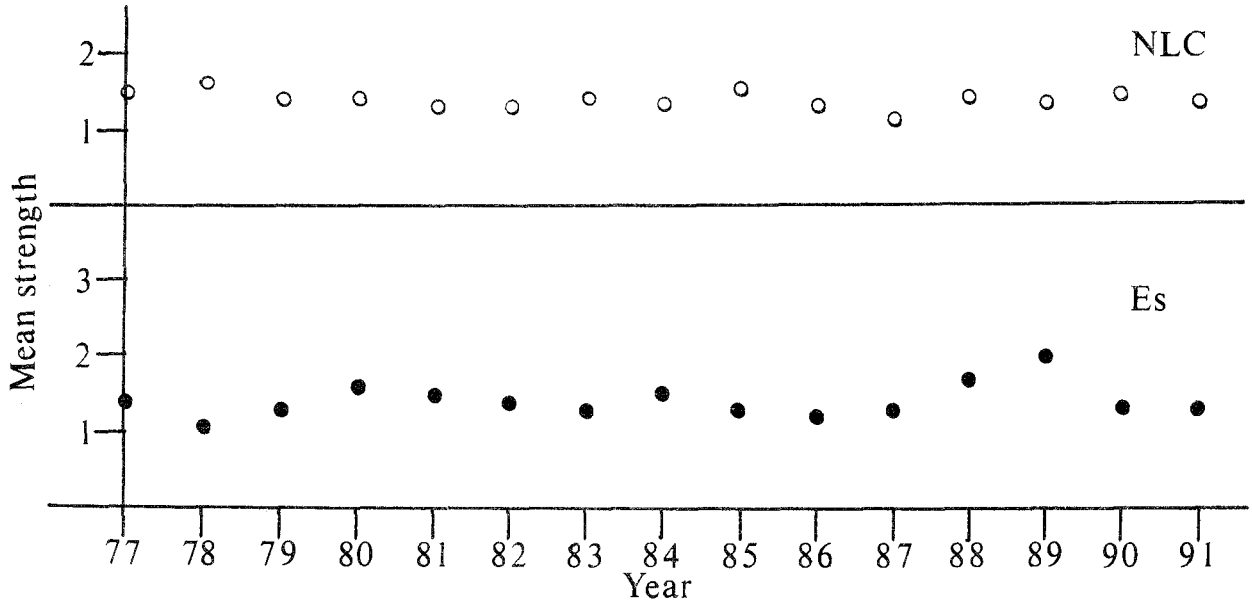

Figure 5 – Es (lower—filled circles) and NLC (upper—open circles) mean display strengths per year, 1977–1991.

10. Numbers of displays per year, 1977–1991

Figure 6 shows the numbers of Es and NLC displays recorded in each calendar year, based on reports from May to August only. A line indicating the annual Mean Daily Frequency (MDF) for sunspots, extracted from *JAS* Solar Section results published between July 1977 and February 1992 in *JAS Circulars* 81–168, is also appended. References for these sunspot numbers are too numerous to mention here, but can be supplied to those seriously interested on request.

Correlations between these three graphs are not immediately apparent, but Es activity seems to reach a peak a year or two before solar maximum, and again about halfway through the declining phase of the sunspot cycle. NLC displays appear quite regularly in the lower solar activity stages, and only drop significantly as the sunspot peak approaches. NLC do seem to take some time to recover after solar maximum, however, and seem to reach a trough only one or two years before sunspot minimum. The 1981 NLC peak may be viewed as somewhat anomalous, occurring so soon after the solar peak, especially as preliminary results from the similar solar cycle period in 1992 [46] suggest lower NLC numbers than in 1991. The solar cycle has an important effect on atmospheric ionization generally (cfr. [44]), which needs to be considered in an examination such as this, although the effect on Es and NLC numbers is not in-step with the higher ionization levels expected near solar maximum, as has already been discussed.

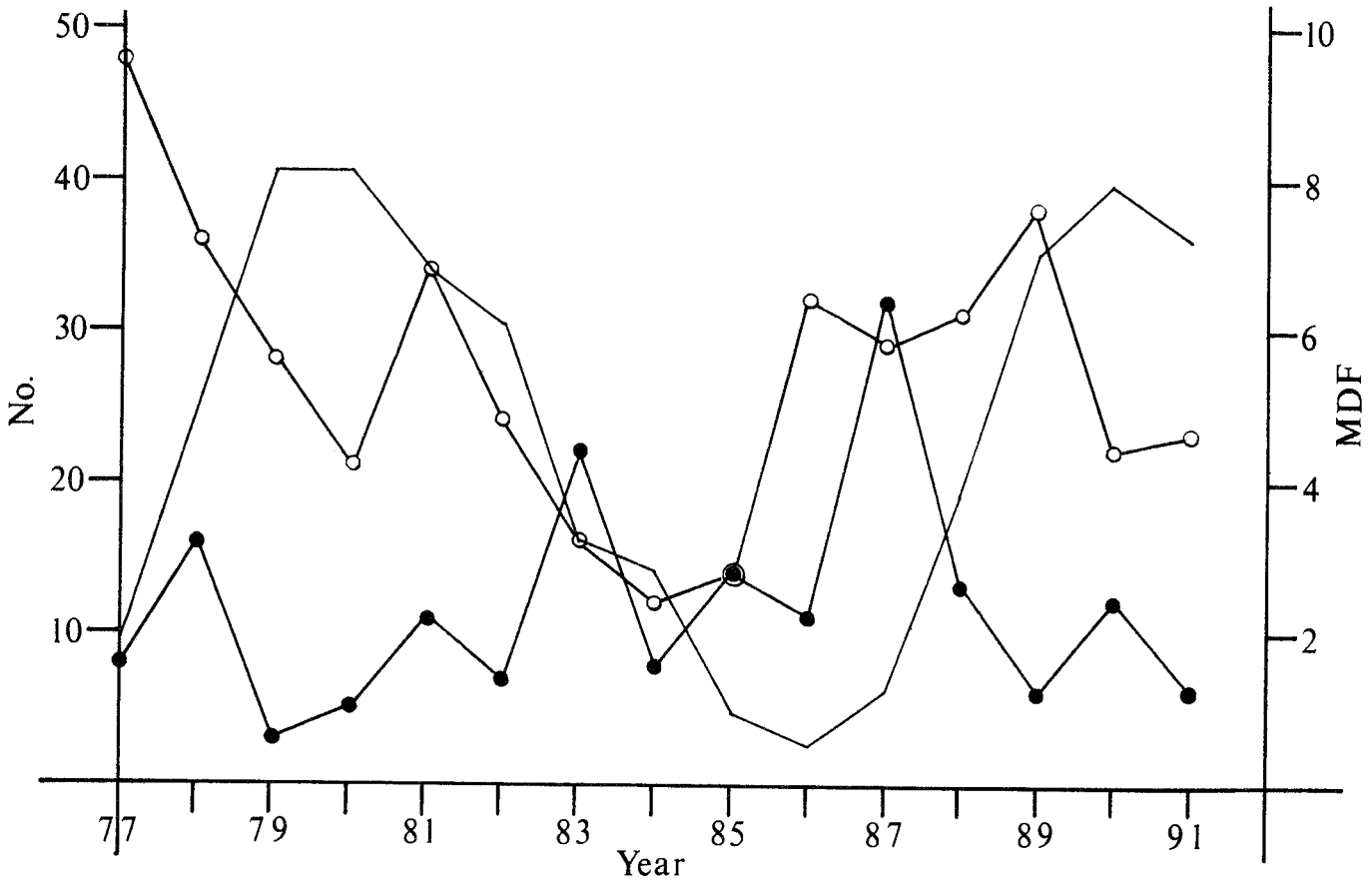

Figure 6 – Es (filled circles) and NLC (open circles) display numbers per year, 1977–1991. A simplified MDF sunspot curve (unmarked line) for the period has been added.

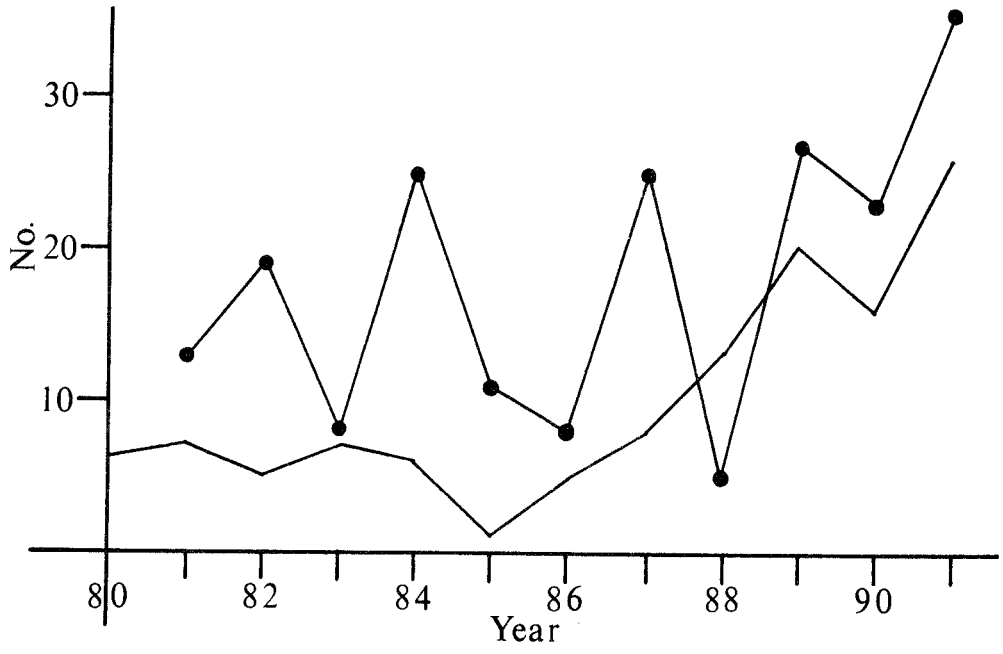

Figure 7 – Visual (unmarked line) and radio (filled circles) aurorae recorded between May and August from 1980 (visual) and 1981 (radio) to 1991.

Figure 7 illustrates the numbers of visual and radio auroral events detected from May to August in each year from 1980 (visual) or 1981 (radio) to 1991. This graph can be directly compared to Figure 6.

Table 5 gives the strength classes for visual auroral displays from 1980 to 1991.

Table 5 – Display strengths for visual aurorae seen May–August, 1980–1991. Overall percentages (%) and mean numbers per year (N) are noted as well.

Year	1	2	3	Total
1980	1	4	1	6
1981	2	2	3	7
1982	1	2	2	5
1983	1	0	6	7
1984	6	0	0	6
1985	0	0	1	1
1986	0	1	4	5
1987	3	2	3	8
1988	8	1	4	13
1989	12	1	7	20
1990	9	4	3	16
1991	7	11	8	26
Total	50	28	42	120
%	41.7	23.3	35	
N	4.2	2.3	3.5	10

Visual auroral sightings, though depressed in numbers due to the difficulty of their observation in the brightly-twilit summer skies, do tend to show a pattern typical of the expected overall behavior of mid-latitude aurorae, i.e., a twin peak to either side of the sunspot maximum, and a trough around solar minimum. The greater numbers of reported events in more recent years may well be a result of increased observer activity and auroral awareness, following several campaigns to highlight the appearance and characteristic features of aurorae since the mid-1980s, but larger numbers of visible aurorae, apparently representative of genuinely more events taking place, have been consistently reported during Cycle 22, up until 1992. The pattern shown tends to loosely mirror, to within a year or so, the trends found in the NLC curve. An approximate antiphase correlation is suggested, compared to Es, but this is not at all clear. The various auroral display strengths indicate no real tendencies, but events do seem to polarize towards either weak or strong ones, perhaps due largely to the problems with twilight observing.

Radio aurorae register a very irregular pattern of occurrence, similar to the "spiky" nature of the annual Es numbers graph. A trough coincident with sunspot minimum, and peaks to either side of Cycle 22's maximum are obvious enough, but other, almost random-seeming highs and lows feature throughout the eleven years of data. These features fail to correlate significantly, or with any real repetition, with either the Es or NLC lines. Indeed, both clear phase and antiphase correlations between radio auroral numbers and Es numbers are seen from 1981 to 1985 (antiphase) and 1986 to 1988 (in phase), for example.

11. Discussion

Sections 6–10 above have established several main periods of Es and NLC activity, but have also raised a number of points and problems needing further discussion.

Firstly, we have the difficulty of establishing definite negative Es reports. Forward scatter radio work generally, including Es, meteor scatter and Auroral-E propagation modes, is nothing like so clear-cut as visual observing, for instance. A visual event can either be detected or not, and a negative report under good circumstances usually indicates a definite absence of the phenomenon. With radio observing, a negative report simply shows no contact was possible at that time, with that specific equipment and frequency set-up, not that the phenomenon was actually absent. The fact that peaks and troughs can be defined in the Es graphs at all, speaks volumes for the ability, dedication and persistence of the radio observers.

Then there is the lack of an immediate correlation between meteor activity and Es/NLC events, although the *o*-Cetid and β-Taurid maxima do coincide with NLC peaks found in the analysis. Interestingly, the Arietid, ζ-Perseid and Southern δ-Aquarid peaks all occur within 2°–6° of solar longitude of NLC maxima too. The correlation with Es events is much poorer, although the 1991 Perseid peak, like the 1946 Draconid storm [43], produced Es for several hours at a major shower maximum. This does not seem to happen with every unusual shower return, however. It is conceivable that occasionally Es and NLC could be produced simultaneously by meteor activity, based on the above statements. More normally, as has been established for some time, there is a delay between meteor activity and Es occurrence, amounting to some 6–15 days on average, but possibly longer [47], which, if allowed for, would bring Es peaks well into line with origins due to to the η-Aquarids (Es-$\lambda_\odot \approx 55°$), *o*-Cetids (Es-$\lambda_\odot \approx 66°$–$69°$), Arietids/$\zeta$-Perseids (Es-$\lambda_\odot \approx 84°$–$86°$+), and the β-Taurids (Es-$\lambda_\odot \approx 105°$–$119°$—very approximately). The Es peak around $\lambda_\odot \approx 126°$ coincides quite well with the Southern δ-Aquarid maximum without the need for any shift. Once shifted, the Es-$\lambda_\odot \approx 132°$ is a better fit for this shower, leaving the $\lambda_\odot \approx 126°$ peak anomalous, along with the far more significant major Es peak at $\lambda_\odot \approx 71°$–$82°$. The highest part of this latter peak will fit to the *o*-Cetids by invoking a 15–16 day shift, however, which is not beyond the realms of possibility. This may mean the *o*-Cetids and possibly the Southern δ-Aquarids give rise to two Es peaks, of course. One further point is worth mentioning here. A shift of 14–16 days would produce a near-perfect coincidence between virtually all the main NLC and Es peaks from NLC-$\lambda_\odot \approx 59°$–$150°$. We shall return to this topic at the end of this section.

Meteor activity is relatively constant during the May–August period at a background level (i.e., sporadics and minor showers), and even the lesser shower peaks seem to have little influence on the observed Es and NLC distributions. The pattern compared to the major shower peaks is very different, however, as has been indicated already. The contribution of meteoric input to improving the chances of occurrence as well as the strengths of displays produced seems quite marked, although it would have been interesting to compare the very active visually-observable η-Aquarids and Perseids to Es and NLC activity, if these showers had taken place away from the outer fringes of the chief "seasons." The velocity/height relationship for meteors commented on in Section 4 above is probably of little importance, as already suggested, but further data, particularly for the Perseids, might have revealed differences from the results found here. The fact that the *o*-Cetids, β-Taurids and Southern δ-Aquarids coincide best with NLC and the shifted Es peaks does imply that lower, but sustained, meteor activity is a more important contributor than a large, but short-lived, flux. The exception may be when very high rates manifest for a short time (e.g., the 1991 Perseids).

Looking at display strengths, there is the possibility that a gradual build-up of material, whether dust or ions, may be represented, especially by the NLC data. This is rather less obvious from the Es results, which may well be linked to more immediate causes of material loss for whatever reason. With NLC, brighter events appear to trail the most likely times of occurrence by one day, which again perhaps suggests some form of "collection" mechanism for material in the NLC zone. NLC strength is also apparently boosted by the β-Taurids in particular, with a greater degree of consistency over time than is present at any other stage during the NLC "season."

Since the total mean strengths and relative proportions of both Es and NLC were so similar, a link between their formation mechanisms can at least be implied, although other causes could well give rise to comparable effects. That such a similarity is found at all is not wholly unexpected, as additional features support this view, e.g., sheet nuclei particles and their origins. The fifteen-year strength trends are very slight, Es perhaps increasing, NLC decreasing, but only a longer time-series of results would be liable to confirm these changes.

The assumed negative link between solar/auroral activity and NLC had already begun to be questioned in recent years, with several simultaneous aurora/NLC sightings taking place, and the number of photographic reports of these have increased notably since the late 1980s. Higher

solar activity does seem to promote a fall-off in NLC events, but in Cycle 22, this drop took place at a somewhat later stage than in Cycle 21. Es activity peaks shortly before and after solar maximum, although events are generally commoner close to solar minimum. These points are much as expected from previous results, and although there is some suggestion of a 4–6 year "cycle" for both Es and NLC, and a shorter 4–8 day "cycle" within the summer's activity, these are not really convincing, and the conclusions for Es from [3] are not well-confirmed by this present paper. The general annual trends are reasonably similar, however, which implies there is some global mechanism at work, since the data in [3] were obtained from Texas, USA, and covered a very different area of the world to those used here.

The peak in NLC found in 1981, very soon after solar maximum, is unusual, and does not appear to have recurred in 1992 at a comparable stage in the present solar cycle. The slight increase in 1991 may represent this feature, however, especially bearing in mind that subsequent solar cycles do not repeat exactly, nor at equivalent times, whereas the NLC "season" is effectively fixed by the conditions of twilight illumination.

Radio aurorae numbers seem to fluctuate almost at random from year to year, perhaps as a result of their detectability. It was not felt feasible to try to correlate this phenomenon further with the other subjects under consideration, except in a general way.

Es and NLC trends from year to year are broadly similar, but there are often smaller-scale contradictions. The state of the Earth's upper atmosphere in preventing or promoting Es formation—and as with many radio propagation modes, these conditions may well be quite exacting, see for instance the discussion of over and underdense radio meteor trails in [48]—may well be critically important here.

Finally, we return to the 14–16 day shift of Es relative to NLC, which creates a reasonably good coincidence in activity peaks, as shown earlier. The following notes propose a possible sequence of events which may give rise to this pattern. This is likely to be superimposed on an underlying, lower-level of activity, produced by the constant influx of sporadic and minor shower meteors, as well as solar/auroral ions.

Initially, Es forms as a result of the input of mainly meteoric ions after a major shower peak. This may take up to two weeks to occur, and the concentration of the ions is likely to be due to wind shears and/or internal gravity waves [47,2,4]. These sheets, or the particles comprising them, then descend to the NLC level, and there act as at least part of the nuclei for NLC formation a further two weeks later. The lifetime of these ions must therefore be at least four weeks. This is a not unreasonable length of time from theoretical studies (e.g., [47]). The implied fall-rate for such ions would be an average of about 2.7 km/day, although it is not at all certain the fall-rate would be constant. Though most studies show both Es and NLC tend to descend over time, EISCAT radar observations have detected ascending Es areas too [49]. This could add to the overall time delay, both for Es and NLC via Es formation, and may be capable of creating multiple, or enhanced subsequent, Es events, if it takes place regularly. Wind speeds and directions are also very different to one another only a few kilometers apart in the upper atmosphere, particularly vertically, so sufficient transportation and collection mechanisms for the ions are apparently present. It is even possible that weather systems, such as are found lower in the atmosphere, exist at these heights too, affecting exactly what can happen in this region (cfr. [6]).

Meteoric dust input seems able to reach and concentrate in the NLC layer, and acts as condensation nuclei there, very quickly after major meteor shower maxima, giving rise to NLC within a few days at most. Then follows the "Es-ion" NLC circa two weeks later, but as time progresses, this pattern will become more complex, if indeed it is ever this simplified in the first instance, with both meteoric dust and ions mixing to produce NLC. A gradual build-up of, perhaps, residual material would naturally help produce the post-solstice skew found in NLC probabilities.

As internal gravity waves are known to affect NLC (the characteristic, short-amplitude, billow wave-formations in NLC in particular illustrate this, as well as the longer amplitude bands and complex—turbulent?—whirl forms), there is also the intriguing possibility that NLC nuclei may be carried back up to the Es layer, for a further repeat performance. This is far from proven, however.

So far, this analysis has dealt solely with statistical results, which are not necessarily open to only one interpretation. The logical next step following on from the above proposals, was to plot out the Es, NLC and auroral data for each year, looking for actual, not simply statistical, correlations.

12. Annual Es and NLC occurrence, 1977–1991

Figure 8 contains the plots of the actual occurrence of Es, NLC and auroral displays per degree of solar longitude per year, with a simplified meteor index showing only the maxima of the seven main showers during this period. In studying these graphs, it must be borne in mind that not all displays will be recorded, either visually or by radio, due to poor observing conditions or the requirements for radio propagation not being met. It is therefore quite likely that not every event will appear to produce a correlation, as suggested by the preceding section.

Up to around 1981, there seems to be a coincidence of Es and NLC at roughly the same time. However, in most of these years, a 7–15 day shift would also allow equally good—in some cases better—coincidences to be made. The 1982–1986 data would generally benefit from such a shift, but the unprecedented burst of radio aurorae during the early part of the 1987 "season" from $\lambda_\odot \approx 65°$–$87°$, seems to have had a highly adverse effect on the strength (though not the numbers) of the NLC displays subsequently, while possibly enhancing the Es events then. With Es so prevalent, almost any coincidence devised can be accommodated, a sound reason for using a statistical base to draw initial conclusions from, rather than individual years. The less intense spates of radio aurorae early in the "seasons" of 1982 and 1984 seem not to have shown this effect.

In 1988, a return to the pre-1982 pattern seems to occur, while the lack of Es in 1989 makes correlating the results difficult for that year. The three main Es peaks during 1989 also took place very close to a spell of radio aurorae. 1990 is suggestive of the desirability of the shift suitable for 1982–1986, while in 1991, a strong burst of radio aurorae seems to have coincided with a reduction in the Es population in that year, and perhaps weakened the NLC displays (e.g., no class 3 NLC events).

Overall, the evidence for a shift of about 7–15 days to bring Es and NLC events together does seem to be present, albeit not especially strongly in several years. The reduced Es numbers in 1989 and 1991 make these years' data unreliable for tracing possible links, although the major Es spike due to the Perseid outburst at $\lambda_\odot = 140°$ is clear enough. Further data are required to help demonstrate or deny the existence of this postulated Es/NLC-meteor link.

Radio aurorae, already found to be somewhat odd in their occurrence, seem to rarely take place in isolation. Groups of events lasting for about 4+ days are relatively common, and with the uncertainties involved, may perhaps produce occasional spurious Es events, or vice versa. Radio aurorae may also boost ion-input to create more Es, and possibly more, but weaker, NLC (perhaps because of the largely ion condensation nuclei for the ice crystals, giving rise to smaller crystals at such times, if this is so. A higher ratio of dust to ions may be required to yield stronger NLC displays in this case). Visual aurorae often do happen as one-off events, and may occur simultaneously with either Es, NLC or neither. Both radio and visual aurorae do sometimes seem to precede NLC events by about one day or so, although once again, this does not undisputably demonstrate a link.

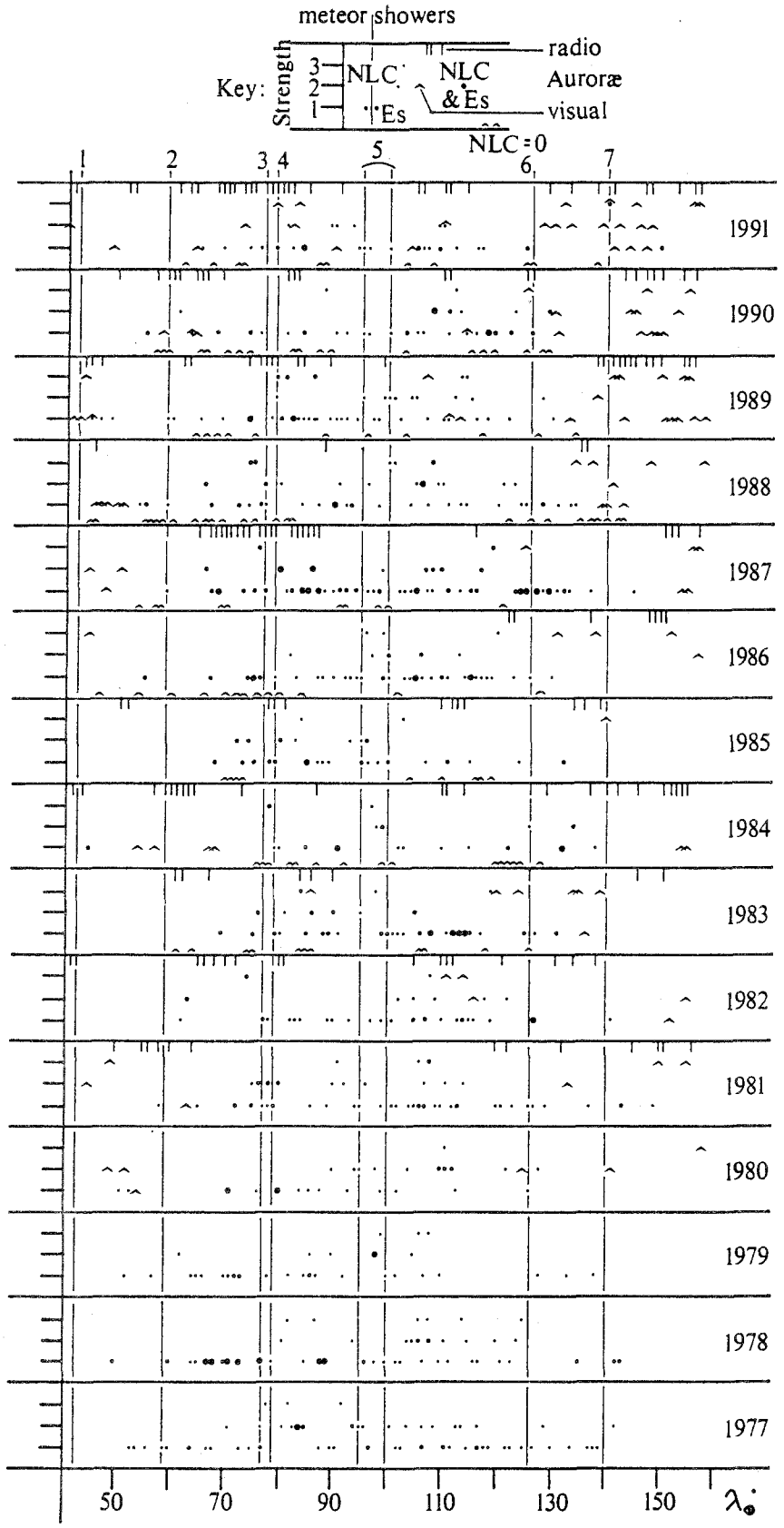

Figure 8 – Es, NLC, visual and radio aurorae per year per degree of solar longitude. The strength of each display is also shown, except for radio aurorae. The maxima of the seven major meteor showers active at this time are drawn-in too. Note that zero points for NLC indicate occasions when no NLC was observed in clear skies.

13. Conclusion

The analysis of fifteen years of Es and NLC with meteor and auroral data essentially confirms the links between meteors and Es found by earlier workers, including the time delay in Es formation of roughly two weeks. Major meteor activity also correlates well with NLC events, and a further link between Es and NLC, again with an average time delay of about a further two weeks, may well have been found. This implies that both meteoric dust and meteoric ions are capable of producing NLC, and thanks to the coincidence of major meteor inputs (e.g., the 1991 Perseids) with high Es peaks, some occasions can clearly produce "instant" Es from meteor debris too. The same meteor activity may give rise to two NLC peaks, one almost immediately, the other delayed until the Es sheet ions descend to the NLC level. Aurorae too may be capable of generating ions suitable for Es and NLC formation, and while the suggestion that NLC will dissipate as aurorae occur now seems less likely, auroral activity may well help moderate the strength of NLC, and perhaps Es too. All of this awaits further confirmatory—or negatory—evidence, and a longer time-series of results, particularly including negative date results for NLC and perhaps even Es, should be worth studying in this regard, when it becomes available.

Acknowledgments

Apart from all the observers, mainly from the amateur astronomical and radio communities, whose contributions over the years have been absolutely essential to this work, I am especially grateful to Mick Toms, for providing the catalyst to nearly ten years of considering these topics with his article on Es results [5], to the *IMO*'s Radio Commission Director Jeroen Van Wassenhove for help with the radio data, both meteor and Es, but particularly to the *BAA* Aurora Section's Assistant Director Dr. David Gavine for advice, encouragement, invaluable discussions of these subjects, and assistance in obtaining many of the NLC references.

References

[1] L. Neuzil, "Meteoric influences on the Sporadic-E layer", in *Meteors*, T. Kaiser, ed., Pergamon Press, 1955, pp. 96–98.

[2] J. Bacon, "An introduction to Sporadic E", *Radio Communication* 65:5, 1989, pp. 37–41.

[3] E. Pocock, P.J. Dyer, "Eleven years of Sporadic E", *QST*, March 1992, pp. 23–28.

[4] J. Bacon, "An introduction to Sporadic E (part 2)", *Radio Communication* 65:6, pp. 37–39.

[5] M. Toms, "Sporadic E data", *VHF-UHF Dxer* 1:1, 1992, pp. 13–15.

[6] M. Gadsden, W. Schröder, "Noctilucent Clouds", Springer-Verlag, 1989.

[7] M. Gadsden, "Noctilucent Clouds", *Quarterly Journal of the Royal Astronomical Society* 27:3, 1986, pp. 351–366.

[8] A. McBeath, "Noctilucent Cloud observing", in *Handbook for Astronomical Societies 1988*, B. Jones, ed., Federation of Astronomical Societies, 1987, pp. 31–36.

[9] D.H. McIntosh, M. Hallissey, "Noctilucent Clouds over Western Europe and the Atlantic during 1977", *Meteorological Magazine* 107, 1978, pp. 182–187.

[10] D.H. McIntosh, M. Hallissey, "Noctilucent Clouds over Western Europe during 1978", *Meteorological Magazine* 108, 1979, pp. 185–189.

[11] D.H. McIntosh, M. Hallissey, "Noctilucent Clouds over Western Europe during 1979", *Meteorological Magazine* 109, 1980, pp. 182–184.

[12] D.H. McIntosh, M. Hallissey, "Noctilucent Clouds over Western Europe during 1980", *Meteorological Magazine* 110, 1981, pp. 109–112.

[13] D.H. McIntosh, M. Hallissey, "Noctilucent Clouds over Western Europe during 1981", *Meteorological Magazine* 111, 1982, pp. 122–125.

[14] D.H. McIntosh, M. Hallissey, "Noctilucent Clouds over Western Europe during 1982", *Meteorological Magazine* 112, 1983, pp. 245–249.

[15] D.M. Gavine, "Noctilucent Clouds over Western Europe during 1983", *Meteorological Magazine* 113, 1984, pp. 272–277.
[16] D.M. Gavine, "Noctilucent Clouds over Western Europe during 1984", *Meteorological Magazine* 114, 1985, pp. 349–356.
[17] D.M. Gavine, "Noctilucent Clouds over Western Europe during 1985", *Meteorological Magazine* 115, 1986, pp. 361–370.
[18] D.M. Gavine, "Noctilucent Clouds over Western Europe during 1986", *Meteorological Magazine* 116, 1987, pp. 386–388.
[19] D.M. Gavine, "Noctilucent Clouds over Western Europe during 1987", *Meteorological Magazine* 118, 1989, pp. 16–18.
[20] D.M. Gavine, "Noctilucent Clouds over Western Europe during 1988", *Meteorological Magazine* 118, 1989, pp. 214–216.
[21] D.M. Gavine, "Noctilucent Clouds over Western Europe during 1989", *Meteorological Magazine* 120, 1991, pp. 65–66.
[22] D.M. Gavine, "Noctilucent Clouds over Western Europe during 1990", *Meteorological Magazine* 121, 1992, pp. 53–54.
[23] D.M. Gavine, "Noctilucent Clouds over Western Europe during 1991", *Meteorological Magazine* 121, 1992, pp. 284–285.
[24] W.J. Baggaley, in *IAU Symposium 90: Solid Particles in the Solar System*, I. Halliday, B.A. McIntosh, eds., D. Reidel, 1980.
[25] V.A. Bronshten, "Physics of meteoric phenomena", D. Reidel, 1983.
[26] P. Roggemans (ed.), "Handbook for visual meteor observations", Sky Publ. Co., 1989.
[27] A McBeath (comp.), "1993 Meteor Shower Calendar", IMO, 1992.
[28] G.W. Kronk, "Meteor showers—a descriptive catalog", Enslow Publishers, 1988.
[29] A. McBeath, "An analysis of sporadic meteors", *WGN* 17:6, 1989, pp. 267–272.
[30] C. Newton, "Radio auroras", Radio Society of Great Britain, 1991.
[31] R.J. Livesey, "The aurora in 1980", *Journal of the BAA* 93:3, 1983, pp. 114–116.
[32] R.J. Livesey, "The aurora in 1981", *Journal of the BAA* 93:6, 1983, pp. 254–258.
[33] R.J. Livesey, "The aurora in 1982", *Journal of the BAA* 94:4, 1984, pp. 158–162.
[34] R.J. Livesey, "The aurora in 1983", *Journal of the BAA* 95:3, 1985, pp. 100–105.
[35] R.J. Livesey, "The aurora in 1984", *Journal of the BAA* 96:5, 1986, pp. 278–283.
[36] R.J. Livesey, "The aurora in 1985", *Journal of the BAA* 98:1, 1988, pp. 18–22.
[37] R.J. Livesey, "The aurora in 1986", *Journal of the BAA* 98:6, 1988, pp. 301–307.
[38] R.J. Livesey, "The aurora in 1987", *Journal of the BAA* 99:4, 1989, pp. 172–178.
[39] R.J. Livesey, "The aurora in 1988", *Journal of the BAA* 100:2, 1990, pp. 73–78.
[40] R.J. Livesey, "The aurora in 1989", *Journal of the BAA* 101:3, 1991, pp. 153–161.
[41] R.J. Livesey, "The aurora in 1990", *Journal of the BAA* 102:3, 1992, pp. 151–157.
[42] R.J. Livesey, "The aurora in 1991", *Journal of the BAA* 103:2, 1993, pp. 77–83.
[43] A.C.B. Lovell, "Meteor Astronomy", Oxford University Press, 1954.
[44] "Chapter 11: Propagation", in *Radio Communication Handbook*, 5th Edition, Radio Society of Great Britain, 1982.
[45] J. Van Wassenhove, *personal communications*, 1993.
[46] D.M. Gavine, *personal communications*, 1993.
[47] K. Sinno, "On the time delay of the appearance of sporadic E following meteor activity", *Journal of Atmospheric and Terrestrial Physics* 42, 1980, pp. 35–39.
[48] J. Van Wassenhove (comp.), "IMO Radio Handbook", in preparation.
[49] T. Nygren, "Studies of Sporadic E layer using the EISCAT incoherent scatter radar", in *Advances in Space Science*, COSPAR, 1989.

The Makings of Meteor Astronomy: Part IV

Martin Beech, University of Western Ontario

The history of meteor astronomy is rich in both folklore and mythology. One particularly interesting folkloric connection with shooting stars is that related to the appearance of mushrooms. For all its modern day absurdity this folklore connection proved a difficult notion to dispel.

1. Go, and catch a falling star

When the poet John Donne (1571–1631) wrote the whimsical song [1]

Goe, and catche a falling starre,
Get with child a mandrake roote,
Tell, me where all past years are,
Or who cleft the Divels foot...

he was outlining a series of impossible tasks and tricky to answer questions. While to the modern day reader it is obvious that the task of catching a falling star is impossible, it is in fact not obviously clear whether Donne would have truly believed the task to be inherently impossible.

The reason why Donne and his contemporaries may have considered such a task as being, say very difficult, rather than just plainly impossible was hinted at last time when we presented William Caxton's explanation of the origin of meteors [2]. The view expounded by Caxton in his *The Mirror of the World* was inherently Aristotelean, and meteors were deemed to be produced by the ignition of volatile vapors in the Earth's upper atmosphere. Indeed, Donne echoes the Aristotelean idea of meteor origins in his poem *A Fever*. He writes [1]

These burning fits but meteors bee,
Whose matter in thee is soone spent.
Thy beauty, and all parts, which are thee,
Are unchangeable firmament.

The interesting non-Aristotelean addition to Caxton's explanation of meteor origins, however, and the reason why we can question the meaning behind Donne's song, is that Caxton added to his commentary the idea that meteors can produce a residuum that falls to the ground after their passage. That Donne was aware of such ideas is apparent in his poem *Epithalamions X* where he writes [3]

As he that sees a starre fall, runs apace,
And finds a gellie in the place,
So doth the bridegroome hast as much
Being told this starre is faln, and finds such.

The term "gellie" is the forerunner of our present day "jelly," and is derived from the Latin verb "gelare," which means to freeze or coagulate. Donne's "gellie" is the residuum *like som leef of a tree roten, that were weet* described by Caxton.

Further poetic allusion to meteoric residue can be found in the writings of Donne's contemporary Robert Heath (1635–1559). In his poem *Clarastella*, Heath writes [4] *So have I seen bright falling stars in show, Quench in dark gellies here below.* Abraham Cowley (1618–1667) further expounds [5] in his poem *Reason*

So stars appear to drop to us from the skie.
And gild the passage as they fly,
But when they fall, and meet th' opposing ground,
What but a sordid slime is found?

Clearly the idea that meteors could produce some form of residue was well established by the 17th century. Indeed, the idea was probably well established much earlier than the seventeenth century, as is evidenced by several folkloric stories that relate the appearance of mushrooms with bright shooting stars.

2. Meteors and mushrooms

To the modern day observer there are no obvious connections between the appearance of mushrooms and shooting stars. The one property that they might be reasoned to have in common is there (mostly) unpredictable appearance. Aristotle, for example, advocated the idea that fungi were formed by a process of spontaneous generation. Plutarch (146 A.D.–170 A.D.) explained in book IV of his *Symposiacs*, however, that mushrooms were created whenever thunderous lightning struck the ground.

The idea that mushrooms were created by lightning strikes proved popular, and held prominence well into the 18th century. In 1790, for example Erasmus Darwin wrote [6] in his epic poem *Botanic Garden*, *So from dark clouds the playful lightning springs, rives the firm Oak, or prints the fairy ring.* Fairy ring is, to this day, the common name for those darker circles of lush grass often found in pasture land which produce numerous mushrooms.

As we shall see in subsequent essays, the idea that shooting stars might be a form of lightning has been developed on several occasions. In particular, however, prior to the mid-19th century it was a common belief that the stones which supposedly fell from the sky (i.e., what we would call meteorites) were in fact produced by lightning. These so called thunder stones were formed whenever lightning struck a terrestrial rock.

The lightning strike was not the only way in which fairy rings could be formed. One Italian folk-tale explains [7] that on the nights of August 10 and November 11 a winged dragon flies over the fields scorching the ground with his tail of fire. Wherever the dragon has scorched the ground nothing will grow for seven years. After seven years, however, a circle of mushrooms will appear. The connection between this folk tale and meteors is twofold. Firstly, from the earliest medieval times bright meteors have been referred to as *Draco Volans*, literally flying dragon, and secondly, the nights on which the supposed dragon flies are near the peak nights of the Perseid and Leonid meteor showers.

I have not been able to discover at what time the flying dragon story was collected, or how ancient it might be. It would be interesting to do so, however, since the story implies that people were aware of at least two nights of the year when meteors were more common. The flying dragon story has parallels with the Irish folkloric association of the Perseid meteor shower and the burning tears of the martyred Saint Lawrence. The interesting feature of these tails (should the Italian story indeed prove to be ancient) is that they imply a common knowledge of periodic meteor displays. In an ironic sense it may be that an important clue to the extraterrestrial origin of meteors was known in folklore long before it was revealed through scientific study.

3. Star-jelly

The folk stories presented in the previous section can be viewed as early attempts to unify and explain the appearance of two poorly understood phenomena. The unifying feature in the folkloric sense was probably that both mushrooms and shooting stars appeared seemingly out of nowhere, and in an unpredictable fashion.

One example of a very specific folkloric association, however, exists for the gelatinous fungus *Tremella Mesenterica*. This fungus, sometimes called the "yellow-brain fungus" today was more commonly known as "fairy-butter" or "star-jelly" in the nineteenth century. In his collected fairy folklore notes of 1891, M.A. Denham [8] noted of Tremella that it was a substance occasionally found after rain on rotten wood or fallen timber, with a consistency and color much like genuine butter. He continued that it is a yellow gelatinous matter supposed by the country people to fall from the clouds. In Lincolnshire, England, the same fungus is called starshoot [9].

4. The folkloric legacy

The importance of studying the ancient accounts of meteor storms and fireballs was recognized long ago. Such accounts can, for example, give clues as to the evolution and structure of meteoroid streams.

A systematic study of say, European meteoric folklore has yet to be produced. Such a study could prove very rewarding, and I in particular would be pleased to hear from any *WGN* readers who have any meteoric folk-tales to relate.

References

[1] Lewalski B.K., Sabol A.J., eds., "Major Poets of the Earlier Seventeenth Century", The Odyssey Press, New York, 1973.
[2] Beech M., *WGN* 21:2, 1993, p. 67.
[3] Milgate W., ed., "John Donne—The Epithalamions, Anniversaries, and Epicedes", Clarendon Press, Oxford, 1978.
[4] Heath R., 1650 in *Clarastella together with Poems occasional, Elergies, Epigrams, Satyrs*, Scholars Facsimilies and Reprints, Gainsville, Florida, 1970.
[5] Waller A.R., ed., "Poems of Abraham Cowley", Cambridge University Press, Cambridge, 1905.
[6] Darwin E., "The Botanic Garden, a poem", J. Johnston, London, 1790.
[7] Ramsbottom J., "Mushrooms and Toadstools", Collins, London, 1953.
[8] Denham M.A., *Publications of the Folk-lore Society* 29, 1891, p. 1.
[9] Gutch I., Peacock M., *Publications of the Folk-lore Society* 53, 1908, p. 1.

Interview Series

Dr. P.B. Babadzhanov

Paul Roggemans and Peter Brown

The purpose of this series of interviews with distinguished professional meteor astronomers is to provide another perspective on the work undertaken by professional meteor workers and in doing so create more personal contact between professional and amateur meteor astronomers. This interview was conducted by Paul Roggemans on July 10, 1992, at Smolenice, Slovakia, after the *International Meteor Conference*. Dr. Babadzhanov is from Dushanbe, in the Republic of Tadjikistan (part of the former Soviet Union) where he heads the institute for meteor studies. His interests include meteor fragmentation, stream evolution, and photographic orbital work.

Question: The first question I would like to ask you is when and how you got started in astronomy?

Answer: I became interested in astronomy when I was a student in the faculty of physics and mathematics. After I graduated I became a post-graduate student in the institute of astrophysics and became interested in comets and meteors. For our practical work in those days we would be sent from Dushanbe to Moscow and that is where I met professor Arlov of Moscow University who was one of the leading experts in cometary and meteor science in the country. He suggested I begin investigations in meteor astronomy. From that time forward I became a post-graduate student at Moscow University studying meteor research. My first research project was dedicated to the study of the ejection velocities of meteoroids from comets.

Q: When did these events occur?

A: My early work at Dushanbe occurred in 1950–1951. From 1951 to 1954, I was in Moscow University for training. During the summer, however, I would return to Dushanbe for observational research. My dissertation was connected to the Perseid meteor shower and studying the stream using photographical techniques.

Q: Did you grow up in Dushanbe as well as study there?

A: No. I was born in a town in Tadjikistan which now has a population near 60 000 inhabitants. It is one of the oldest towns in Tadjikistan; in 1993 it will celebrate its 2500th anniversary, as a matter of fact.

Q: Could you summarize for us some of the investigations you have been involved in during the years you have studied in the field of meteor science?

A: At the Dushanbe Astronomical Observatory in 1958 the institute of astrophysics was founded. From the very beginning this institute was connected with meteor investigations. The rich observational material accumulated at the observatory on meteors permitted us to study the evolution and activity, particularly photographic activity, of many showers. At this time the observational program at the institute was quite broad encompassing such things as visual work, photographic work, radar etc. Today there is not as much work being done in all these areas, but we are trying to establish a television observational program.

Q: How many people are currently involved in the observational program at the institute?

A: Today the meteor department at the institute consists of 25 people, though only 10 of them are actually scientists; the rest are technicians and engineers since our work is connected to TV and radar observations and requires much technical support.

Q: What are some of the current research programs at the institute?

A: One of our major programs is carrying out photographic work by the method of instantaneous exposure. *(Ed. note: This method uses a fast rotating shutter to produce exposures of the order of thousandths of a second, effectively "freezing" the meteor image in flight.)* This was first done at our institute many years ago and now we are the only group still carrying out such investigations. This technique yields data concerning the fragmentation of meteoroids in the Earth's atmosphere.

A second major program at our institute concerns the evolution of meteoroid streams. The standard picture of a meteoroid stream is of a flat stream that moves in the same orbit as the parent comet. But when you take into account the differences in semi-major axis and eccentricities of the meteoroids ejected from the comet you arrive at a new result; that each comet or source of meteoroids can produce several meteor showers. For example, the Quadrantid stream is genetically linked by our simulations to eight other streams, for the Geminid stream we found four linked meteor showers. If we take into account long-term perturbations, we find that P/Encke is connected with 12 meteor showers.

Another interesting project took place in 1968–1970 when our Institute was part of a special expedition along with the Kharkov institute to Somalia where we observed southern hemisphere meteors by radar.

Q: What is the most challenging research you have undertaken?

A: A difficult problem which is also interesting is the physical nature of meteoroids. It is valuable research because it gives information concerning the parent bodies of meteoroids—comets and asteroids. This is a long-standing problem. For a long time we have tried to obtain results on this problem, specifically concerning the density of meteoroids.

Q: Have you ever encountered problems in the past such that the institute could not study meteors any longer or that the institute was nearing closure?

A: No. But, for some time I was more connected with the administration work at the institute, more precisely I was head of the Astrophysics Institute from 1959 to 1971. After this time, from 1971–1982 I was appointed as rector of Tadjik State University. In these years I had much less time for scientific research.

Q: What is your current research topic? What are your future plans?

A: Currently we study the evolution of meteoroid streams. In the future we plan two-station TV observations, a program which has already begun in 1991.

Q: How do you see amateur-professional cooperation? Not only here with the IMO, but also in your country?

A: As for amateur-professional cooperation I am quite positive as it is very useful for both the professionals and amateurs. Many great astronomers began from meteor astronomy. Often they went on to study comets, galactic structure etc., but they started from meteor astronomy as this field offers the possibility of becoming acquainted with other fields of astronomy.

Q: Do you have some examples from the former Soviet Union?

A: Levin, Fedensky, who was president of *IAU* 22, Bronshten and others. All of them started from the amateur meteor organizations in the Soviet Union.

Q: Are you optimistic for the future of meteor science now with all the political and economic changes in your country? Compared with the West, for example, there are many more meteor workers in your country.

A: I want to be optimistic. But, you see, the level of scientific work in Tadjikistan does not correspond to the economic level. The scientific level is very high, as, for example, before last year our Institute was the main institute in the field of comet and meteor research for the entire USSR. But now, with the low Tadjikistan economic situation it is much harder to support our institute. But we hope with the support of other organizations we can continue with comet and meteor investigations.

Q: Do similar situations exist in the surrounding former republics of the Soviet Union, for example in Turkmenistan and Uzbekistan?

A: Of course the same situation exists. But, you see, some republics are richer. For example some meteor investigations were being carried out in Turkmenistan, particularly TV observations. But the same basic problem exists for other republics.

Q: What sort of advice would you have for students or amateurs who are contemplating specializing in meteors?

A: I think that sometimes there is an attitude that there are no new problems in meteor astronomy and that the field is dying; but this is wrong. There are still many problems to be solved in meteor astronomy. For example, we have very little information about meteoroid streams which encounter the Earth's orbit and have small orbits. Perhaps they have flux densities which are greater than the Perseid or Geminid streams.

Q: For young scientists do you think that there is still a future in meteor science? Or do you think the trend that we see now, with more and more institutes and radar installations closing, will continue?

A: This is not only true for meteor astronomy but for all branches of astronomy. I think that the problem of Earth-crossing asteroids may hold some of the future for meteor science. It has been proposed that half of them are extinct comets and they are of course connected with meteoroids.

Q: What about theoretical research in meteor work?

A: As for theoretical research, you see, meteoroids as well as comets and asteroids give us information about the origin of the solar system which is quite important. Without knowledge concerning the origin of meteoroids and these related objects we cannot say anything concrete about the origin of the solar system, so I think some theoretical research must continue in meteor astronomy.

Fireballs and Meteorites

Two Meteorite Falls in Japan

Yasuo Yabu

Two meteorite falls in Japan, respectively on December 10, 1992, and March 26, 1991, are described. Tentative orbital data for the 1992 meteorite are presented, and an association with asteroid 1983 VA is suggested.

1. Mihonoseki meteorite

A meteorite directly fell on Mr. Matsumoto's house (Souzu, Mihonoseki-Cho, Yatsuka-Gun, Shimane-Ken) at 11^h59^m UT on December 10, 1992, and was named Mihonoseki Meteorite.

Figure 1 – Damage caused by the Mihonoseki Meteorite to Mr. Matsumoto's house. The red brick is hanging from the point at the ceiling where the meteorite penetrated the roof. The meteorite made an angle with the cord of 8° to the east. The hole through which the meteorite passed the second floor is clearly visible.

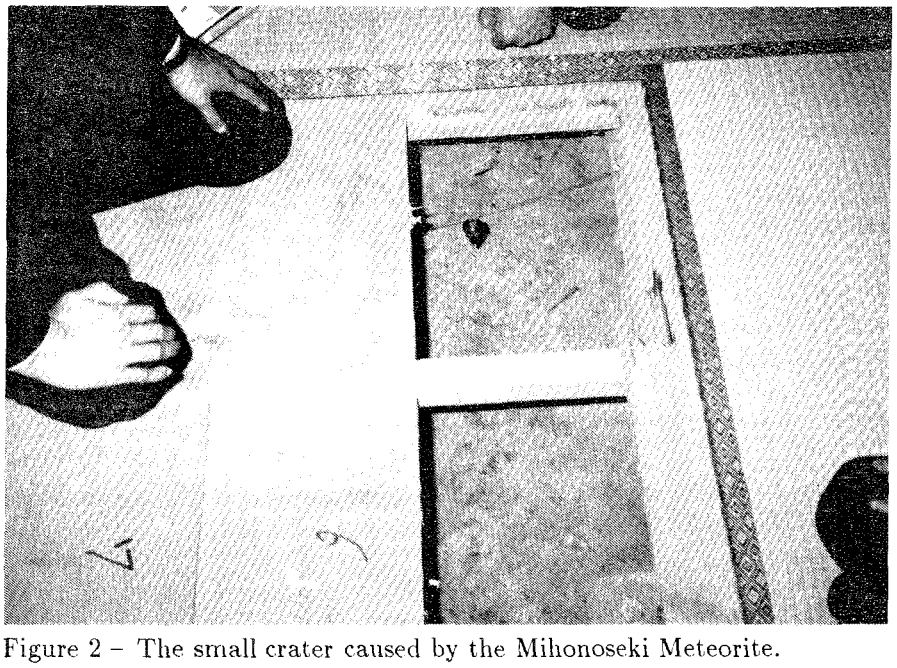

Figure 2 – The small crater caused by the Mihonoseki Meteorite.

Figure 3 – The Mihonoseki meteorite

The meteorite passed through the roof of Mr. Matsumoto's house, the second floor, the tatami (Japanese mat), the first floor and fell to the ground beneath the floor. At that time, it was raining hard with thunder and strong winds. Mr. Matsumoto mistook the meteorite for lightning striking his house. He discovered the meteorite on the evening of December 11.

The meteorite is an aerolite, size 24 cm × 14 cm × 11 cm and weighs 6.5 kg. The coordinates of the impact point are $\lambda = 133°13'09''$ E and $\varphi = 35°34'04''$ N. About 50 or more reports of the event were gathered but all of these are inaccurate and nothing was photographed. The corresponding fireball was of magnitude −6 or brighter.

Mr. T. Sowa calculated the orbit on the assumption that the meteorite was at an altitude of 100 km over Ashizuri's Cape. The orbit is shown in Table 1.

Table 1 – Orbital data and radiant information for the Mihonoseki Meteorite and the asteroid 1983 VA (eq. 2000.0).

	Mihonoseki	1983 VA [1]
Time	1992 December 10.4997 UT	December 10
Apparent radiant	$\alpha = 24°.5$ $\delta = -30°.4$	
Observed velocity	15.0 km/s	
Geocentric velocity	10.1 km/s	12.9 kms/s
Corrected radiant	$\alpha = 20°.2$ $\delta = -44°.9$	$\alpha = 38°.4$ $\delta = -45°.9$
Arg. perihelion ω	2°.82	11°.68
Long. asc. node Ω	78°.8	78°.87
Inclination i	11°.3	16°.24
Eccentricity e	0.593	0.6917
Perihelion dist. q	0.984 AU	0.8065 AU
Period P	3.76 years	4.22 years

The orbital data in Table 1 are uncertain because there may possibly have been two fireballs: one coming from the south and another one from the south-west, 4 minutes later. Indeed, a few observers saw two fireballs within 4 minutes.

A point of reference is asteroid 1983 VA which has a comparable orbit and radiant point. Only a few reports mentioned an explosion.

Mr. Matsumoto's mother used to live in the room on the first floor through which the meteorite passed. However, she went to the hospital a few days earlier because she was ill. She was extremely lucky to have escaped the direct hit of the meteorite.

The meteorite was investigated by Dr. Masako Shima from December 13 at the National Science Museum in Tokyo and reported to be an L6-type chondrite, having a cosmic ray age exposure of 61 million years. The meteorite is now exhibited in the Mihonoseki Data Center as a treasure of the town, together with a broken board of ceiling, floor, tatami, etc. Figure 3 was taken by Mr. H. Abe and Figures 1 and 2 are by the author.

2. Tahara meteorite

Another new meteorite was discovered as a result of newspaper reports on the Mihonoseki meteorite. Mr. Hidenobu Minao picked up a fragment of a stone which fell on the deck of a transport ship *Century Highway No. 1* (23 000 tons) on March 26, 1991. Mr. Minao lives near Mihonoseki and he thought the stone might be a meteorite. He carried it into a newspaper office the consequence of which it was that it was examined by amateur astronomers of this region.

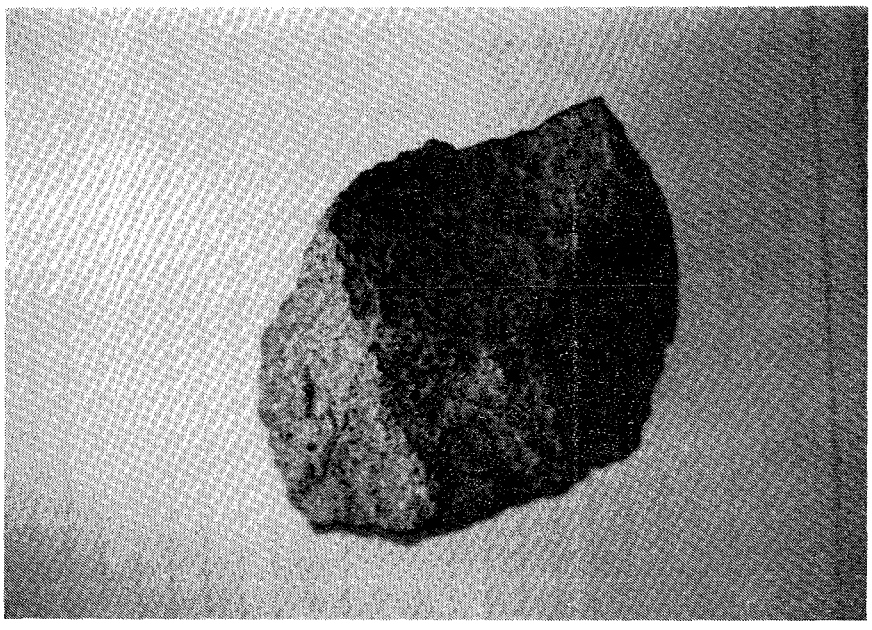

Figure 4 – Mr. Minao's fragment of the Tahara Meteorite.

The meteorite is an aerolite and was named "Tahara Meteorite." Dr. Sadao Murayama and Dr. Masako Shima investigated the ship. The fall of the meteorite happened between 8^h30^m and 12^h JST on March 26, 1991, at Tahara Port in Mikawa Bay, Aichi-Ken, $\lambda = 137°.292$ E, $\varphi = 34°.664$ N.

Supposedly, the meteorite came from the east-southeast. The meteorite dented the steel deck about 3 cm and broken fragments spread out in a fan shape. There were 10 or more fragments. The largest remained in the ship and was later thrown overboard. Other fragments were divided between 7 persons.

The fragments gathered now are that of Mr. Minao, size 85 mm × 65 mm × 50 mm, weight 430 g, and those of Mr. Ayabe, a little one and three weighing 800 g, 200 g, and 80 g, respectively. Figure 4 was taken by Mr. H. Abe.

Reference

[1] I. Hasegawa, Y. Ueyama, K. Ohtsuka, "Prediction of the Meteor Radiant Point Associated with an Earth-Approaching Minor Planet", *Publ. Astron. Soc. Japan* 44, 1992, pp. 45–54.

Orionid Fireball over Japan

October 21, 1992, $16^h31^m05^s$ UT

Katsuhito Ohtsuka and Hiroyuki Tomioka

The results of orbital calculations of a fireball photographed over Japan on October 21, 1992, are presented. The fireball was a member of the Orionids.

A fireball (no. T9210-01) with a terminal burst of magnitude −7 was photographed simultaneously from two stations in the *Tokyo Meteor Network* on October 21, 1992, at $16^h31^m05^s$ UT, using 85–100 mm class lenses [1,2]. The trajectory and orbital elements are as in Table 1. The fireball, an Orionid, is shown on the front cover of volume 5 of the *WGN Report Series*.

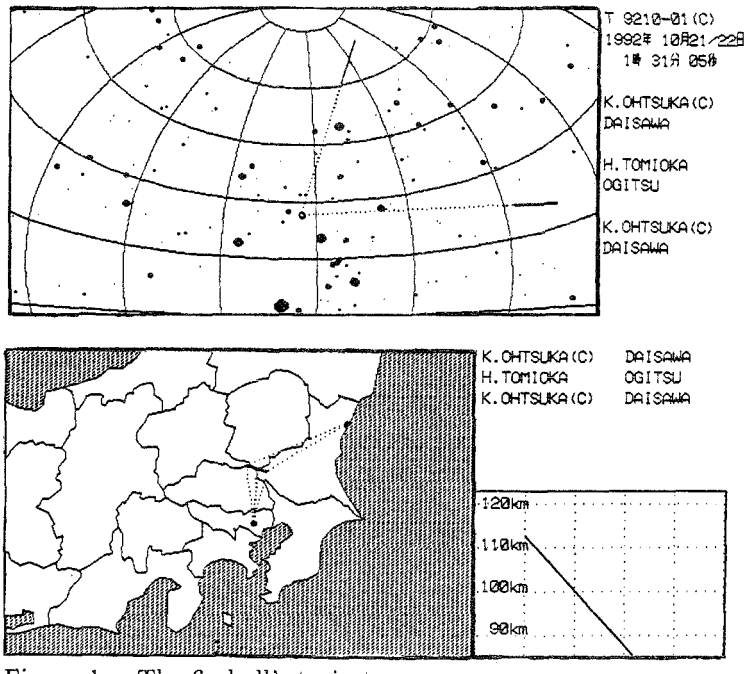

Figure 1 – The fireball's trajectory.

Table 1 – Results of trajectory and orbital calculations of T9210-01 (eq. 1950.0).

Time of appearance	1992 October 21.68825 UT
Apparent radiant position	$\alpha = 94.^\circ75 \quad \delta = +15.^\circ71$
Corrected radiant position	$\alpha = 94.^\circ71 \quad \delta = +15.^\circ59$
	$\sin Q = 0.949$
Begin	$\lambda = 139^\circ49'.5$ E $\quad \varphi = +36^\circ09'.1$ N $\quad h = 112.4$ km
Maximum	$\lambda = 139^\circ39'.6$ E $\quad \varphi = +36^\circ12'.3$ N $\quad h = 92.3$ km
End	$\lambda = 139^\circ36'.2$ E $\quad \varphi = +36^\circ13'.4$ N $\quad h = 85.4$ km
Velocity	$v_\infty = (67.90 \pm 0.19)$ km/s $\quad v_{geo} = 66.77$ km/s $\quad v_{hel} = 41.75$ km/s
Angular elements	$\omega = 27.^\circ927 \quad \Omega = 80.^\circ8 \quad i = 163.^\circ7$
Other elements	$e = 0.974 \quad q = 0.5830$ AU $\quad a = 22.3$ AU

References

[1] Ohtsuka K., Tomioka H., "Photographic Meteor Observations in the Tokyo Meteor Network", *WGN* 19:1, February 1991, pp. 14–16.

[2] Ohtsuka K., Tomioka H., Murayama H., Hidaka E., "TMN Photographic Meteor Observing Program", *Tokyo Meteor Network Report* 12, September 1992, pp. 69–78 (in Japanese).

A New Zealand Fireball with an Unusual Curved Trajectory

Graham W. Wolf

A New Zealand Fireball of visual magnitude −4 was seen from the Pauatahanui (pronounce *pah-wah-tah-har-noo-ee*) Observatory, located some 40 km north-west of the capital city of Wellington. The fireball, which had a distinct and unusually curved trajectory, was observed at $12^h17^m15^s$ UT on 1993 February 15 under perfectly clear skies and with a zenith limiting magnitude of 6.8.

The Pauatahanui Observatory is administered by the *Wellington Astronomical Society (WAS)* and is located at $\varphi = 41°07'40''$ S and $\lambda = 174°56'00''$ E, at an altitude of 60 m above sea level. The site is some 40 km north-west of the author's flat. At $12^h17^m15^s$ UT on February 15, 1993, a fireball with a strongly curved trajectory was observed peaking at magnitude −4 from this location. It started some 2° west of Achernar (α Eridani). At this stage, the fireball was some 22° above the southwestern horizon at magnitude −2 (the same brightness as the planet Jupiter that night, which itself was near Spica in the constellation of Virgo, low in the East).

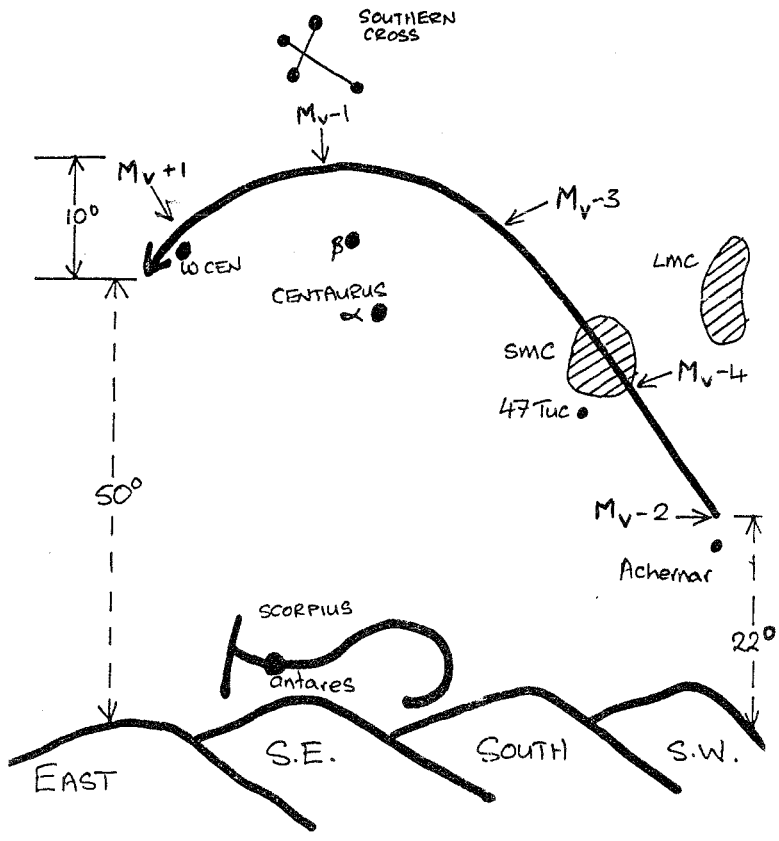

Figure 1 – Fireball trajectory across the southern sky.

Scorpius, with its bright star Antares, was some 5° above the southeastern horizon. The fireball then proceeded to brighten to a peak brilliance of −4 and stay bright yellow, as it passed through the Small Magellanic Cloud (SMC), just to the right of the globular cluster 47 Tucanae nearby. Heading upwards at an angle of about 45°, it began to level off once it had passed near β Centauri (one of the Southern Cross "pointers"), and at this stage had faded from −3 to −1, the latter being confirmed by comparing with the magnitude −0.72 star Canopus (α Carinae). By the time the fireball had passed halfway between β Centauri and the Southern Cross, it had leveled off and began then to arch leftward and downward in the vicinity of the magnitude

+3.4 globular cluster ω Centauri (NGC 5139), whereupon it had faded to magnitude +1 and headed downwards at an angle of about 30°. About 5° past ω Centauri, the fireball suddenly extinguished at an altitude of some 50° above the eastern horizon.

Its angular speed also varied. Firstly, at about Achernar where it commenced, the fireball was traveling at about 5°/s and somewhat obliquely, suggesting that perhaps, it was approaching the Earth's atmosphere at a rather flat trajectory. Between the SMC and β Centauri, at the point where it was of magnitude −3, the velocity peaked at 10°/s. By the time it had passed under the Southern Cross, its velocity had dropped back to about 5°/s, and by the time it extinguished near ω Centauri, its velocity had dropped further to about 2°/s. The fireball had a duration of 8 seconds, and left a train of 5 seconds. Meteorological conditions at the time were as follows: temperature 12.4° C, 87% humidity, wind calm, and 1020 hPa barometric pressure. The zenith limiting magnitude for that hour was 6.8.

What caused the curved trajectory of the fireball, is still a matter for heated debate. Certainly, the observer's head was not turned during the flight path (although the eyes were) as he was watching the vicinity of Centaurus for January shower meteors and saw the initial path out to the right edge of his centered vision. The trajectory did in fact bend only during the later stages of its path. It must be stressed that the path did not pass through the zenith, but to the front, then left of the observer (myself), unlike a previous −7 electrophonic fireball (with a remarkable 150° trail from low East at the horizon through the zenith, to the South) on December 8, 1986, at the R.F. Joyce Observatory at West Melton, near Christchurch. This electrophonic event was reported in more detail in *CASMAG* [1].

By all means, curved meteor trajectories are not unique in the astronomical world. Gotfred Kristensen has reported a rather jerky trajectory in *WGN* [2], and Ralf Koschack (*IMO* Visual Commission Director) has responded with some thoughts of his own on the matter [3]. In *Sky and Telescope* [4], there appears a photograph of a "wobbly" meteor trajectory taken on August 13, 1988, near Washington, USA, by Roy Gephart, perhaps the first such photographed event to be published. Furthermore, Dr. Martin Beech of the University of Western Ontario has provided valuable input on the subject, with articles in *WGN* [5] and *Sky and Telescope* [4]. Dr. Beech [4] suspects that Ralf Koschack has a valid criticism in many cases of curved meteor trails being due to either psychological or head-turning reflex events [3,5]. However, Dr. Beech suggests that there may in fact be some events that are not spurious, and perhaps due to spinning of the meteoroid in the upper atmosphere itself [5].

Dr. Beech explains in greater detail in *Sky and Telescope* [4], that the famous "Magnus Effect," which typically makes a spinning golf ball curve in flight, may in fact be responsible for non-linear meteor trails. W. Jones [6] has proved conclusively, from other studies, that it is indeed possible for a meteor to spin heavily in flight.

Referring back to the 1986 electrophonic fireball observed at West Melton on December 8, the head of that fireball was indeed observed to be spinning (at a frequency of about 1 revolution per second)... perhaps not so fast as to provide a perceivably curved path. That fireball did, however, pass through the zenith, and from a perspective point of view, could have been judged to be on a curved path, due to the long trajectory of some 150° to 160°, as it passed from just above one horizon to the other [1].

Shallow angle trajectories have indeed been suspected of causing curved meteor paths [2], but this is still controversial [3], and needs closer scientific study. A more restrained and less sensational attitude to the problem would certainly help matters considerably. Certainly, a careful examination of the immense *FIDAC* data held by the *IMO*, could provide researchers with more cases of non-linear paths, provided of course that the fireball observers were considerate enough in the first place to provide trajectory diagrams with their submitted reports.

It is interesting to note that Marc Gyssens makes a similar view regarding shallow entry angles, at the bottom of Kristensen's report [2]. Dr. Beech has suggested that less than 0.05% of all

meteor trails are curved [4]. Dr. Beech also remarks that non-linear meteor reports date only back to the last two centuries [4], and it is interesting to speculate that earlier observers, perhaps as far back as 5 centuries or more in China for example, may have seen such events and not apparently recorded them.

Like the enigma of electrophonic fireballs, non-linear meteor paths require further study and scientific investigation, before the phenomena and, particularly, its physical mechanism, can be accurately ascertained. This is a task for which the global characteristics and resources of the *IMO* are admirably equipped.

Comments and constructive criticisms are welcomed on this event, directed through the pages of *WGN*.

Acknowledgments

I wish to thank the Carter National Observatory of New Zealand (where the author is now employed) for encouragement and bibliographical assistance, the Wellington Astronomical Society (WAS), for use of the facilities at the Pauatahanui Observatory, Wellington, Jürgen Rendtel, Alastair McBeath, and Paul Roggemans of the *IMO*, whose encouragements are highly valued and appreciated, and the late Peter A. Read, populariser and mentor, for his inspiration and example.

References

[1] G. Wolf, "Observations", *CASMAG* 38:3, March 1987, pp. 10–11.
[2] G.M. Kristensen, "Unusual Meteor Track", *WGN* 19:4, August 1991 p. 136.
[3] R. Koschack, "Letter to WGN", *WGN* 19:5, October 1991, p. 170.
[4] M. Beech, *Sky and Telescope*, January 1989, pp. 11–12.
[5] M. Beech, "Letter to WGN", *WGN* 20:1, February 1992, pp. 2–3.
[6] W. Jones, "Rotational Damping of Small Interplanetary Particles", *Mon. Not. Roy. Astron. Soc.* 247, 1990, pp. 257–259.

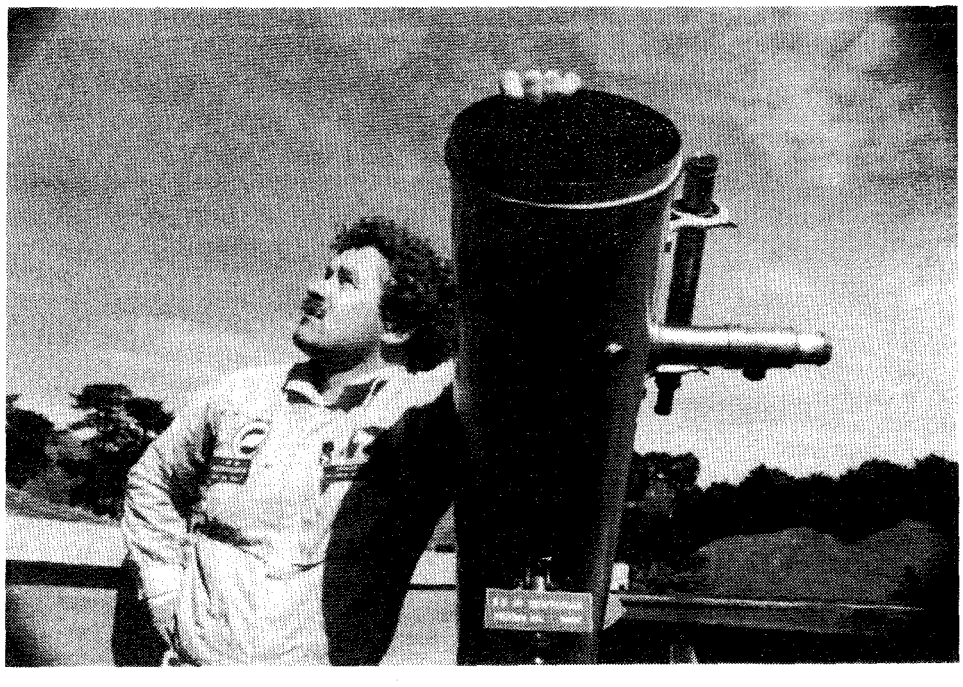

Figure 2 – Graham Wolf at the Panatahanui Observatory.

Fireball above the North Sea

April 15, 1993, $21^h14^m30^s$ UT

Ben Apeldoorn and Niek de Kort

A description is given of a simultaneously-observed fireball on April 15, 1993, over the North Sea. With an all-sky photograph and 3 visual reports, a trajectory was determined suggesting the fireball belonged to shower complex in Leo and Virgo.

At $21^h14^m30^s$ UT on April 15, 1993, a −9.5 magnitude fireball appeared roughly above the Dutch North Sea coastline. More than 40 visual reports, several from amateur-astronomers, were collected by the Meteor Section of the *Dutch Association for Meteorology and Astronomy (NVWS)*, after announcements in newspapers and on the radio. Some eye-witnesses reported "anomalous" sounds, such as "hissing" and "cracking" accompanying the fireballs appearance.

Although the weather conditions above the Netherlands were rather poor, one of the all-sky meteor stations of the Meteor Section, situated in the village of Hoogmade ("ASH," All-Sky Hoogmade, $\lambda = 4°34'42''$ E, $\varphi = 52°10'16''$ N), captured the fireball with a 16 mm Nikkor fish-eye lens ($f/4$) during a 62 minute exposure. The photograph started a mere 78 seconds before the fireball flashed "beside" the bowl of the Big Dipper. A $2 \times 90°$ rotating shutter (12.5 rps) and Kodak T-Max-400 film were used.

A rough atmospheric trajectory was derived from the "ASH" picture and three more or less accurate visual reports collected by one of us (De Kort). The fireball became visible at an altitude of 98 ± 5 km above the Valkenburg airbase ($\lambda = 4°56'21''$ E, $\varphi = 52°10'45''$ N, exactly 10 km west of Hoogmade), and ended its trajectory 3.5 seconds later at an altitude of 75 ± 5 km above the point $\lambda = 4°30'25''$ E, $\varphi = 52°27'45''$ N (this is 6 km west of the town of IJmuiden).

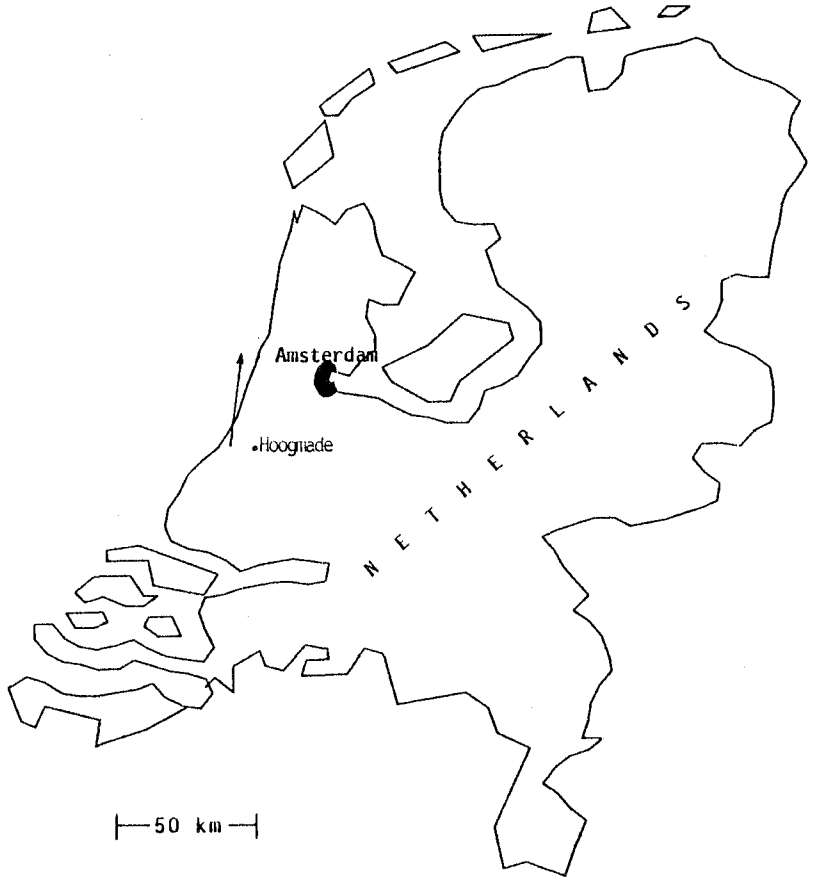

Figure 1 – Ground-based trajectory of the fireball.

The initial velocity was 10–14 km per second and the apparent radiant was in Sextans ($\alpha = 10^h36^m$, $\delta = -04°$) which suggests that the fragment belongs to the Leo-Virgo-complex active in March, April, and May. Many reports indicated that the fireball was fragmenting during the final second of its flight; this agrees with the photograph in which shutter breaks in the last part of the trail are barely visible. The meteoroid seems to be a typical "earth-grazer."

Four more, but (far) less luminous meteors (two of them probably also Virginids) have been captured by "ASH" in March and April. Last year (1992) on May 4, a −5 magnitude Virginid was simultaneously photographed by 3 all-sky stations of both the *NVWS* Meteor Section and the *Dutch Meteor Society.*

The Virginids are probably responsible for a number of dazzling slow moving fireballs with exceptionally long atmospheric trajectories, appearing in the period of April 15–30 during the last 20 to 30 years. The "European record holder" of that family undoubtedly was the −15 to −20 magnitude fireball on the evening of April 25, 1975. It was observed by thousands of eye-witnesses in Northwestern Europe, before ending its fiery path through the sky with two terminal bursts less than 20 km above the Noordoostpolder region. Despite intensive searching in Gaaster- and Lemsterland, in the province of Friesland, no meteorites were found.

A photograph of this fireball appears on the front cover. (Ed.)

Visual, Radio, and Photographic Fireball

N.E. Germany, January 28, 1993, $4^h02^m22^s$ UT

André Knöfel, Jürgen Rendtel and Gotfred M. Kristensen

A fireball simultaneously observed by different techniques is described.

On January 28, 1993, at $4^h02^m22^s$ UT, Gotfred M. Kristensen observed a bright, flickering light behind his house in a southern direction from his hometown Havdrup (Denmark). The light lasted 2 seconds and was as bright as the rising Full Moon. The color was described as orange and red. On this particular night, Kristensen's radio receiver was tuned to a frequency of 100.5 MHz. Exactly at $04^h02^m22^s$ the penrecorder registered an unusually powerful signal lasting 124 seconds (Figure 1).

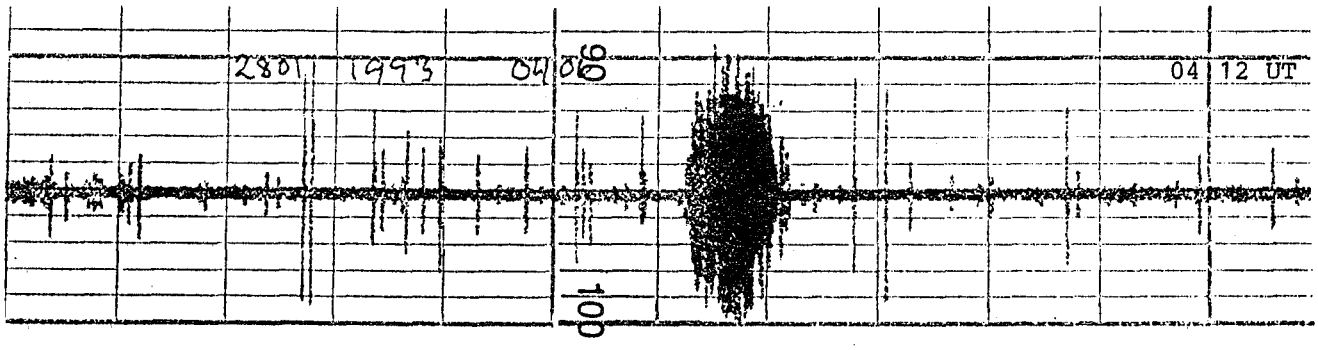

Figure 1 – Part of the pen-recorder registration of G.M. Kristensen from Havdrup (Denmark) on a frequency of 100.5 MHz between 3^h50^m and 4^h14^m UT on January 28, 1993.

Despite the hazy sky, the photographic fireball patrol of Jürgen Rendtel in Potsdam (Germany) was active during this night as well. The film was exposed from $17^h00^m50^s$ UT to $5^h53^m35^s$ UT. On this photo, which appeared in *FIDAC News*, the fireball of approximately −8 can be seen close to the northern horizon. There also exists another photograph of this fireball from a mirror all-sky station of the German fireball survey network.

Video Observational Results

Orbits of TV η-Aquarid Meteors Obtained in 1988

K. Suzuki, T. Akebo, S. Suzuki, T. Yoshida, and K. Ohtsuka

Orbits of 5 TV η-Aquarid meteors obtained in 1988 have been determined. The orbital data are more similar to those of P/Halley than other meteor orbits determined in the past.

High sensitivity TV meteor observations were carried out in early May 1998, around the shower maximum of the η-Aquarids, by the Damine TV meteor observing program. As a result, 5 η-Aquarids were recorded simultaneously on VHS video tapes at two Damine meteor stations: Toyokawa (λ = 137°19′23.″9 E, φ = 34°48′44.″4 N, h = 10 m) and Okazaki (λ = 137°13′28.″4 E, φ = 34°54′37.″2 N, h = 52 m). Of these, 4 meteors were obtained on the night of May 7, and one was obtained on May 4. The TV system consists of an image intensifier (Hamamatsu Photonics V1366P) with CCD video camera (Panasonic MC15 at Toyokawa; Panasonic AG400 at Okazaki). The lenses used are a Pentax 135 mm $f/2.8$ at Toyokawa and a Nikon 85 mm $f/1.4$ at Okazaki; their fields of view are 10° and 16°, respectively. We estimate that the limiting magnitude for meteors is near +7 to +8 under the best night conditions. The time and date are superposed on the corner of each video frame every 1/30 second. For image processing, video frames are digitized (512 × 512 dots) by Fujitsu FM-Towns (80386SX computer). Meteor images are measured with the graphic software "Newtransfer 1.1." Between 6 and 17 reference stars surrounding the trail are taken from the AGK3 Catalogue. The positions of each meteor are reduced and fitted using the general linear constants and taking the optical distortion into account. In this system, we estimate that the positional accuracy of the meteor is about 1′–2′. This procedure is almost the same as Hawkes's method [1].

The trajectories and orbital data are listed in Table 1 where *Date* is the observed time of meteor appearance in UT given as a decimal day in May, 1988; $\lambda_\odot$ is the solar longitude (eq. 1950.0); α and δ are the coordinates of the corrected radiant (eq. 1950); V_∞ is the no-atmosphere velocity (km/sec); $V_{\rm geo}$ is the geocentric velocity (km/sec); $V_{\rm hel}$ is the heliocentric velocity (km/sec); $h_{\rm beg}$ is the begin height (km); $h_{\rm end}$ is the end height (km); $\cos Z_R$ is the cosine of the zenithal angle of the apparent radiant; e, q, a, i, ω, and Ω are orbital elements (eq. 1950); λ and β are longitude and latitude of the perihelion; $\sin Q$ is the sine of the angle between the two great circles of the meteor paths as seen from the two stations; *Magnitude* is the approximate TV magnitude; and *Frames* is the number of frames on which the meteor appears at the two stations (30 frames/second).

The orbits of TV η-Aquarids are well determined as can be seen from Table 1. In particular, the linear elements, and λ and β are more similar to the corresponding elements of P/Halley (1986 III) [2] than those orbits derived from photographic and radar observations in [3].

The values of $\sin Q$ from our data are somewhat small for the accurate determination of orbits. But the meteor trails are rather long, and therefore we believe that the orbits of these TV η-Aquarids are reliable. We have also recorded some other double-images of η-Aquarids at two stations. However, the values of $\sin Q$ are also small, and the meteor trails in these cases are so short, that we cannot compute reliable orbits.

References

[1] Hawkes R.L., "Constructing a Video-Based Meteor Observatory", *WGN* 18:4, August 1990, pp. 145-151.

[2] Marsden B.G., "Catalogue of Cometary Orbits", 6th edition, Minor Planet Center, 1989.

[3] Lindblad B.A., "The Orbit of the Eta Aquarid Meteor Stream", in *Asteroids, Comets, Meteors* III, C.-I. Lagerkvist, H. Rickman, B.A. Lindblad, and M. Lindgren, eds., Uppsala Univ., 1990, pp. 551-553.

Table 1 – Orbits of TV η-Aquarids (eq. 1950.0). Explanations are given in the text.

	DMA801	DMA802	DMA803	DMA804	DMA805	Mean	Photo [3]	Radar [3]	Halley [2]
Date (UT)	7.72182	7.75317	7.74698	7.76258	4.73713				
$\lambda_\odot$	46°.80	46°.83	46°.83	46°.84	43°.91				
α	338°.24	338°.80	338°.09	338°.88	336°.71				
δ	−0°.55	−0°.08	−0°.04	−0°.36	−1°.48				
V_∞ (km/s)	67.8	67.4	66.0	67.5	66.2				
V_{geo} (km/s)	66.5	66.2	64.7	66.2	64.9				
V_{hel} (km/s)	41.6	41.6	40.0	41.6	40.5				
h_{beg} (km)	118.7	113.6	113.5	116.5	116.0				
h_{end} (km)	106.7	101.9	93.3	107.1	103.0				
$\cos Z_R$	0.233	0.374	0.356	0.411	0.277				
e	0.984	0.979	0.898	0.981	0.924	0.953	0.983	0.882	0.967
q (AU)	0.612	0.593	0.581	0.593	0.555	0.587	0.612	0.584	0.587
a (AU)	37.0	28.2	05.7	30.9	07.3	12.3	29.8	05.0	17.9
i	163°.5	162°.8	162°.0	163°.4	163°.5	163°.0	165°.5	165°.7	162°.2
ω	101°.9	99°.5	96°.0	99°.7	93°.7	98.2	101°.5	95°.9	111°.8
Ω	46°.80	46°.83	46°.83	46°.84	43°.91	46°.24	45°.8	45°.5	58°.1
λ	304°.4	306°.9	310°.5	306°.7	310°.1	307°.7	303°.9	309°.4	305°.3
β	+16°.1	+17°.0	+17°.9	+16°.4	+16°.5	+16°.8	+14°.2	+14°.2	+16°.4
$\sin Q$	0.080	0.078	0.117	0.071	0.083				
Magnitude	+5	+5	+4	+5	+5				
Frames	12, 24	15, 14	15, 28	11, 12	22, 22				

TV Observations of the 1991 Geminid Meteor Shower

Masayoshi Ueda and Yasunori Fujiwara

TV Observations of faint meteors were carried out during the period of Geminid activity in 1991. The magnitude distribution of 583 meteors, of which 205 belong to the Geminids, was studied. A deficiency of faint meteors in the Geminids as compared with sporadic meteors was confirmed.

1. Introduction

Television (hereafter, TV) systems including image intensifiers have great potential for observing faint meteors, which cannot be observed by the usual photographic or visual methods [1]. Such TV observations provide us with valuable data not only on the precise orbit, but also on the magnitude distribution of faint meteors. This magnitude distribution is strongly related to the mass distribution of meteoroids, which gives important information on the evolution of meteor streams. Because of the Poynting-Robertson effect, the evolution of each meteoroid's orbit depends on its mass. Therefore, the magnitude distribution should be studied over a wide range. The magnitude distribution extending to 7th magnitude, however, has not been studied sufficiently.

Using the TV system we observed 583 meteors, of which 205 belong to the Geminids. These data include faint meteors of the 7th magnitude. In this paper, we present preliminary results of the magnitude distribution extending to the 7th magnitude, and discuss the difference between the Geminid meteors and sporadic meteors.

2. Observations and reduction

The TV observations were carried out from December 12 to 14, 1991, at the site of the MU radar, belonging to the Radio Atmospheric Science Center, Kyoto University. It is located at Shiga, Japan (λ = 136°07′ E, φ = 34°51′ N). The TV system consists of an image-intensifier

(Hamamatsu Photonics V3287P), objective lens (Nikon 85 mm $f/1.8$), and video camera (Sony CCD-V90). The field of view is circular and 16°.9 in diameter. The limiting magnitude of this system is in the range 7.5–8.0 for stars, depending on the spectral type.

The center of the field of view was at an azimuth of 131° and an altitude of 65°. The video signal was recorded onto videotapes, which were inspected on a TV-monitor after the observation by one of the authors (M. Ueda). This inspection provided the number of meteors with their apparent magnitude. Using this inspection method, the limiting magnitude for meteors is about 7. It is thought that no meteors of magnitude 6 or brighter are overlooked. The apparent magnitude of each meteor was determined by comparing its brightness to that of field stars. Because this method of estimating magnitudes is not very accurate, the magnitudes were rounded to integers.

3. Rate profiles

The number of observed meteors is listed in Table 1. Although the Geminid maximum occurred around December 14 UT, 1991, as determined by visual observations [2], the explicit maximum was not clear from our TV-observations. The meteor rate profiles have shapes which vary as a function of the brightness of the observed meteors [3]. Poole et al. showed in 1972 that the rate profile for the brighter meteors was skewed as determined by radar observation. The lack of explicit maximum in the TV observation indicates a slowly varying rate profile. The number of sporadic meteors increases clearly towards the morning. This diurnal variation is similar to that of radar meteors [4].

Table 1 – Number of observed Geminid and sporadic TV meteors on December 12–14, 1991, by M. Ueda.

Date	Period (UT)	T_{eff}	Lm	Gem	HR_{Gem}	Spor	HR_{Spor}
Dec 12	$15^{\text{h}}57^{\text{m}}$–$17^{\text{h}}00^{\text{m}}$	1.05	8	18	17.1	18	17.1
	$17^{\text{h}}00^{\text{m}}$–$19^{\text{h}}00^{\text{m}}$	2.00	8	25	12.5	52	26.0
	$19^{\text{h}}01^{\text{m}}$–$20^{\text{h}}46^{\text{m}}$	1.75	8	9	5.1	50	28.6
Dec 13	$12^{\text{h}}52^{\text{m}}$–$14^{\text{h}}52^{\text{m}}$	2.00	8	18	9.0	16	8.0
	$14^{\text{h}}53^{\text{m}}$–$16^{\text{h}}54^{\text{m}}$	2.02	8	29	14.3	30	14.9
	$16^{\text{h}}56^{\text{m}}$–$18^{\text{h}}53^{\text{m}}$	1.95	8	34	17.4	49	25.1
	$18^{\text{h}}55^{\text{m}}$–$20^{\text{h}}37^{\text{m}}$	1.70	8	26	15.3	54	31.8
Dec 14	$14^{\text{h}}50^{\text{m}}$–$16^{\text{h}}00^{\text{m}}$	1.17	8	9	7.7	19	16.3
	$16^{\text{h}}01^{\text{m}}$–$18^{\text{h}}01^{\text{m}}$	2.00	8	23	11.5	37	18.5
	$18^{\text{h}}02^{\text{m}}$–$19^{\text{h}}55^{\text{m}}$	1.88	8	14	7.4	53	28.1
Total		17.52	8	205	11.7	378	21.6

4. Magnitude distribution

The magnitude distribution of the observed meteors is shown in Figure 1. Figure 2 is the relationship between the magnitude and the cumulative number of meteors. The difference between the Geminids and the sporadic meteors is clear. While the maximum number of Geminid meteors appears in the 4th magnitude bin in Figure 1, the maximum for the sporadic meteors appears in the 6th magnitude bin. As it is easy to overlook 7th magnitude and fainter meteors, the number of sporadic meteors can be expected to increase with decreasing magnitude.

This result demonstrates the difference in the mass distribution between the Geminids and sporadic meteors. Since the orbital evolution of the meteoroids depends strongly on their mass, massive meteoroids tend to remain in their original orbit. Such mass segregation has been theoretically studied by many researchers [3]. The results of the present study reveals some of the important observational constraints on such evolutional theories.

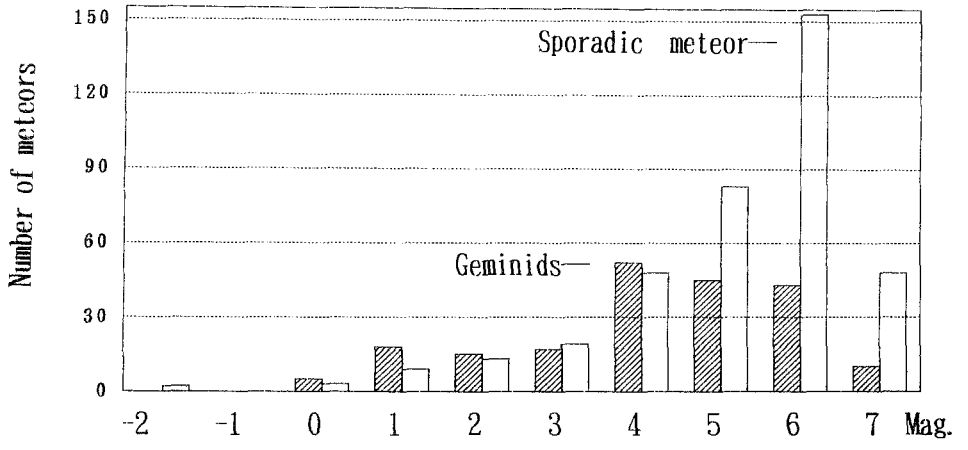

Figure 1 – The magnitude distributions of M. Ueda on the TV meteors during the nights of December 12–14, 1991.

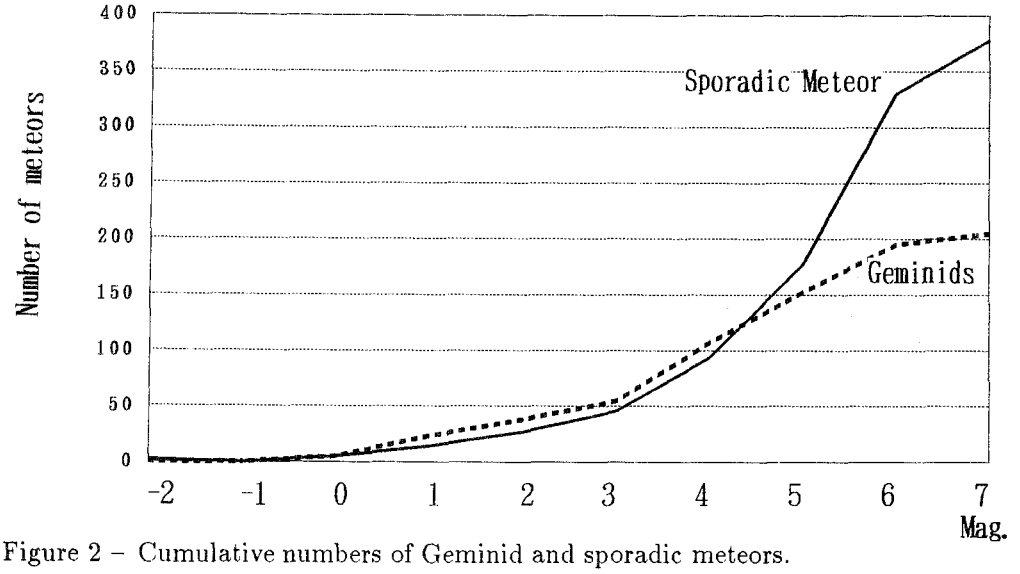

Figure 2 – Cumulative numbers of Geminid and sporadic meteors.

Continued efforts should be made to obtain more data from TV observations, in order to clarify the evolutionary status of not only the Geminids, but also of other meteor showers.

Acknowledgment

The authors would like to thank the staff of the Kyoto university Radio Atmospheric Science Center, Dr. Junichi Watanabe (National Astronomical Observatory of Japan), and Mr. Yasuo Yabu and Mr. Kazuhiro Suzuki (Nippon Meteor Society) for their beneficial guidance during the course of this study.

References

[1] Hawkes R.L., "Television Meteors", in *Proc. International Astronomical Symposium: Meteoroids and their Parent Bodies*, 1993, p. 227.

[2] Ueda M., *Tenmonkaihou (the Nippon Meteor Society)* 595, 1992, pp. 3–17 (in Japanese).

[3] Fox K., Williams I.P., Hughes D.W., *Mon. Not. R. Astr. Soc.* 205, 1983, pp. 1155–1169.

[4] Watanabe J., Nakamura T., Tsutsumi M., Tsuda T., *Publ. Astron. Soc. Japan* 44, 1992, pp. 677–685.

Latest News

Space Shuttle "Discovery" is Delayed by the 1993 Perseids

Peter Brown

A brief summary is given of the causes of the delay of the Space Shuttle *Discovery* and the subsequent heightened interest by the popular media in the event.

As this issue was going to press we learned how serious some are taking the possibility that the forthcoming Perseid return will be of storm proportions. On July 31, NASA announced that they were delaying the scheduled August 4 launch of the Space Shuttle *Discovery* until at least August 12 as a direct result of the danger posed by meteoroidal debris from the Perseid stream. The genesis of this decision goes all the way back to basic research the *IMO* performed several years ago.

The first step toward this decision to ground the shuttle was taken by Paul Roggemans and Ralf Koschack when they analyzed the 1989 Perseid display and derived (for the first time) accurate spatial number densities for the stream using visual observations. Other data from radar have given estimates of the spatial number densities, but these are often less accurate in defining the lower mass limit involved and are affected by other observational biases which make interpretations more open to question.

After this article, the Japanese meteor observers were alerted to the possibility of enhanced activity some 12 hours before the normal maximum in 1991. As we all know now, they saw the first strong activity heralding the return of Swift-Tuttle. After the recovery of the comet, it became apparent that the 1993 Perseid return might be something special. In this respect, Beech et al. published a short letter in *MNRAS* Letters calculating the impact probability on various sized space platforms from the Perseids based on the spatial number density data that Roggemans and Koschack had derived from analysis of visual data in 1989.

After the *MNRAS* paper had been published, officials in charge of the Hubble Space Telescope (HST) read the article and began a separate series of calculations to verify the impact probabilities given in the Beech et al. work. This being verified and the HST people satisfied with the believability of the *IMO* results which form the ground work for such calculations, a decision was made to reorient the HST for 6 hours on either side of the potential storm peak near 1^h UT on August 12. This decision went largely unnoticed by the media and public at large. Indeed, even the specialized astronomy based media missed this event initially.

However, when, as the result of a delay, the shuttle launch date was set back until early August, the media inquired of NASA about the danger to the shuttle and pointed to the HST decision. NASA then worked back the results that HST officials had already crunched, came to the same answer and decided to delay. What is more all of this was due to basic research the *IMO* undertook several years ago as a matter of course. If you ever thought your visual observations were not valuable consider what they lead to in a direct way in the summer of 1993!

As a final note, only a few days before the actual Perseid maximum, a paper by Williams submitted to *MNRAS* raised exceptional interest by the media after being released by the *RAS*. In it, Williams suggested that the 1994 Perseids would in fact be the stronger of the displays in 1993 and 1994. Perhaps you saw extracts of this in your local media. However, also these calculations confirm that 1993 will yield a magnificent display!

By the time you get this issue of *WGN*, the Perseids will be over. Hence, only you, the readers of *WGN*, know the true outcome of these exciting series of events!

The International Meteor Organization

Council

President: Jürgen Rendtel, Gontardstraße 11, D-14471 Potsdam, *Germ.*, tel. 49 (331) 960 727

Vice-President: Alastair McBeath, 25 West Park, Morpeth, Northumberld. NE61 2JP, *England*

Secretary-General: Paul Roggemans, Pijnboomstraat 25, B-2800 Mechelen, *Belgium*, tel. 32 (15) 41 12 25

Treasurer: Ina Rendtel, Gontardstraße 11, D-14471 Potsdam, *Germany*,
postal (giro) account number: 547234-107
post office code: 100 100 10 Postgiroamt 1000 Berlin
(post office code and postgiroamt to be mentioned together with account number!)

Other council members:
Peter Brown, Dept. of Physics, Univ. of Western Ontario, London, *Ont., N6A 3K7, Canada*
Malcolm Currie, 25 Collett Way, Grove, Wantage, Oxon. OX12 0NT, *England*
Marc Gyssens, Heerbaan 74, B-2530 Boechout, *Belgium*
Robert Hawkes, Mt. Allison Univ., Physics Dept., Sackville, *N.B. E0A 3C0, Canada*
Detlef Koschny, Ostpreußenstraße 51, D-81927 München 81, *Germany*
Masahiro Koseki, 4-3-5 Annaka, Annaka-shi, Gunma-ken 379-01, *Japan*
Vasilii Martynenko, Astronomical Observatory of the Crimean Regional Young Technicians Station, P.O. Box 52, Simferopol, *Crimea* 333 000, *Ukraine*
D. Steel, Anglo-Australian Observatory, Private Bag, Coonabarabran, *N.S.W. 2357, Australia*
Christian Steyaert, Dr. Van de Perrestraat 83, B-2440 Geel, *Belgium*
A. Terentjeva, Astronomical Council, Pjatnitskaja 48, Moscow 109 017, *Russia*
Casper ter Kuile, Akker 145, NL-3732 XD De Bilt, *the Netherlands*
Jeff Wood, 126 Lansdowne Street, Kensington, *West-Australia 6151, Australia*

Commission Directors

Visual Commission: Ralf Koschack, Prof.-Wagenfeld-Ring 33, D-02943 Weißwasser, *Germ.*
Input *Visual Meteor Database*: Rainer Arlt, Berliner Straße 41, D-14467 Potsdam, *Germ.*
email: `100114.1361@compuserve.com`
Telescopic Commission: Malcolm Currie
FIreball DAta Center: André Knöfel, Saarbrücker Straße 8, D-40476 Düsseldorf, *Germany*
Photographic Commission: Dieter Heinlein, Lilienstraße 3, D-86156 Augsburg, *Germany*
Radio Commission: Jeroen Van Wassenhove, 's-Gravenstraat 66, B-9810 Nazareth, *Belgium*

WGN — The Journal of the IMO and Observational Report Series

Editor-in-chief: Marc Gyssens, tel. 32 (3) 455 68 18, e-mail: `gyssens@wins.uia.ac.be`
fax: 32 (3) 820 24 21 (mention "for Marc Gyssens")

Editorial board: R. Arlt, D. Asher, M. Beech, P. Brown, M.J. Currie, M. de Lignie, W.G. Elford, G.W. Kronk, R. Hawkes, J. Jones, C. Keay, R. Koschack, A. McBeath, D. Meisel, P. Pravec, J. Rendtel, M. Šimek, G. Spalding, I.P. Williams.

Typesetting: Urania, the Public Observatory of Antwerp
Printing: André Gabriël

Other author's addresses

Addresses not listed can be found in a previous issue of this volume.

D.W. Olson et al., Dept. Phys., S.W. Texas State Univ., San Marcos, *TX 78666-4616, USA*
Y. Yabu, NMS, Maruyama-cho 878, 523 Omihachiman-shi, *Japan*
K. Ohtsuka et al., 1-27-5 Daisawa, Setagaya-ku, 155 Tokyo, *Japan*
B. Apeldoorn, Graaf Willem II-laan 30, NL-2355 BH Hoogmade, *the Netherlands*
M. Ueda et al., 43-2 Asuka Habikino-shi, 583 Osaka, *Japan*

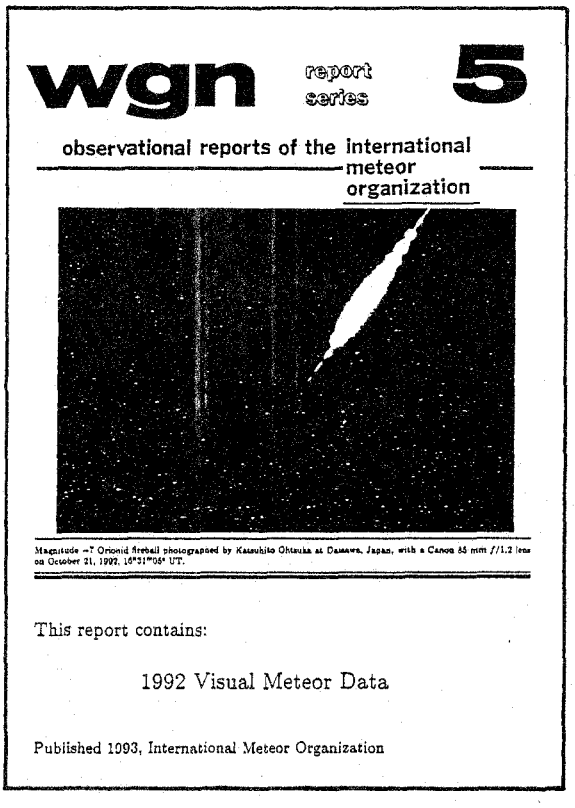

Observational Report Series vol. 5

edited by Marc Gyssens

Volume 5 contains 148 pages with all *IMO* visual observations of 1992! In total, you will find 71 909 visual meteors seen during 4094 hours by 317 observers from 29 different countries. As usual, Paul Roggemans composed this report, which is a must for every meteor observer!

An invaluable work for meteor workers wishing to carry out further analyses or for meteor observers wanting to know how their contributions fit in on a global scale.

The price for this fifth issue of *WGN*'s Report Series has *not* been raised: for only 15 DEM post paid (surface mail delivery), this huge list of observations is yours!

Available now: Proceedings

International Meteor Conference 1992

Smolenice, Slovakia, July 2–5, 1992

The proceedings of this International Meteor Conference are available now! The book contains articles about various fields of meteor astronomy—almost entirely covering the conference.

Included are: visual and photographic observations, radio meteor work, telescopic and video observations, new techniques in meteor observation, data processing, investigations on meteorite events in the past, meteor physics and the International Meteor Organization itself.

These proceedings are published by the *International Meteor Organization* and can be ordered at only 10 DEM per copy (surface mail delivery). Note that the proceedings were included in the registration fee for the participants of the 1992 *IMC*; they should already have received their copy now. Non-participants can order these proceedings in the same way as paying for *WGN*!